

**CARDIAC MAGNETIC RESONANCE
IMAGING IN ISCHEMIC
HEART DISEASE**

Sharon Wilhelmina Maria Kirschbaum

ISBN: 9789491211249

Printed by Ipskamp Drukkers B.V., Enschede

Cover design by Sharon Kirschbaum and Ton Everaers

Layout by Ton Everaers and Sanne Evers

© 2011 Sharon Kirschbaum

All rights reserved. No part of this thesis may be reproduced or transmitted in any form or by any means, electronic or mechanical, including photocopying, recording, or any information storage and retrieval system, without prior written permission from the copyright owner.

Cardiac Magnetic Resonance Imaging in Ischemic Heart Disease

Cardiale Magnetic Resonance Imaging in Ischemische Hartziekten

Proefschrift

ter verkrijging van de graad van doctor aan de
Erasmus Universiteit Rotterdam
op gezag van de
rector magnificus

Prof.dr. H.G. Schmidt

en volgens besluit van het College voor Promoties.

De openbare verdediging zal plaatsvinden op
vrijdag 20 mei 2011 om 13:30 uur

door

Sharon Wilhelmina Maria Kirschbaum
geboren te Weert



Promotiecommissie

Promotoren: Prof.dr. P.J. de Feyter
Prof.dr. G.P. Krestin

Overige leden: Prof.dr. D.J.G.M. Duncker
Prof.dr. F. Zijlstra
Prof.dr. W.J. Niessen

Copromotor: Dr. R.J.M. van Geuns

Financial support by the Netherlands Heart Foundation and the department of Radiology Erasmus MC for the publication of this thesis is gratefully acknowledged.

Content

Part 1: Introduction **11**

Chapter 1 **13**

General introduction and outline of the thesis

Chapter 2 **19**

Cardiac magnetic resonance imaging in stable ischemic heart disease

Netherlands Heart Journal, accepted

Sharon W. Kirschbaum, Pim J. de Feyter, Robert-Jan M. van Geuns

Part 2: Validation **33**

Chapter 3 **35**

Addition of the long axis information to short axis contours reduces interstudy variability of left ventricular analysis in cardiac magnetic resonance studies

Investigative Radiology. 2008 Jan;43(1):1-6.

Sharon W. Kirschbaum, Timo Baks, Ed H. Gronenschild, Jean-Paul Aben,

Annick C. Weustink, Piotr A. Wielopolski, Gabriel, P. Krestin, Pim J. de

Feyter, Robert-Jan M. van Geuns

Chapter 4 **51**

Accurate automatic papillary muscle identification for quantitative left ventricular mass measurements in cardiac magnetic resonance imaging

Acad Radiol. 2008 Oct;15(10):1227-33.

Sharon W. Kirschbaum, Jean-Paul Aben, Timo Baks, Amber Moelker,

Katherina Gruszczynska, Piotr Wielopolski, Gabriel P. Krestin, Wim J. van

de Giessen, Dirk J. Duncker, Pim J. de Feyter, Robert-Jan M. van Geuns

Part 3: Detection of ischemic heart disease **65**

Chapter 5 **67**

Comparison of adenosine magnetic resonance perfusion imaging with invasive CFR and FFR in patients with suspected coronary artery disease

International journal of cardiology, accepted

Sharon W. Kirschbaum, Tirza Springeling, Alexia Rossi, Eric Duckers, Juan Luis Gutiérrez-Chico, Eveline Regar, Pim J. de Feyter and Robert-Jan M. van Geuns.

Chapter 6 **75**

Non-invasive diagnostic workup of patients with suspected stable angina by computed tomography coronary angiography and magnetic resonance perfusion imaging

Circulation Journal, accepted

Sharon W. Kirschbaum, Koen Nieman, Tirza Springeling, Annick C. Weustink, Steve Ramcharitar, Carlos van Mieghem, Alexia Rossi, Eric Duckers, Patrick W. Serruys, Eric Boersma, Pim J. de Feyter and Robert-Jan M. van Geuns

Chapter 7 **91**

Contractile reserve in segments with non-transmural infarction in chronic dysfunctional myocardium using low dose dobutamine CMR

Journal of the american college of cardiology Cardiovasc Imaging. 2010 Jun;3(6):614-22

Sharon W. Kirschbaum, Alexia Rossi, Ron T. van Domburg, Katerina Gruszczynska, Gabriel P. Krestin, Patrick W. Serruys, Dirk J. Duncker, Pim J. de Feyter, Robert-Jan M van Geuns

Part 4: Magnetic resonance imaging guided management of ischemic heart disease **109**

Chapter 8 **111**

Combining magnetic resonance viability variables better predicts improvement of myocardial function prior to percutaneous coronary intervention

International Journal of Cardiology, accepted

Sharon W. Kirschbaum, Alexia Rossi, Eric Boersma, Tirza Springeling, Martin van de Ent, Gabriel P. Krestin, Patrick W. Serruys, Dirk J. Duncker, Pim J. de Feyter, Robert-Jan M. van Geuns

Chapter 9 **131**

Evaluation of left ventricular function 3 years after percutaneous recanalisation of chronic total coronary occlusions.

American journal of cardiology. 2008 Jan 15;101(2):179-85.

Sharon W. Kirschbaum, Timo Baks, Martin van den Ent, George Sianos, Gabriel P. Krestin, MD, Patrick W. Serruys, Pim J. de Feyter, Robert-Jan M. van Geuns

Chapter 10 **147**

Complete percutaneous revascularization for multivessel disease in patients with impaired left ventricular function. Pre- and post procedural evaluation by cardiac magnetic resonance imaging

Journal of the american college of cardiology Cardiovasc Interv. 2010 Apr;3(4):392-400

Sharon W. Kirschbaum, Tirza Springeling, Eric Boersma, Adriaan Moelker, Wim J. van der Giessen, Patrick W. Serruys, Pim J. de Feyter, Robert-Jan M. van Geuns.

Interlude **169**

Cardiac amyloidosis mimics fabry's disease in cardiac magnetic resonance imaging

Clinical Radiology 2008 Nov;63(11):1274-6. Epub 2008 Jun 27.

Sharon W. Kirschbaum, Timo Baks, Marcel J. M. Kofflard, Robert-Jan M. van Geuns

| | |
|----------------------------------------|------------|
| Part 5: Summary and conclusions | 175 |
| Chapter 11 | 177 |
| Summary and conclusions | |
| Samenvatting en conclusies | |
| Acknowledgements | |
| Publications | |
| Presentations | |
| Curriculum vitae | |
| PhD portfolio | |

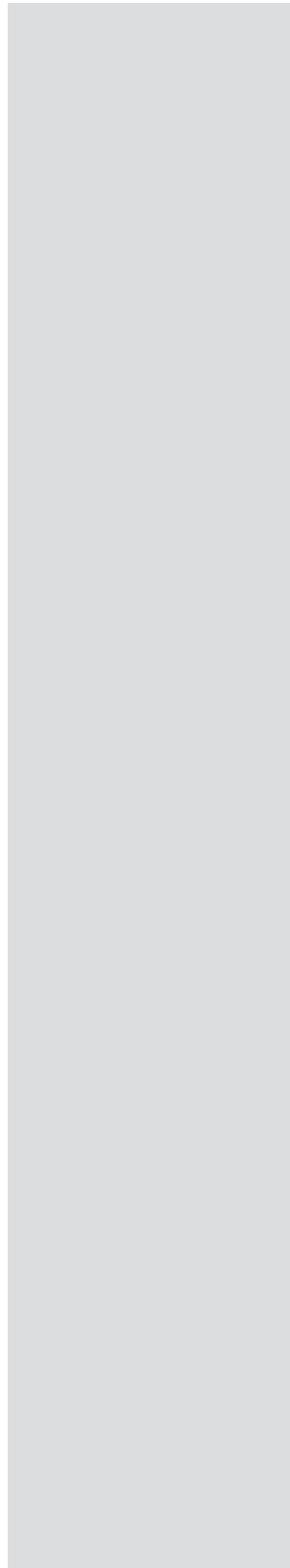
Part **1**

Introduction



Chapter 1

**General introduction
and outline of the thesis**



Introduction

Ischemic heart disease is the leading cause of morbidity and mortality in the western world¹ in particularly in the elderly and as medical and revascularization therapy is improving and life expectancy is increasing, the number of patients having ischemic heart disease is expected to increase. Chronic ischemic heart disease may be associated with depressed left ventricular function due to a state called ‘hibernation’ or “sleeping” myocardium or scarred myocardium. Scarred myocardium will not improve after revascularization therapy but hibernating myocardium may recover after restoration of myocardial blood flow. The time of blood flow obstruction and the extent of myocardial damage is related to the ability of ischemic myocardium to improve². Therefore early accurate assessment of viability and necrosis is important for optimal management of patients with chronic ischemic heart disease.

Non invasive imaging modalities are becoming key diagnostic tools in coronary artery disease detection, evaluation and guidance for revascularization therapy. To detect and evaluate ischemic heart disease different imaging modalities are available including echocardiography, nuclear imaging like SPECT or PET, computed tomography or magnetic resonance imaging³. This thesis will evaluate and discuss magnetic resonance imaging which is a relatively new imaging technique that allows imaging of the beating heart and evaluation of cardiac anatomy, ventricular function, ischemia and viability. Cardiac magnetic resonance imaging (CMR) is an enormous versatile imaging tool and all these parameters can be measured in one imaging session.

The technique has an excellent reproducibility^{4,5}, it has proven its advantage over other imaging modalities⁶ and is therefore nowadays considered the reference standard for the evaluation of cardiac function. However we have to keep in mind that CMR is not perfect and variability in measurements is still present. The second part of the thesis concerns the validation of outcome parameters: left ventricular function and cardiac mass. Cardiac function is usually measured from a stack of short axis images covering the entire ventricle from base to apex. At the base and apex of the heart it is often difficult to determine which slice should be included in left ventricular volume measurements therefore we wanted to investigate if addition of long axis contours in left ventricular functional measurement could reduce variability (chapter 2) and if incor-

poration of the papillary muscle influences left ventricular mass measurements (chapter 3).

Part 3 mainly focussed on the detection of ischemic heart disease. Adenosine Cardiac Magnetic Resonance perfusion imaging (MRP) has emerged as a safe non invasive imaging technique to detect stress induced myocardial perfusion abnormalities. Most studies compared visual interpretation of MRP with visual assessment of invasive coronary angiography. We compared the ability of MRP to detect presence of myocardial ischemia with invasive fractional flow reserve and coronary flow reserve as standard of reference in patients with stable angina (chapter 5). Not only non invasive MRP but also CTCA is useful to detect coronary artery disease. Many studies have demonstrated that CTCA has a high negative predictive value to exclude coronary artery disease but correlation of the degree of severity of a stenosis, in particular intermediate lesions, with the hemodynamic relevance of a lesion is poor. Therefore the combination of CTCA and adenosine MRP may complement each other and allows comprehensive evaluation of anatomy and hemodynamic relevance of a lesion (chapter 6). Not only the hemodynamic relevance of a lesion but also the amount of scar tissue and the presence of contractile reserve gives us information about ischemic heart disease. We studied the relation between the quantitative amount of contractile reserve during dobutamine and infarct size which was not investigated thus far (chapter 7).

Part 4 mainly focused on CMR guided management of ischemic heart disease. In patients with coronary artery disease and depressed myocardial function, CMR can predict if myocardial tissue will benefit from restoration of coronary blood flow. Myocardium will only improve after revascularization if the dysfunctional myocardium is viable. CMR is able to detect both viability and myocardial necrosis and can therefore predict the presence of improvement of left ventricular function after revascularization. A widely used technique for the detection of viability is delayed enhancement imaging, but its diagnostic accuracy is low due to the limited predictive value of this technique in segments with an intermediate transmural extent of infarction. In chapter 8 we describe the effect of combined viability assessment using different CMR parameters for the prediction of improvement of myocardial function after revascularization, where we evaluated the presence of viability on a per segment level.

In chapter 9 we evaluated the predictive possibilities of CMR on a per patient level in patients with multivessel coronary artery disease and also evaluated the effect of treatment on left ventricular ejection fraction. In patients with multivessel coronary artery disease and depressed left ventricular function, PCI is increasingly used as revascularization strategy instead of CABG because both therapies have the same outcome in terms of survival and rates of myocardial infarction in patients with syntax score <30. Due to extensive disease or depressed left ventricular systolic function which is thought to be irreversible, PCI may result in incomplete revascularization. We hypothesize that complete revascularization may better improve left ventricular ejection fraction as compared to incomplete or unsuccessful revascularization (chapter 7) and investigated the diagnostic accuracy of CMR in this patient population. Most studies that investigated the effect of revascularization on left ventricular function were performed with a follow-up duration of 5 to 6 months, however it is currently unknown in what time span recovery of dysfunctional but viable myocardium can be seen. Therefore we evaluated myocardial function after percutaneous coronary intervention of a chronic total occlusion at 6 months and at 3 years (chapter 10) and measured the improvement in left ventricular function on both time frames.

References

1. Fox CS, Evans JC, Larson MG, Kannel WB, Levy D. Temporal trends in coronary heart disease mortality and sudden cardiac death from 1950 to 1999: the Framingham Heart Study. *Circulation* 2004;110:522-527.
2. Haas F, Augustin N, Holper K, Wottke M, Haehnel C, Nekolla S, Meisner H, Lange R, Schwaiger M. Time course and extent of improvement of dysfunctioning myocardium in patients with coronary artery disease and severely depressed left ventricular function after revascularization: correlation with positron emission tomographic findings. *J Am Coll Cardiol* 2000;36:1927-1934.
3. Mazeika PK, Nadazdin A, Oakley CM. Dobutamine stress echocardiography for detection and assessment of coronary artery disease. *J Am Coll Cardiol* 1992;19:1203-1211.
4. van Geuns RJ, Baks T, Gronenschild EH, Aben JP, Wielopolski PA, Cademartiri F, de Feyter PJ. Automatic quantitative left ventricular analysis of cine MR images by using three-dimensional information for contour detection. *Radiology* 2006;240:215-221.

5. Kirschbaum SW, Baks T, Gronenschild EH, Aben JP, Weustink AC, Wielopolski PA, Krestin GP, de Feyter PJ, van Geuns RJ. Addition of the long-axis information to short-axis contours reduces interstudy variability of left-ventricular analysis in cardiac magnetic resonance studies. *Invest Radiol* 2008;43:1-6.
6. Grothues F, Smith GC, Moon JC, Bellenger NG, Collins P, Klein HU, Pennell DJ. Comparison of interstudy reproducibility of cardiovascular magnetic resonance with two-dimensional echocardiography in normal subjects and in patients with heart failure or left ventricular hypertrophy. *Am J Cardiol* 2002;90:29-34.

Chapter 2

Cardiac magnetic resonance imaging in stable ischemic heart disease

Netherlands Heart Journal, accepted

Sharon W Kirschbaum
Pim J de Feyter
Robert-Jan M van Geuns

Department of
Cardiology, Erasmus
University Medical Center
Rotterdam

Introduction

Ischemic heart disease, despite advances of detection and treatment remains the leading cause of morbidity and mortality in the Netherlands and more accurate detection and evaluation of coronary atherosclerosis may further reduce adverse outcome. Cardiac magnetic resonance imaging (CMR) is a new robust versatile non-invasive imaging technique that can detect global and regional myocardial dysfunction, presence of myocardial ischemia and myocardial scar tissue and has the advantage that it can evaluate all these parameters in one imaging session with freedom of ionizing radiation and with the use of relatively safe contrast material. CMR has demonstrated a high interstudy reproducibility which make it possible to use this technique for serial assessment in an individual patient to evaluate the effect of treatment. The different diagnostic possibilities of CMR in patients with ischemic heart disease will be discussed with the focus on the strengths and weaknesses of each particular feature.

MR for the assessment of left ventricular function

CMR is a precise and highly reproducible technique to assess left ventricular (LV) function, volume and mass with a lower intraobserver- interobserver- and inter-study variability[1, 2] as compared to LV angiography or cardiac echocardiography[3, 4, 5]. CMR is currently considered the standard of reference for these parameters and is frequently used as a surrogate end point in clinical trials[6, 7]. These measurements are obtained using dynamic imaging where a series of

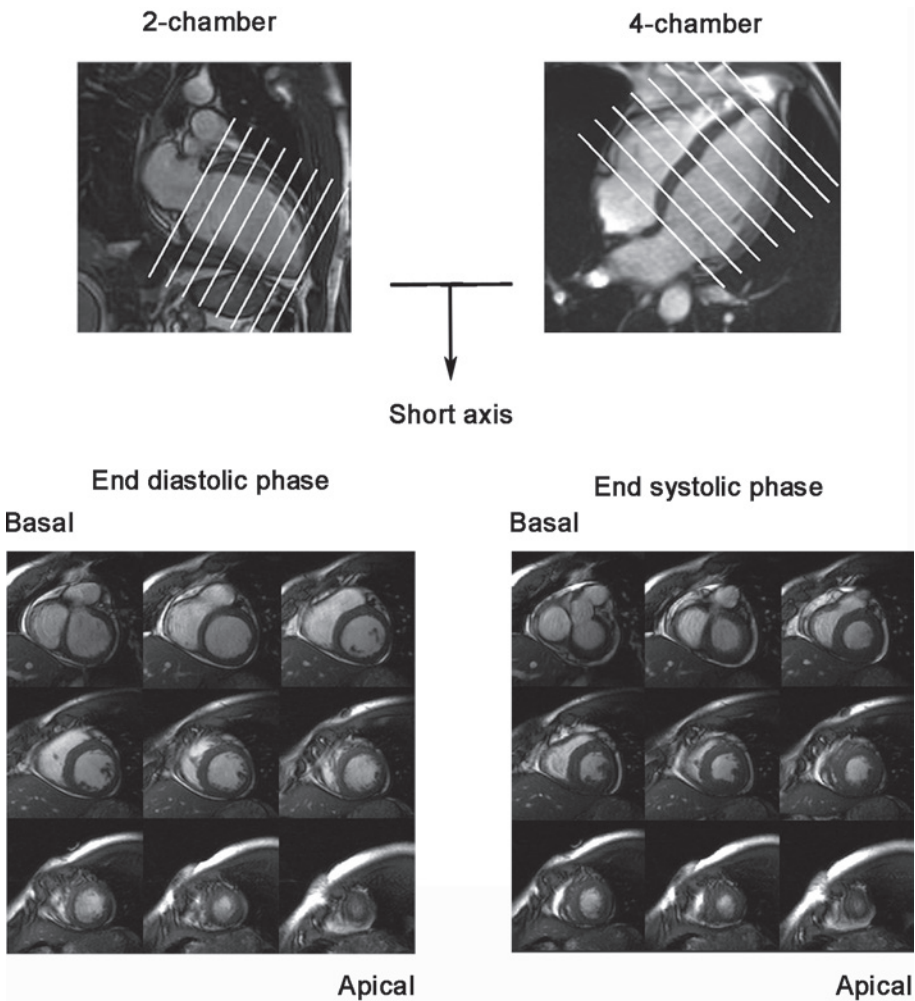


Figure 1 The end diastolic image of the two and four chamber image (upper part) is used to position a stack of short axis images (bottom) from basal to apical with a slice thickness of 8 mm.

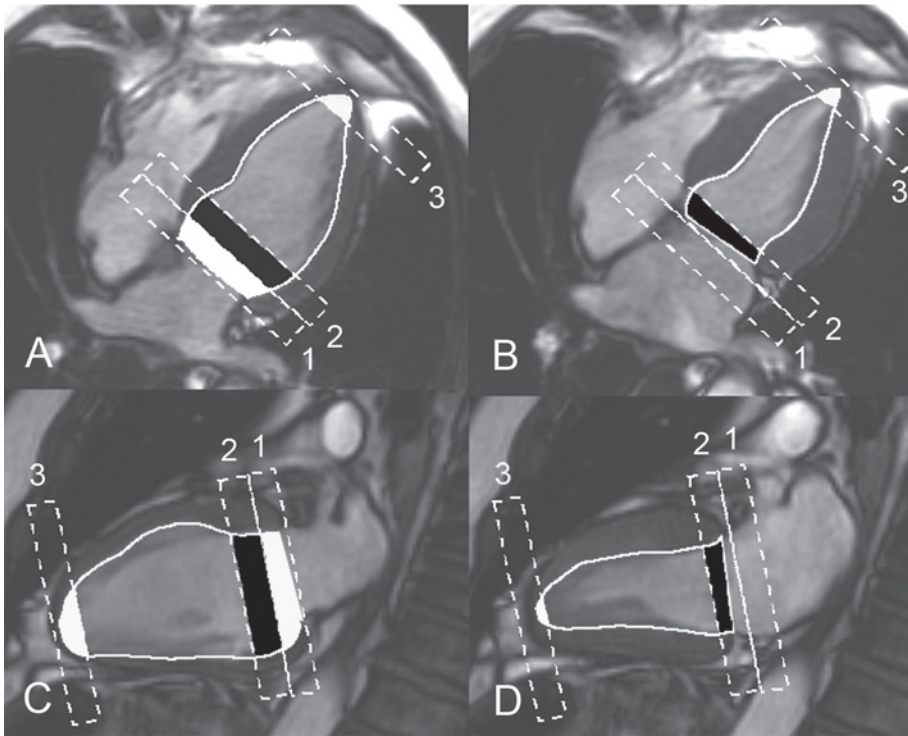


Figure 2 Illustration of the method using the information of the long axis to achieve left ventricular volumes mass and function. During the end diastolic phase (figure A, C), slice 1 is partially included in the LV volume, slice 2 is totally included based on the long axis areas, while during systole (figure B, D) 0% is included of slice 1 and slice 2 is only partially included. At the apex, slice 3 is partially included for both phases (figure A, B, C and D) in LV functional assessment. By integrating the long axis and thereby more accurately indicating left ventricular borders the variability can be significantly reduced.

parallel short axis images is acquired covering the whole ventricle from the atrio-ventricular transition to the apex. The long axis images of both the 2- and 4-chamber in the end-diastolic phase at end-expiration provide the reference images to acquire a series of short axis images (figure 1). To estimate left ventricular functional volume and mass, the Simpson method is used where the volume of each individual slice is calculated and added[8]. Even though the Simpson's method has been the standard method of CMR LV analysis for many years, variability in left ventricular measurements is still present. Sources of variability are inconsistency in planning of the images during acquisition and post procedure analysis, when the analyst has to indicate the most upper and lower border of the left ventricle. Integrating the contours of the long axis to short axis contours significantly reduces

interstudy variability of all left ventricular functional parameters and may be the preferred analysis method (figure 2)[1].

Using CMR the left ventricle can be studied in detail (figure 3) and even thin structures such as the heart valves and papillary muscles can be visualized. A regular heart rhythm and consistent breath holding are essential for highly detailed imaging as each dynamic loop is acquired during a 10 to 12 second period of suspended breathing. When patients cannot hold their breath or have an irregular heart rhythm image quality may be poor and is often not good enough for accurate analysis due to respiratory motion or mistrigging of the ECG. In these cases real time dynamic acquisition

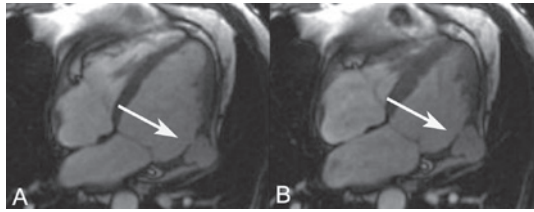


Figure 3 This is a 4-chamber view of a 64-year old patient, with a recent history of a myocardial infarction, complicated by a pseudo aneurysm (arrow) of the anterolateral wall (end diastolic phase, A; end systolic phase, B).

without breath holding can be performed and each image is acquired during a single heartbeat. A disadvantage of this technique is the lower spatial and temporal resolution which may hamper precise LV analysis [9].

MR for the detection of ischemia

If a treadmill electrocardiography test for the identification of ischemia is physically impossible or the test is inconclusive, non invasive perfusion imaging may be indicated. CMR has been the latest addition to the spectrum of non invasive myocardial perfusion or wall motion imaging modalities. The advantage of CMR over other technologies is its high resolution and contrast to noise ratio. The two main CMR methods for the assessment of myocardial ischemia are high dose dobutamine stress test with wall motion assessment and first pass myocardial perfusion under pharmacological stress with adenosine. The patient should be closely monitored during stress CMR by measuring blood pressure and heart rhythm during infusion of these pharmacological stressors. One must keep in mind that the ST-segment deviation is disturbed in the static magnetic field and detection of ischemia by ECG-monitoring is not possible.

High dose dobutamine stress with wall motion assessment

During dobutamine infusion, similar to echocardiography, functional imaging is used to detect the ischemia induced wall motion abnormalities at increasing dose from 10, 20, 30 and 40 mcg/kg/min every 3 minutes at each stress level and imaging is repeated at every stress level in both long and short axis orientations. It is important to closely monitor the development of wall-thickening abnormalities and if these develop the test is considered positive for a hemodynamic significant coronary stenosis. In a meta analysis of the pooled data of 13 publications investigating 735 patients using dobutamine stress CMR for the detection of ischemia, sensitivity was 83% (95% CI 79-88%) and specificity 86% (95% CI 81-91%) when analysed on a per patient level[10]. Nagel et al. compared dobutamine stress CMR with dobutamine stress echocardiography in patients with suspected coronary artery disease[11]. They found that dobutamine stress CMR had a higher diagnostic performance. The sensitivity increased from 74% to 86% and specificity increased from 70% to 86% (both $p < 0.05$) using coronary angiography as the standard of reference. Also in patients with a poor acoustic echo window, image quality of CMR was able to detect the presence of coronary artery disease with a sensitivity varying from 75% to 92% depending on the extent of coronary artery disease and a specificity of 83% using quantitative coronary angiography as standard of reference[12].

Although CMR is a relatively new technology it has proven prognostic value, patients with inducible ischemia were at higher risk of developing a myocardial infarction or cardiac death independent and incremental to the presence of conventional risk factors for coronary arteriosclerosis [13].

Adenosine stressed first pass myocardial perfusion

Myocardial perfusion imaging is based on the changes of myocardial signal intensity during the first passage of a contrast bolus into the myocardium of intravenously injected contrast agent at rest and during stress using adenosine as a pharmacological stressor. Flow limiting coronary stenosis during stress causes less perfusion of the subtended myocardium than myocardium that is supplied by normal vessels. This is visualized on CMR images as a darker myocardial area (less perfusion, less contrast) during stress as compared to normal perfused myocardial areas. Perfusion of the myocardium can be assessed visually (perfusion present or absent) or quantitatively by calculating the myocardial perfusion reserve index.[14]

The MR-Impact trial[15], a multicenter multivendor prospective trial, compared perfusion CMR with single photon emission tomography (SPECT) and concluded that perfusion CMR in the entire study population was superior to SPECT. The superior sensitivity and specificity of stress perfusion CMR is most likely due to the better spatial resolution as compared to SPECT. In addition SPECT is hampered by its radiation exposure and attenuation artifacts that makes it sometimes difficult to correctly interpret the scans. Visual assessment of perfusion images, as in the MR-Impact trial by experienced readers has sufficient diagnostic accuracy, but this simple approach is not always sufficient and subtle differences may be missed as might be needed for follow-up examination or to evaluate therapeutic effects on myocardial perfusion. Quantitative analysis is more objective, it has also the advantage that in patients with three vessel disease, balanced perfusion defects can be detected.

To determine the myocardial perfusion reserve index for quantitative assessment, the relative upslope of a given segment during stress is divided by the relative upslope of a given segment at rest[16, 17]. Relative upslope is defined as the maximum upslope of the signal intensity curve divided by the maximum upslope of the LV cavity curve.

A disadvantage of perfusion CMR is the fact that the investigation is cumbersome, time consuming and acquisition and interpretation of images requires extensive experience. In a meta analysis of 14 studies of 1183 patients, pooled data analysis showed a sensitivity of 91% (95% CI 88-94) and a specificity of 81% (95%CI 77-85) for adenosine perfusion CMR on a per patient level compared to coronary angiography as standard of reference[10]. Two more recent studies showed the same diagnostic accuracy (table)[18, 19].

Table Sensitivity and specificity of perfusion MRI

| Author [ref#] | N | Sensitivity (%) | Specificity (%) |
|----------------|------|-----------------|-----------------|
| Gebker [19] | 455 | 91 | 70 |
| Klem [18] | 136 | 84 | 88 |
| Nandalur [10] | 1183 | 91 | 81 |
| Schwitzer [15] | 234 | 85 | 67 |

N = number of patients

CMR for the assessment of viability

Left ventricular dysfunction may be the result of viable or non viable dysfunctional myocardium. The latter may not recover after revascularization therapy while viable myocardium in patients with chronic ischemic heart disease will recover in weeks, months or years after revascularization. Viable myocardium is associated with repetitive transient ischemia or persistent reduced myocardial blood flow so called hibernating myocardium that must be distinguished from permanently damaged infarcted myocardium. Viable dysfunctional myocardium is defined as recovery of regional myocardial dysfunction after revascularization. CMR viability assessment is achieved using low dose dobutamine as a functional response to examine contractile reserve or late gadolinium enhancement as necrosis imaging or simply assessing end diastolic wall thickness.

End diastolic wall thickness was the first parameter that has been used as a viability parameter prior to late gadolinium enhancement and an end diastolic wall thickness of < 5.5 mm represented non viable tissue[20, 21, 22].

Low dose dobutamine

Dobutamine is known to stimulate the beta receptors of the myocytes, increases the ATP and oxygen consumption and therefore improves contraction. The presence of contractile reserve during low dose dobutamine which is tested at two different doses (5 and 10 mcg/kg/min) has a higher predictive accuracy as compared to the end diastolic wall thickness (91% vs. 79% for preserved wall thickness)[23]. With current fast CMR techniques one is able to scan the left ventricle at both stress levels and a useful approach is to acquire 3 short axis view and 3 long axis views within 4 breath holds during each stress level. An example of a patient with contractile reserve during dobutamine in a region perfused by a chronic total occlusion is presented in figure 4.

CMR late gadolinium enhancement

Contrast late enhancement CMR allows visualization of the distribution of myocardial scarring in post infarction patients[24, 25, 26, 27, 28, 29]. Kim et al. [24] were the first to show that delayed enhancement strongly predict functional improvement after revascularization. In segments with no infarction the likelihood

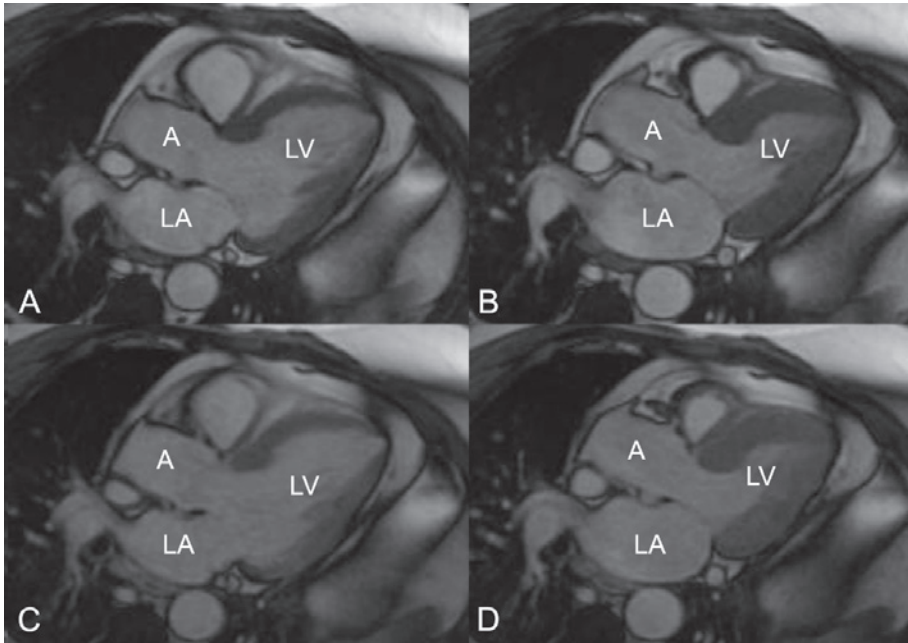


Figure 4 A 3 chamber view in the end diastolic phase (A) and the end systolic phase (B) at rest of a patient with an old anterior wall infarction and a chronic total coronary occlusion of the left anterior descending artery, and a 3 chamber view of the same patient after administration of low dose dobutamine in the end diastolic phase (C) and the end systolic phase (D) where an improvement in contractility was detected in the anteroseptal wall. LA, left atrium; A, aorta; LV, left ventricle.

of recovery was high, 78% of the segment recovered after revascularization while only 1 segment with >75% infarct transmuralty improved.

Delayed enhancement images are acquired 10-20 minutes after administration of gadolinium based contrast agent. The resulting image will show normal myocardium as black and infarcted myocardium as white (figure 5). In acute myocardial infarction the contrast agent passively diffuses into the intracellular space because the membrane is ruptured while chronic myocardial infarctions contains collagenous material replacing the myocytes which increases the extra cellular space causing increased contrast concentration and thus enhancement on delayed imaging CMR [30]. Gadolinium itself is toxic but when chelated to other molecules can be safely administered to most patients. However in patients with severe kidney disease gadolinium based contrast agents may increase the risk of developing a rare and potentially fatal condition known as nephrogenic systemic fibrosis. It involves the formation of excess fibrous connective tissue in the skin,

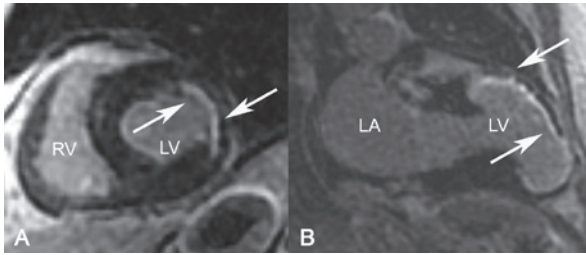


Figure 5 Short axis delayed enhancement image (A) with a sub-endocardial infarct in the lateral wall between the white arrows. A 2-chamber delayed enhancement image with a transmural infarction of the anterior wall between arrows (B). RV, right ventricle; LV, left ventricle; LA, left atrium.

eyes, joints and body organs. Symptom may include stiffness, hardening and tightening of the skin. If body organs are involved it eventually lead to death. The federation of food and drug administration (FDA) advises not to use this agent in patients

with acute kidney injury or chronic, severe kidney disease (with a glomerular filtration rate $< 30 \text{ mL/min/1.73m}^2$).

When to assess functional improvement of viable myocardium after revascularization?

Initial studies examining the functional recovery of revascularised viable myocardium were performed at 6 months after revascularization. It was assumed that this time period was sufficient for the processes underlying restoration of dysfunctional myocardium. However we hypothesized that it may require longer time for recovery and we examined patients at 6 months and again at 3 years of follow-up[31]. Improvement in segments with a small subendocardial infarction (a transmural extent of infarction of $<25\%$) was observed at 6 months and further improvement occurred at 3 years follow up. In segments with more extensive scarring, a transmural extent of infarction between 25-75%, improvement was only observed 3 year follow up but not at 6 months.

Non-ischemic heart disease

Abnormal enhancement may also be present in patients with other myocardial diseases like myocarditis, infiltrative cardiomyopathy such as amyloidosis or Fabry's disease, hypertrophic cardiomyopathy or tumors. The enhancement pattern in these patients is different from the enhancement pattern seen in patients with a myocardial infarction where it usually involves the endocardium and may extent to the epicardium and is linked with a specific coronary vessel territory. In patients with non ischemic heart disease, enhancement patterns are different

and vary between midmyocardial enhancement, a more patchy multifocal distribution or epicardial enhancement. Myocardial contraction may also be impaired in these regions [30].

Conclusion

CMR is considered as the standard of reference for comprehensive assessment of the left ventricle that can measure cardiac function, detect ischemia and has the ability to assess viable myocardium in one imaging session without the use of ionizing radiation. However patients with stable anginal symptoms also require anatomical information of the coronary vessel for clinical decision making. CMR falls short to adequately visualize the coronary artery and improvements are highly desirable to achieve complimentary anatomical and functional information in one investigational session.

References

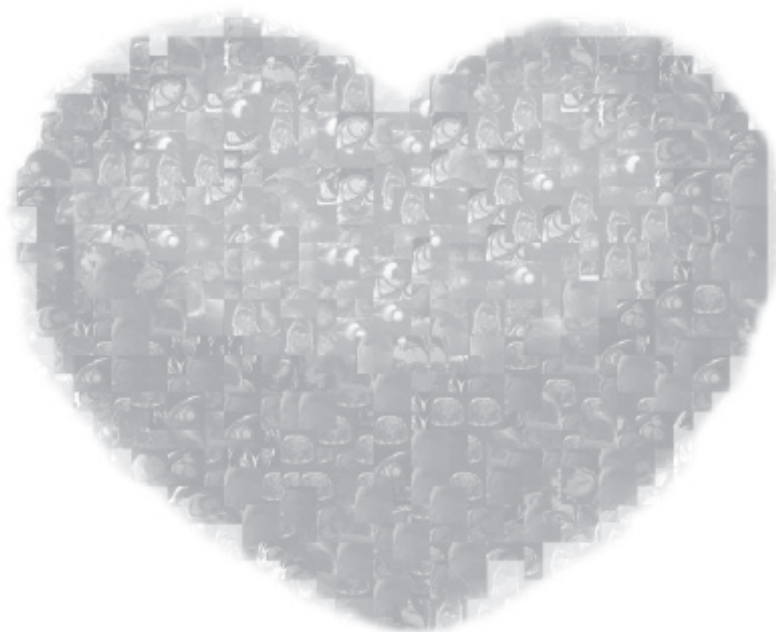
- 1 Kirschbaum SW, Baks T, Gronenschild EH, et al. Addition of the long-axis information to short-axis contours reduces interstudy variability of left-ventricular analysis in cardiac magnetic resonance studies. *Invest Radiol* 2008;43:1-6.
- 2 Bellenger NG, Davies LC, Francis JM, et al. Reduction in sample size for studies of remodeling in heart failure by the use of cardiovascular magnetic resonance. *J Cardiovasc Magn Reson* 2000;2:271-8.
- 3 Danilouchkine MG, Westenberg JJ, de Roos A, et al. Operator induced variability in cardiovascular MR: left ventricular measurements and their reproducibility. *J Cardiovasc Magn Reson* 2005;7:447-57.
- 4 Bogaert JG, Bosmans HT, Rademakers FE, et al. Left ventricular quantification with breath-hold MR imaging: comparison with echocardiography. *Magma* 1995;3:5-12.
- 5 Grothues F, Smith GC, Moon JC, et al. Comparison of interstudy reproducibility of cardiovascular magnetic resonance with two-dimensional echocardiography in normal subjects and in patients with heart failure or left ventricular hypertrophy. *Am J Cardiol* 2002;90:29-34.
- 6 Schachinger V, Assmus B, Britten MB, et al. Transplantation of progenitor cells and regeneration enhancement in acute myocardial infarction: final one-year results of the TOPCARE-AMI Trial. *Journal of the American College of Cardiology* 2004;44:1690-9.

- 7 Meyer GP, Wollert KC, Lotz J, et al. Intracoronary bone marrow cell transfer after myocardial infarction: eighteen months' follow-up data from the randomized, controlled BOOST (BOne marROw transfer to enhance ST-elevation infarct regeneration) trial. *Circulation* 2006;113:1287-94.
- 8 Dulce MC, Mostbeck GH, Friese KK, et al. Quantification of the left ventricular volumes and function with cine MR imaging: comparison of geometric models with three-dimensional data. *Radiology* 1993;188:371-6.
- 9 Setser RM, Fischer SE, Lorenz CH. Quantification of left ventricular function with magnetic resonance images acquired in real time. *J Magn Reson Imaging* 2000;12:430-8.
- 10 Nandalur KR, Dwamena BA, Choudhri AF, et al. Diagnostic performance of stress cardiac magnetic resonance imaging in the detection of coronary artery disease: a meta-analysis. *J Am Coll Cardiol* 2007;50:1343-53.
- 11 Nagel E, Lehmkühl HB, Bocksch W, et al. Noninvasive diagnosis of ischemia-induced wall motion abnormalities with the use of high-dose dobutamine stress MRI: comparison with dobutamine stress echocardiography. *Circulation* 1999;99:763-70.
- 12 Hundley WG, Hamilton CA, Thomas MS, et al. Utility of fast cine magnetic resonance imaging and display for the detection of myocardial ischemia in patients not well suited for second harmonic stress echocardiography. *Circulation* 1999;100:1697-702.
- 13 Hundley WG, Morgan TM, Neagle CM, et al. Magnetic resonance imaging determination of cardiac prognosis. *Circulation* 2002;106:2328-33.
- 14 Wilke N, Jerosch-Herold M, Wang Y, et al. Myocardial perfusion reserve: assessment with multi-section, quantitative, first-pass MR imaging. *Radiology* 1997;204:373-84.
- 15 Schwitler J, Wacker CM, van Rossum AC, et al. MR-IMPACT: comparison of perfusion-cardiac magnetic resonance with single-photon emission computed tomography for the detection of coronary artery disease in a multicentre, multivendor, randomized trial. *Eur Heart J* 2008;29:480-9.
- 16 Al-Saadi N, Nagel E, Gross M, et al. Noninvasive detection of myocardial ischemia from perfusion reserve based on cardiovascular magnetic resonance. *Circulation* 2000;101:1379-83.
- 17 Jerosch-Herold M, Seethamraju RT, Swingen CM, et al. Analysis of myocardial perfusion MRI. *J Magn Reson Imaging* 2004;19:758-70.
- 18 Klem I, Greulich S, Heitner JF, et al. Value of cardiovascular magnetic resonance stress perfusion testing for the detection of coronary artery disease in women. *JACC* 2008;1:436-45.
- 19 Gebker R, Jahnke C, Manka R, et al. Additional value of myocardial perfusion imaging during dobutamine stress magnetic resonance for the assessment of coronary artery disease. *Circ Cardiovasc Imaging* 2008;1:122-30.
- 20 Baer FM, Voth E, Schneider CA, et al. Comparison of low-dose dobutamine-gradient-echo magnetic resonance imaging and positron emission tomography with [18F]fluorodeoxyglucose in patients with chronic coronary artery disease. A functional and morphological approach to the detection of residual myocardial viability. *Circulation* 1995;91:1006-15.

- 21 Baer FM, Smolarz K, Theissen P, et al. Regional ^{99m}Tc -methoxyisobutyl-isonitrile-uptake at rest in patients with myocardial infarcts: comparison with morphological and functional parameters obtained from gradient-echo magnetic resonance imaging. *European heart journal* 1994;15:97-107.
- 22 Baer FM, Smolarz K, Jungehulsing M, et al. Chronic myocardial infarction: assessment of morphology, function, and perfusion by gradient echo magnetic resonance imaging and ^{99m}Tc -methoxyisobutyl-isonitrile SPECT. *American heart journal* 1992;123:636-45.
- 23 Baer FM, Theissen P, Schneider CA, et al. Dobutamine magnetic resonance imaging predicts contractile recovery of chronically dysfunctional myocardium after successful revascularization. *J Am Coll Cardiol* 1998;31:1040-8.
- 24 Kim RJ, Wu E, Rafael A, et al. The use of contrast-enhanced magnetic resonance imaging to identify reversible myocardial dysfunction. *The New England journal of medicine* 2000;343:1445-53.
- 25 Kim RJ, Fieno DS, Parrish TB, et al. Relationship of MRI delayed contrast enhancement to irreversible injury, infarct age, and contractile function. *Circulation* 1999;100:1992-2002.
- 26 Wu E, Judd RM, Vargas JD, et al. Visualisation of presence, location, and transmural extent of healed Q-wave and non-Q-wave myocardial infarction. *Lancet* 2001;357:21-8.
- 27 Wagner A, Mahrholdt H, Holly TA, et al. Contrast-enhanced MRI and routine single photon emission computed tomography (SPECT) perfusion imaging for detection of subendocardial myocardial infarcts: an imaging study. *Lancet* 2003;361:374-9.
- 28 Judd RM, Lugo-Olivieri CH, Arai M, et al. Physiological basis of myocardial contrast enhancement in fast magnetic resonance images of 2-day-old reperfused canine infarcts. *Circulation* 1995;92:1902-10.
- 29 Baks T, van Geuns RJ, Duncker DJ, et al. Prediction of left ventricular function after drug-eluting stent implantation for chronic total coronary occlusions. *Journal of the American College of Cardiology* 2006;47:721-5.
- 30 Mahrholdt H, Wagner A, Judd RM, et al. Delayed enhancement cardiovascular magnetic resonance assessment of non-ischaemic cardiomyopathies. *European heart journal* 2005;26:1461-74.
- 31 Kirschbaum SW, Baks T, van den Ent M, et al. Evaluation of left ventricular function three years after percutaneous recanalization of chronic total coronary occlusions. *Am J Cardiol* 2008;101:179-85.

Part 2

Validation



Chapter 3

Addition of the long axis information to short axis contours reduces interstudy variability of left ventricular analysis in cardiac magnetic resonance studies

Investigative Radiology. 2008 Jan;43(1):1-6.

Sharon W. Kirschbaum^{1,2}

Timo Baks^{1,2}

Ed H Gronenschild⁴

Jean-Paul Aben³

Annick C. Weustink²

Piotr A. Wielopolski²

Gabriel, P. Krestin²

Pim J de Feyter^{1,2}

Robert-Jan M van Geuns^{1,2}

1. Department of
Cardiology,

2. Department of
Radiology, Erasmus
University Medical
Center, Rotterdam, The
Netherlands

3. Pie Medical Imaging,
Maastricht, The
Netherlands

4. Department of Medical
informatics, Maastricht
University, Maastricht, the
Netherlands

Abstract

Purpose To reduce interstudy variability using long axis information for correcting short axis contours at basal and apical level for left ventricular (LV) analysis by magnetic resonance imaging.

Materials and Methods A total of twenty patients with documented heart failure and twenty volunteers underwent MRI examination twice for measuring endocardial end diastolic volume (EDV), endocardial end-systolic volume (ESV), mass and ejection fraction (EF). The boundary of the left ventricle, the mitral valve plane and apex were marked manually on the 2 and 4 chamber long axis images. Automatic epicardial and endocardial contour detection was performed on the short axis (SA) images using the intersection of the outlines from the long axis as starting positions. The same observer compared the interstudy variability of this method with analysis that was based on the short axis images only.

Results The interstudy variability decreased when information from the long axis was included; for ESV, 9.6% vs. 4.7%, ($p=0.00014$); for EDV, 4.9% vs. 2.5% ($p=0.0011$); for mass, 7.4% vs. 5.0% ($p=0.11$); and for EF 12.2% vs. 5.6% ($p=0.0017$), respectively.

Conclusion Identification of the mitral valve plane and apex on long axis images to limit the extent of volume at the base and the apex of the heart reduces interstudy variability for LV functional assessment.

Introduction

Left ventricular (LV) function and mass are used in clinical practice as parameters of cardiac function(1, 2) and are frequently used as end-points in clinical trials(3-5) Cardiac MRI has evolved to be a precise and reproducible technique for quantification of LV volumes, mass and function(6-12). These parameters are mostly measured on a stack of short axis (SA) cine images covering the entire left ventricle from base to apex. For this the Simpson rule is used avoiding assumptions on LV morphology. Variability in measurements is present although this is relatively small compared to other techniques such as LV angiography and echocardiography. Variability is introduced during acquisition when the SA series are planned on the 4-chamber localisation images and during post procedure analysis when the observer determines the upper and lower extend of the left ventricular at the base and apex of the heart. Variability can be reduced using guidelines for acquisition and post procedure analysis for acquiring volumetric data(13). However this is still a suboptimal solution for post procedure analysis as these are based only on 2D SA information. Including additional 3D information from the long axis images should provide more detailed information on the location of the mitral valve and apex.

The purpose of the present study was to investigate if identification of the mitral valve plane and apex on long axis images in addition to SA contours, improves the interstudy reproducibility of LV parameters measured by MRI, when compared to using SA images only.

Materials and Methods

Patient selection

A total of 40 subjects were prospectively studied. The study population consisted of 20 healthy volunteers with no history of cardiac disease and 20 patients with documented heart failure (New York Heart Association class I to III). Patients and volunteers were recruited consecutively from February 2006 till May 2006. Study participants underwent two MRI examinations. After the first MRI study the subject was removed from the scanning area, rested, and then repositioned for a second examination with a minimal time interval of 10 minutes. Exclusion criteria were any contraindications for magnetic resonance studies (pacemakers, claustrophobia, cochlea implants). The study was approved by the institutional review board and each subject gave informed consent.

MRI protocol

MR images were acquired using a 1.5 Tesla scanner. Patients were positioned in the supine position with a cardiac eight-element phased-array coil placed over the thorax (Signa CV/i, GE Medical systems, Milwaukee, Wisconsin USA). Repeated breath holds and gating to the electrocardiogram were applied to minimize the influence of cardiac and respiratory motion on data collection. Cine MRI was performed using a steady-state free-precession technique (FIESTA). Imaging parameters were; 10-15 s breath hold (depending on the heart rate); repetition time, 3.4 ms; echo time, 1.5 ms; flip angle, 45 degrees; slice thickness was 8.0 mm with a 2.0 mm slice gap; field of view 36-40 x 28-36 cm; 12 views per segment and matrix size was 192 x 192. These used parameters resulted in a temporal resolution per image of less than 41 ms. Using standard techniques to identify the major cardiac axes, two-chamber and four chamber cine MR images were obtained. The two- and four-chamber end diastolic images at end expiration provided the reference images to obtain a series of SA views. The first slice was positioned at the basis covering the mitral valve and the last slice covering the apex. This resulted in 10-12 cine breath-hold short-axis images to cover the entire left ventricle. All imaging examinations were performed by the same operator (S.W.K).

Data analysis

All images were transferred to a Microsoft Windows™ based personal computer for analysis using the CAAS-MRV program (version 2.0; Pie Medical Imaging,

Maastricht, The Netherlands). This software uses the additional information of the long axis to limit the extent of volumes at the base and apex of the heart. All studies were analysed using classical SA-images only and with a combined approach using long axis and SA images.

The SA end-diastolic (ED) phase was selected as the phase with the largest LV endocardial area. The end systolic (ES) phase was identified as the image with the smallest LV endocardial area. For the LV segmentation procedure both epicardial and endocardial contours are manually drawn on the two and four chamber ED and ES views. Based on the four intersection points between each contour, a first rough endocardial and epicardial contour is prepared in each specific SA image. Using an algorithm based on the concept of “fuzzy objects” in which image

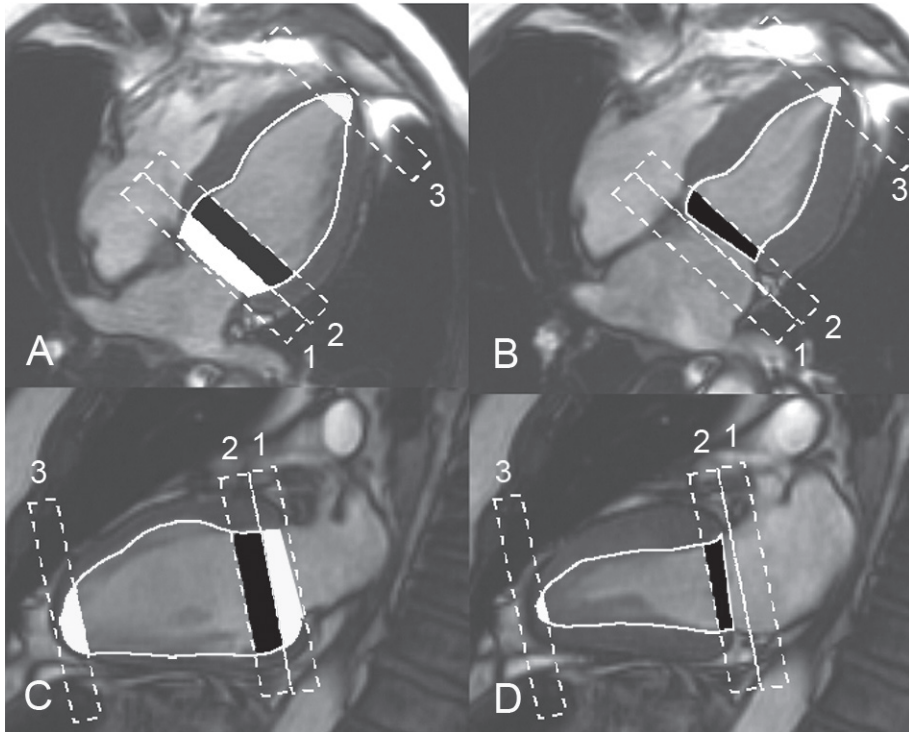


Figure 1 Illustration of the method using the information of the long axis to achieve ventricular volumes mass and function. During the ED phase (figure A, C), slice 1 is partially included in the LV volume, slice 2 is totally included based on the long axis areas, while during systole (figure B, D) 0% is included of slice 1 and slice 2 is only partially included. At the apex, slice 3 is partially included for both phases (figure A, B, C and D) in LV functional assessment.

elements (pixels/voxels) exhibit a similarity both in geometry and in grey-scale values, the final endocardial border is detected in each SA image. More details of this algorithm have been previously reported (14). The average segmentation time is 15 seconds on a 3.8 GHz Pentium IV. Within this time both ED and ES epicardial and endocardial contours are derived for all SA series. Manual corrections were performed afterwards on the SA images where necessary. The guideline for correcting SA contours was to achieve a nearly round contour excluding the papillary muscles and trabeculations from the myocardium(15). Only those contours were corrected that were not accurately on the border between the blood pool and the myocardium.

For LV ES volume and LV ED volumes calculations with the combined approach using the long axis images the Simpson's rule was used where both the first basal and last apical slice are only partly included related to the area each slice contributes to the LV area outlined on the 2 and 4 chamber images (Figure 1). For the classical method (SA-images only) volumes are calculated by the Simpson's rule only. The most basal slice was only included if more than 50% of the total circumference was identified as myocardium(16). LV mass was calculated by taking the difference of the ED epicardial volume and ED endocardial volume multiplied by 1.05 g/cm^3 , the standard mass for each cubic centimetre. The ejection fraction (EF) was determined by calculating the difference of the ED endocardial volume and ES endocardial volume divided by the ED endocardial volume. (15). The MRI studies of all patients and volunteers were analysed in a random order with the investigator blinded to the subjects name and previous result.

Statistical analysis

For each analysis method, SA only and SA combined with long axis, the mean \pm the standard deviation (SD) of each parameter was calculated for all studies. The mean difference between both studies in all patients and volunteers was also calculated for each parameter. The agreement between two MRI studies was calculated for the combined method with the information of the long axis using the coefficient of determination (r^2).

Moreover, we calculated interstudy variability for both methods using combined long axis and SA and the traditional SA only for analysis. The interstudy variability was defined as the absolute value of the difference between two measurements divided by the average value of the paired volumes, mass or EF. To investigate if

there were systematic variances and to compare reproducibility, Bland and Altman plots were used (17).

A two-tailed paired Student-t-test was performed to measure significant difference between the mean values for both methods. Furthermore, a non-parametric Wilcoxon Signed Ranks Test was performed to determine the statistical significant difference between the absolute observed differences for both methods. A p -value of <0.05 was considered to indicate statistical significance.

Results

MRI studies were well tolerated in both groups with no complications. The average time to analyse each study was 4.8 ± 0.79 minutes for the combined method using the long axis images and SA images.

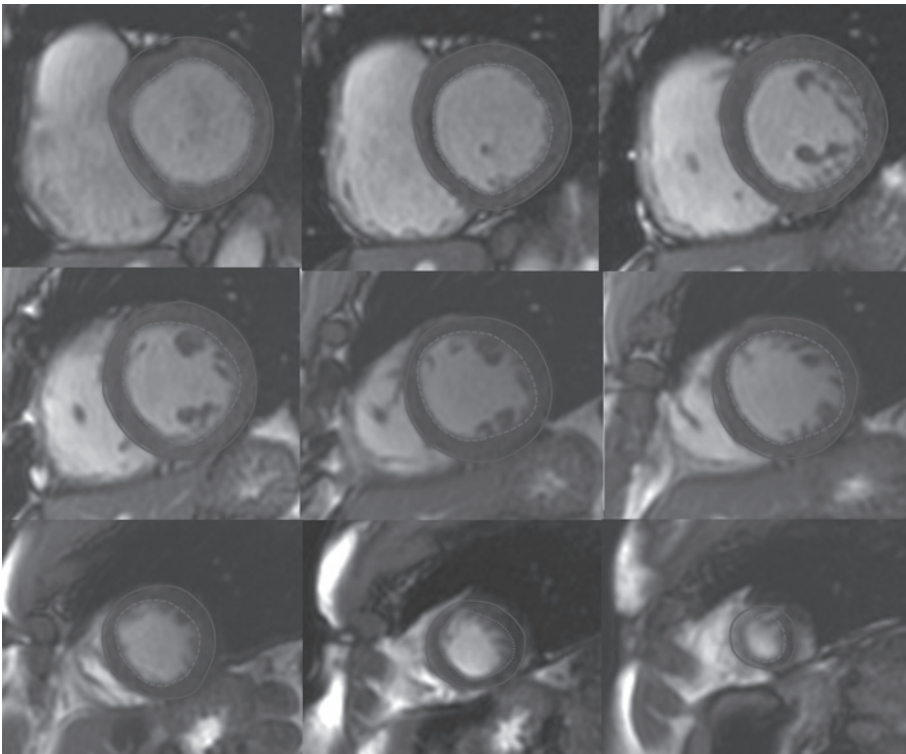


Figure 2 Illustration of the epicardial contour and endocardial contour on the SA images of an individual patient.

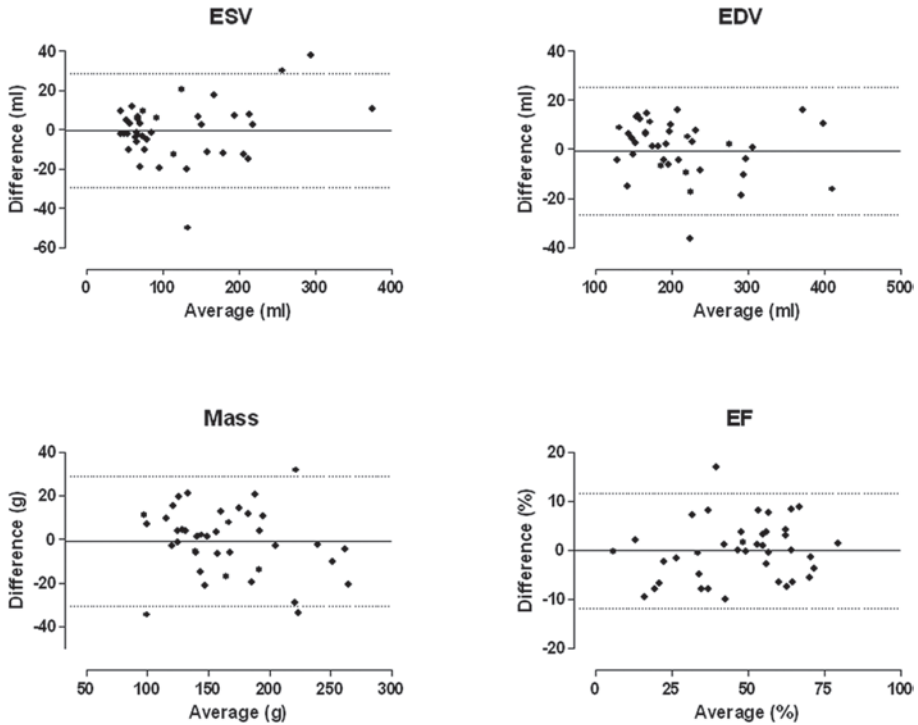


Figure 3 Bland-Altman plots of LV volumes, mass and function derived on the SA images only. The dotted lines show the 95% confidence interval.

The average values for LV volumes mass and function for patients and volunteers with the combined approach and using the SA images only were shown in table 1. An example of the contours of the SA images is shown in Figure 2.

The agreement between both studies for the combined method was for ESV ($r^2=0.98$, SEE 5.75 ml), EDV ($r^2=0.98$, SEE 6.49 ml), mass ($r^2=0.96$, SEE 8.63 g) and EF ($r^2=0.97$, SEE 2.96 %), respectively. Bland Altman analysis (figure 3 and 4) showed good agreement for the SA-only (ESV -0.46 ± 14.80 ml; EDV -0.63 ± 13.18 ml; mass -0.89 ± 15.14 g, and EF -0.07 ± 5.98 %) and when the information of the long axis was included (ESV -0.93 ± 5.71 ml, EDV 0.32 ± 6.56 ml, Mass -2.05 ± 8.22 g and EF -0.27 ± 2.95 %). The advantage of the inclusion of the long axis is illustrated by the marked reduction in the 95% confidence interval (figure 4). Another way to quantify this is by calculating the interstudy variability. The percentage interstudy variability decreased for all parameters when the information of the long axis was included; for ESV, 9.6% vs. 4.7%, ($p=0.00014$); for EDV, 4.9% vs.

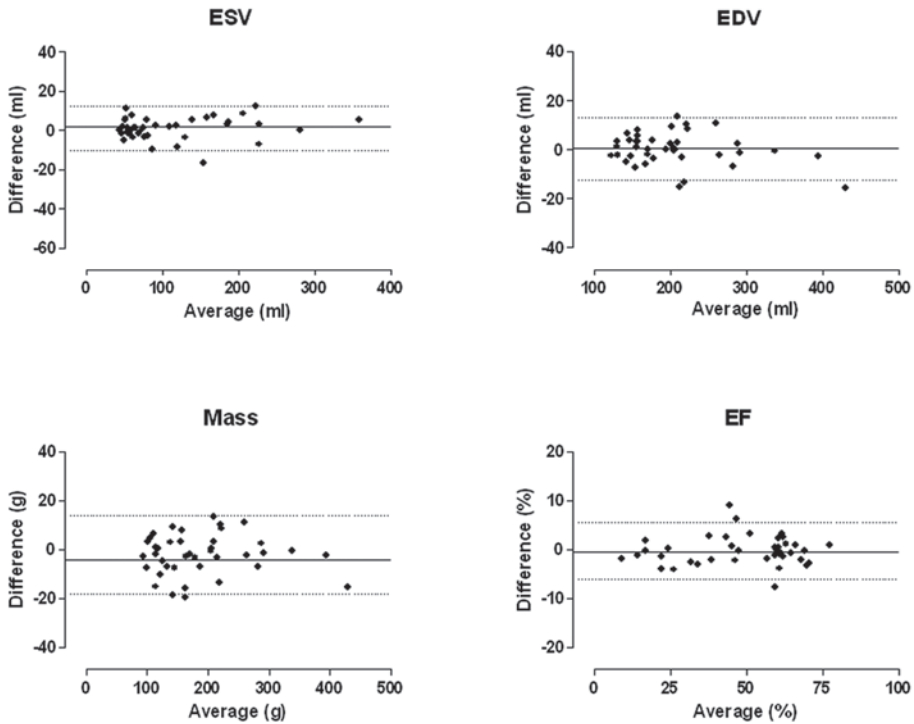


Figure 4 Bland-Altman plots of left ventricular volumes, mass and function derived with the information of the LA. The dotted lines show the 95% confidence interval.

2.5% ($p=0.0011$); mass, 7.4% vs. 5.0% ($p=0.11$); and EF 12.2% vs. 5.6% ($p=0.0017$), respectively. For more detailed results in each group see table 1.

Discussion

This study was performed to evaluate a new method using long axis images designed to further improve reproducibility of LV function assessment with MRI. We compared the values of LV parameters derived by the new methodology with the standard technique using the SA images only. The results from this study confirmed our hypothesis that this combined method significantly reduced interstudy variability.

The mean values of LV volumes and mass for both groups, derived by the combined method, were lower than the values we derived when we used the SA

Table 1 The Interstudy data

| | Volunteers | | | Patients | | | | |
|----------------------------------------------------|------------|-------------|-------------|-----------|-------------|-------------|-------------|------------|
| | ESV (ml) | EDV (ml) | Mass (g) | EF (%) | ESV (ml) | EDV (ml) | Mass (g) | EF (%) |
| SA | | | | | | | | |
| Mean±SD | 64.8±11.2* | 166.4±24.2* | 138.8±26.2* | 60.1±6.9* | 175.5±76.1* | 257.8±71.9* | 191.0±46.1* | 33.9±16.4* |
| Mean diff. ±SD | -0.6±7.6 | 1.4±13.4 | 3.7±10.5 | 0.8±5.2 | -0.26±19.8 | -2.7±13.0 | -5.5±17.8 | -0.9±6.7 |
| Interstudyvariability (%±SD) | 9.4** | 5.6** | 6.3** | 6.9** | 8.6** | 4.0** | 7.8** | 14.9** |
| SA+LA | | | | | | | | |
| Mean±SD | 60.0±10.6* | 162.1±28.0* | 129.7±25.6* | 62.8±4.1* | 164.4±75.0* | 245.6±74.4* | 184.7±39.5* | 34.8±16.4* |
| Mean diff. ±SD | 1.3±4.1 | 0.2±5.6 | -4.6±8.3 | -0.8±2.5 | 0.6±7.1 | 0.5±7.6 | 1.0±9.4 | 0.2±3.4 |
| Interstudyvariability (%) | 5.2** | 2.6** | 5.7** | 3.0** | 3.5** | 2.3** | 4.3** | 7.2** |
| p-value for interstudy variability (SA vs SA+LA)** | 0.010 | 0.021 | 0.852 | 0.033 | 0.002 | 0.021 | 0.037 | 0.028 |
| p-value * | 0.029 | 0.086 | <0.001 | 0.042 | 0.002 | 0.001 | 0.075 | 0.517 |

Mean ± standard deviation (SD) and mean difference ± SD of the difference for all parameters are measured. * Results for the paired t-test for comparison between SA and SA+LA. ** Results for the Wilcoxon Signed Ranks Test for comparison between SA and SA+LA. SA= short axis analysis, SA+LA = combined short and long axis analysis.

images only. The EF was higher for the combined method in both groups. One explanation for this difference may be the difficult identification of the most basal extent of the left ventricle on the SA-images. There are several approaches for standardisation described in the literature, using various methods to identify the most basal slice of the LV. Van der Geest et al(16) reported that for their semi automated method the most basal slice was defined as the last slice where the total amount of myocardium from the circumference of the basal slice was at least 50 %. However this method only allows full inclusion or exclusion of a slice to a volume introduced subjectively and thus remains a suboptimal solution. Pennell's strategy is based on planning of the first basal slice at the location of the atrioventricular groove during diastole(13). For the ES image one slice less is analyzed compensating for the through-plane descent of the atrio-ventricular ring in systole. However in patients with severe heart failure the atrio-ventricular ring may descend less when compared with healthy subjects. When this strategy is used in these patients, stroke volume and EF are probably exaggerated. As the LV parameters are especially important in patients with severe heart failure we considered this as the least optimal method and therefore we used the method of van der Geest mentioned above for comparison.

Several groups have described 3D approaches for LV analysis. For example, Graves et al.(18) described a technique, which makes use of the long axis images from the two- and four-chamber views for automatic detection of endocardial contours in the SA images but do not report a benefit in interstudy reproducibility.

Swingen et al. and Young et al. (19-21) used a 3D model based on a large number of points on the SA and the long axis but do not actually trace the SA contours. With such an approach, LV mass and volumes cannot be accurately measured as the papillary muscle and trabecularisations cannot be identified.

The results of the mean LV EF, volumes and mass in normal volunteers as measured by our novel technique are comparable to figures from previously reported studies(22). In addition, when we compare our results with the information of the long axis with those previously published in literature, our interstudy variability is lower for all parameters except for mass in the volunteers-group(8, 10, 12, 23). In the patient subgroup the results of our methodology are comparable with the literature(6, 9). Because the variability in this subgroup is very low due to the larger LV volume and reduced motion, it is difficult to achieve further

improvement. Another explanation is that in larger volumes it is easier to draw contours. The high level of interstudy reproducibility and the reduction in the 95% confidence interval in the Bland and Altman plots using our novel strategy can be explained by the simplicity of the procedure. The 3D information takes into account the motion of the atrioventricular ring and apex during the systolic phase accurately and it allows definition of atrial volume and ventricular volume.

The high reproducibility suggest that a smaller sample size is possible to detect a change in volumes, mass, and function in comparison with use of the SA images only. The reduction in sample size could lead to a more cost-effective assessment of therapeutic interventions by MRI.

No technique is perfect and the proposed method is depended on reproducible breath hold positions for the long axis and SA acquisitions. Inconsistent breath holding will impede the reliability of the integration of long axis and short axis images which makes assessment of left ventricle parameters more difficult. In our setting all volunteers and patients were instructed in breath holding techniques during which end-expiratory breath holding was explained which resulted in good image quality.

Nowadays, parallel imaging techniques like SMASH and SENSE have accelerated the acquisition speed and allow acquisition of 2 or 3 slices in a single breath hold(24, 25). Additionally, in the future when these techniques are combined with temporal under sampling techniques like k-t SENSE, k-t Blast and k-t GRAP-PA single breath hold 3D cine images are possible with good temporal and spatial resolution(26). If slice thickness is below 5 mm, multiplanar reformations of the SA series can be performed to obtain 2 and 4 chamber views with sufficient spatial resolution for demarcation of the mitral valve and apex. Analysis of these 3D single breath hold acquisitions will benefit from our combined approach using long axis contours from the 2 and 4 chamber view with shorter analysis time compared to the traditional method using only SA images which are increased in number in 3D reconstructions. Recently developed real 4D segmentation algorithms are alternatives when true isotropic voxels can be achieved(27).

In conclusion, the addition of long axis information to short axis contours reduces interstudy variability for all parameters in LV functional assessment. The technique is fast and can be implemented in daily routine.

References

1. Miller S, Helber U, Brechtel K, et al. MR imaging at rest early after myocardial infarction: detection of preserved function in regions with evidence for ischemic injury and non-transmural myocardial infarction. *Eur Radiol* 2003;13(3):498-506.
2. Haider AW, Larson MG, Benjamin EJ, et al. Increased left ventricular mass and hypertrophy are associated with increased risk for sudden death. *J Am Coll Cardiol* 1998;32(5):1454-9.
3. Meyer GP, Wollert KC, Lotz J, et al. Intracoronary bone marrow cell transfer after myocardial infarction: eighteen months' follow-up data from the randomized, controlled BOOST (BOne marROw transfer to enhance ST-elevation infarct regeneration) trial. *Circulation* 2006;113(10):1287-94.
4. Schachinger V, Assmus B, Britten MB, et al. Transplantation of progenitor cells and regeneration enhancement in acute myocardial infarction: final one-year results of the TOPCARE-AMI Trial. *J Am Coll Cardiol* 2004;44(8):1690-9.
5. Janssens S, Dubois C, Bogaert J, et al. Autologous bone marrow-derived stem-cell transfer in patients with ST-segment elevation myocardial infarction: double-blind, randomised controlled trial. *Lancet* 2006;367(9505):113-21.
6. Bellenger NG, Davies LC, Francis JM, et al. Reduction in sample size for studies of remodeling in heart failure by the use of cardiovascular magnetic resonance. *J Cardiovasc Magn Reson* 2000;2(4):271-8.
7. Danilouchkine MG, Westenberg JJ, de Roos A, et al. Operator induced variability in cardiovascular MR: left ventricular measurements and their reproducibility. *J Cardiovasc Magn Reson* 2005;7(2):447-57.
8. Bogaert JG, Bosmans HT, Rademakers FE, et al. Left ventricular quantification with breath-hold MR imaging: comparison with echocardiography. *Magma* 1995;3(1):5-12.
9. Semelka RC, Tomei E, Wagner S, et al. Interstudy reproducibility of dimensional and functional measurements between cine magnetic resonance studies in the morphologically abnormal left ventricle. *Am Heart J* 1990;119(6):1367-73.
10. Semelka RC, Tomei E, Wagner S, et al. Normal left ventricular dimensions and function: interstudy reproducibility of measurements with cine MR imaging. *Radiology* 1990;174(3 Pt 1):763-8.
11. Grothues F, Smith GC, Moon JC, et al. Comparison of interstudy reproducibility of cardiovascular magnetic resonance with two-dimensional echocardiography in normal subjects and in patients with heart failure or left ventricular hypertrophy. *Am J Cardiol* 2002;90(1):29-34.
12. Butler SP, McKay E, Paszkowski AL, et al. Reproducibility study of left ventricular measurements with breath-hold cine MRI using a semiautomated volumetric image analysis program. *J Magn Reson Imaging* 1998;8(2):467-72.

13. Pennell DJ. Ventricular volume and mass by CMR. *J Cardiovasc Magn Reson* 2002;4(4):507-114.
van Geuns RJ, Baks T, Gronenschild EH, et al. Automatic Quantitative Left Ventricular Analysis of Cine MR Images by Using Three-dimensional Information for Contour Detection. *Radiology* 2006;240(1):215-21.
14. van Geuns RJ, Baks T, Gronenschild EH, et al. Automatic Quantitative Left Ventricular Analysis of Cine MR Images by Using Three-dimensional Information for Contour Detection. *Radiology* 2006;240(1):215-21.
15. Sievers B, Kirchberg S, Bakan A, et al. Impact of papillary muscles in ventricular volume and ejection fraction assessment by cardiovascular magnetic resonance. *J Cardiovasc Magn Reson* 2004;6(1):9-16.
16. van der Geest RJ, Buller VG, Jansen E, et al. Comparison between manual and semiautomated analysis of left ventricular volume parameters from short-axis MR images. *J Comput Assist Tomogr* 1997;21(5):756-65.
17. Bland JM, Altman DG. Statistical methods for assessing agreement between two methods of clinical measurement. *Lancet* 1986;1(8476):307-10.
18. Graves MJ, Berry E, Eng AA, et al. A multicenter validation of an active contour-based left ventricular analysis technique. *J Magn Reson Imaging* 2000;12(2):232-9.
19. Swingen C, Wang X, Jerosch-Herold M. Evaluation of myocardial volume heterogeneity during end-diastole and end-systole using cine MRI. *J Cardiovasc Magn Reson* 2004;6(4):829-35.
20. Swingen CM, Seethamraju RT, Jerosch-Herold M. Feedback-assisted three-dimensional reconstruction of the left ventricle with MRI. *J Magn Reson Imaging* 2003;17(5):528-37.
21. Young AA, Cowan BR, Thrupp SF, et al. Left ventricular mass and volume: fast calculation with guide-point modeling on MR images. *Radiology* 2000;216(2):597-602.
22. Clay S, Alfakih K, Messroghli DR, et al. The reproducibility of left ventricular volume and mass measurements: a comparison between dual-inversion-recovery black-blood sequence and SSFP. *Eur Radiol* 2006;16(1):32-7.
23. Moon JC, Lorenz CH, Francis JM, et al. Breath-hold FLASH and FISP cardiovascular MR imaging: left ventricular volume differences and reproducibility. *Radiology* 2002;223(3):789-97.
24. Jakob PM, Griswold MA, Edelman RR, et al. Accelerated cardiac imaging using the SMASH technique. *J Cardiovasc Magn Reson* 1999;1(2):153-7.
25. Pruessmann KP, Weiger M, Boesiger P. Sensitivity encoded cardiac MRI. *J Cardiovasc Magn Reson* 2001;3(1):1-9.
26. Kozerke S, Tsao J, Razavi R, et al. Accelerating cardiac cine 3D imaging using k-t BLAST. *Magn Reson Med* 2004;52(1):19-26.
27. Uzumcu M, van der Geest RJ, Swingen C, et al. Time continuous tracking and segmentation of cardiovascular magnetic resonance images using multidimensional dynamic programming. *Invest Radiol* 2006;41(1):52-62.

Chapter 4

Accurate automatic papillary muscle identification for quantitative left ventricle mass measurements in cardiac magnetic resonance imaging

Acad Radiol. 2008 Oct;15(10):1227-33.

Sharon Kirschbaum^{1,2}

Jean-Paul Aben³

Timo Baks^{1,2}

Amber Moelker¹

Katerina Gruszczynska²

Gabriel P Krestin²

Wim J van der Giessen¹

Dirk J Duncker¹

Pim J de Feyter^{1,2}

Robert-Jan M van Geuns^{1,2}

1. Department of Cardiology, Thoraxcenter, Rotterdam, The Netherlands

2. Department of Radiology, Erasmus MC, Rotterdam, The Netherlands

3. Pie Medical Imaging, Maastricht, The Netherlands

Abstract

Purpose To evaluate the automatic detection of the papillary muscle and to determine its influence on quantitative left ventricular (LV) mass assessment.

Materials and Methods Twenty-eight Yorkshire landrace swine and 10 volunteers underwent cardiac magnetic resonance imaging (CMR) of the left ventricle. The variability in measurements of LV papillary muscles traced automatically and manually were compared to intra- and interobserver variabilities. CMR derived LV mass with the papillary muscle included or excluded from LV mass measurements was compared to true mass at autopsy of the Yorkshire Landrace swine.

Results Automatic LV papillary muscle mass from all subjects correlated well with manually derived LV papillary muscle mass measurements ($r=0.84$) with no significant bias between both measurements (mean difference \pm SD: 0.0 ± 1.5 g; $p=0.98$). The variability in results related to the contour detection method used was not statistically significant different compared to intra- and inter observer variability; $p=0.08$ and $p=0.97$ respectively.

LV mass measurements including the papillary muscle showed significantly less underestimation (-10.6 ± 7.1 g) with the lowest percentage variability (6%) compared to measurements excluding the papillary muscles (mean underestimation: -15.1 ± 7.4 g, percentage variability: 7%).

Conclusion The automatic algorithm for detecting the papillary muscle was accurate with variabilities comparable to intra- and interobserver variability. LV mass is determined most accurately when the papillary muscles are included in the LV mass measurements. Taken together these observations warrant the inclusion of automatic contour detection of papillary muscle mass in studies that involve the determination of LV mass.

Introduction

The measurements of left ventricular (LV) function by cardiac magnetic resonance imaging (CMR) is accurate and reproducible when compared to other imaging modalities [1-4]. Measurement of LV mass by CMR is also highly reproducible but both significant underestimation and overestimation in comparison with LV mass at autopsy has been reported [5, 6]. In previous CMR studies of LV mass the papillary muscles were typically excluded because the manual tracing required to measure these complex structures is time consuming. Recent improvements in CMR sequences have increased both the resolution and contrast ratios making it easier to distinguish between blood pool and muscle[7]. As a result the papillary muscles are presently easier to identify. These improvements in CMR combined with modern analysis software allow automatic identification of papillary muscle, within a short time frame. This study compares the in vivo measurement of LV papillary muscle mass using automatically drawn contours on CMR scans with those obtained manually as well as with ex-vivo LV mass measurements at autopsy

Materials and Methods

Animals

Twenty-eight Yorkshire-landrace swine (35-50 kg) were sedated with 20-mg/kg ketamine and 1 mg/kg midazolam intramuscular, anaesthetized with 12-mg/kg thiopental intravenously, intubated, and mechanically ventilated with a 1:2 mixture of oxygen and nitrogen. Anaesthesia was maintained with fentanyl (12.5 microgram/kilogram/hour). All 28 swine underwent an MRI-scan, and were sacrificed the next day. Subsequently the heart was removed and the left ventricle isolated by dissecting out the mitral and the aortic valve, the atria and the right ventricle. Experiments complied with *The Guide for Care and Use of Laboratory Animals* of the National Institutes of Health (NIH Publication No. 86-23, Revised 1996), and were approved by the Erasmus MC Animal Care Committee.

Volunteers

A total of 10 healthy volunteers with no history of cardiac disease were studied. Mean age was 30 ± 4 years. Sixty percent (n=6) of our patient population were male. Exclusion criteria were all the standard contraindications for magnetic res-

onance studies. The study was approved by the institutional review board and each subject gave informed consent for participating in this study.

MRI-protocol

A similar imaging protocol was used for the swine and for the volunteers. MR images were acquired using a 1.5 Tesla scanner (Signa CV/i, GE Medical Systems, Milwaukee, Wisconsin USA). A dedicated four-element phased array receiver coil was used for imaging the swine and an eight-element phased array receiver coil was used for imaging the volunteers. To minimize the influence of cardiac and respiratory motion on data collection we used repeated breath holds, which were achieved in the swine by turning off the ventilator temporarily, and gating to the electrocardiogram. Cine MRI was performed using a steady-state free-precession technique (FIESTA). Imaging parameters were 24 temporal phases per slice, 12 views per segment; voxel size of 1.8 x 1.5 x 8 mm for the volunteers and 2.0 x 1.9 x 8 mm for the swine; repetition time of 3.0 to 3.6 ms; time to echo 1.4; flip angle 45°; number of averages 0.75. To cover the entire left ventricle, 6-12 consecutive slices of 8 mm were planned in short axis view perpendicular to the long axis of a four-chamber view and a two-chamber view.

Data analysis

All the images were transferred to a remote workstation for analysis using the CAAS-MRV program (version 3.1, Pie Medical Imaging, Maastricht, the Netherlands). The algorithm has been described before [8]. In short the algorithm for the endoluminal contour draws heavily on the concept of fuzzy objects, in which image elements (pixels, voxels) exhibit a similarity or “hanging togetherness” both in geometry and in gray-scale values. The algorithm will properly differentiate the papillary muscles located inside the left ventricle from the blood volume. In the last step a smooth convex hull is created to mark the general endocardial border.

For the purpose of this study the delineation of the papillary muscles should be fully independent of the endocardial border detection, which should not be altered during repetitive analysis. Therefore the software was extended with an extra procedure for extracting the papillary muscles automatically after the definition of the endocardial and epicardial contours by using a threshold technique and a filter operation to reduce the inhomogeneous gray scale distribution caused by the surface coil. The threshold is derived from a statistical analysis

of the intensity information inside the epicardial contour in each frame after pre processing. Two observers blinded to the post mortem results delineated the contours of the papillary muscles manually both in animals and in volunteers. By instruction, structures less than 4 mm^2 and not in contact with the papillary muscle in an adjacent slice should be considered as trabeculations and not be included in the papillary volume. The first observer delineated the papillary contours for a second time in order to define the intra observer variability. The automatic contour detection of the papillary muscles was compared to the manual contours of the first observer. Furthermore, the total LV mass was calculated twice, once with the papillary muscle included and once with the papillary muscle excluded from LV mass measurements. Both were compared to LV mass at autopsy. Myocardial mass was calculated by multiplying the myocardial volume by 1.05 g/cm^3 , the standard mass for each cubic centimeter of muscle.

Statistical analysis

The relation between the automatic and manual derived results for papillary muscle mass for volunteers and swine were analyzed with linear regression analysis and the agreement between both was assessed by the statistical method described by Bland and Altman [9], where the mean difference and standard deviation (SD) are reported. Possible significant bias was evaluated with a two-tailed paired students-t-test on the results of both analysis techniques. A p value of <0.05 was considered statistically significant. Intra and interobserver agreement is reported with the mean difference \pm SD.

To compare the variability related to the analysis technique used with either the intraobserver or interobserver variability a two-tailed paired students-t-test was performed on the absolute differences between two measurements.

The relation between the LV mass determined with MR imaging and the LV mass at autopsy was analyzed with linear regression analysis and the agreement between both was assessed by the statistical method described by Bland and Altman [9]. In vivo mass results derived by MR imaging were compared to ex-vivo LV mass values by using a paired student t-test. The co-efficient of variability was defined as the SD of the differences between in-vivo and ex-vivo measurements divided by their mean.

Results

All swine and volunteer data sets were of sufficient image quality and analysis could be performed with good confidence. Automated epicardial and endocardial contour detection was accurate in all animals and only minor corrections were necessary. Two papillary muscles were detected in all subjects. A split papillary muscle was the most common anatomic variant. An example of automated endocardial and epicardial contour detection was shown in Figure 1.

Automated analysis time was 4.1 ± 0.6 minutes per subject when the papillary muscles were excluded and 5.0 ± 0.3 minutes when the papillary muscles were included in LV mass measurements ($p=0.06$). The average analysis time when papillary muscles were traced manually was 6.9 ± 0.5 minutes ($p<0.0001$ as compared to the time analyzing LV mass excluding the papillary muscle and $p<0.01$ as compared to analyzing LV mass including the papillary muscle). The difference in time to analyze LV mass excluding the papillary muscle and LV mass including the papillary muscle traced manually was 3 minutes. The difference was reduced to 1 minute when the papillary muscle was detected automatically.

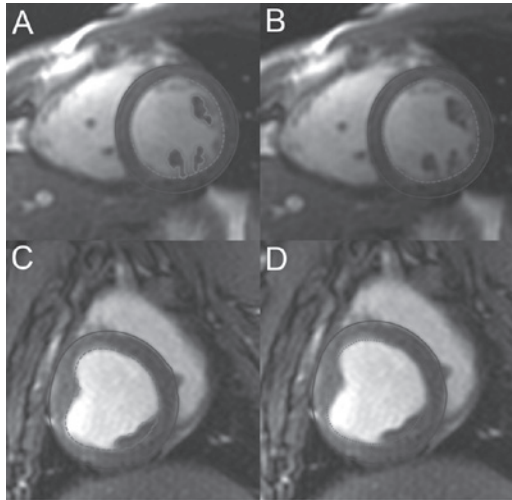


Figure 1. Illustration of the short axis end diastolic phase with automatic delineation of the papillary muscle (a, c) and of the short axis end diastolic phase with the papillary muscle excluded from the LV mass (b, d) in a human volunteer (a, b) and a swine (c, d).

Papillary Muscle Mass

The mean \pm SD of papillary muscle mass for swine was 4.7 ± 1.8 g and accounted for 4.5% of the total measured LV mass. The mean papillary muscle mass for volunteers was 6.9 ± 3.0 g and accounted for 5.4 % of the total LV mass. Automated and manual measurements of papillary muscle mass were strongly correlated ($r=0.83$; $p<0.0001$; Figure 2a). Bland-Altman analysis (Figure 2b) showed a mean differ-

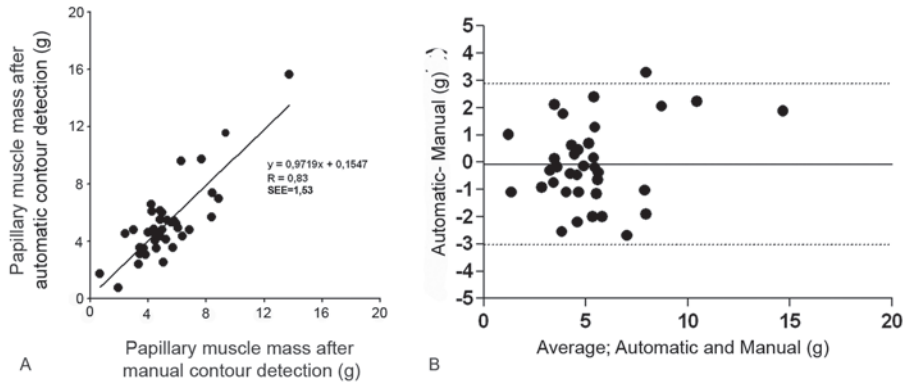


Figure 2 Regression plot (a) of automatic LV papillary muscle mass measurement compared to manual LV papillary muscle mass measurement and Bland-Altman plot (b) of LV papillary muscle mass measurements for both methods. Dotted lines represent the 95% confidence interval.

ence \pm SD of 0.0 ± 1.5 g. No bias ($p=0.98$) and no correlation ($r=0.27$; $p=0.11$) between the difference and the size of the mean of the two measurements were observed. Intraobserver and interobserver agreement for the manual measurements for LV papillary muscle mass was 0.1 ± 1.1 g ($r=0.92$; $p<0.0001$) and 1.4 ± 1.6 g ($r=0.83$; $p<0.0001$), respectively. For more detailed results in each group see table 1.

Table 1. Agreement between automatic and manual papillary muscle mass in respective to intra- and interobserver variability of manual contouring.

| | Massa | Automatic vs. manueel | Intraobserver | Interobserver |
|-----------------------|---------------|-----------------------|----------------|----------------|
| Volunteer (g) | 6.9 ± 3.0 | 0.1 ± 1.6 | 0.1 ± 1.0 | -2.1 ± 1.7 |
| Swine (g) | 4.7 ± 1.8 | -0.0 ± 1.5 | -0.4 ± 1.3 | 0.6 ± 0.9 |
| Volunteer + Swine (g) | 5.3 ± 2.4 | 0.0 ± 1.5 | 0.2 ± 1.1 | 1.4 ± 1.6 |

The values are expressed as mean \pm standard deviation

The variability in results related to the contour detection method used was not significantly different compared to intra-observer variability for all subjects ($p=0.08$) and for volunteers ($p=0.13$) and pigs ($p=0.07$) separately. The variability in results related to the contour detection method was not statistically different compared to inter-observer variability for all subjects ($p=0.97$) and for volunteers ($p=0.17$) and pigs ($p=0.05$) separately.

Total LV Mass

Mean±SD of ex-vivo LV mass was 114.6±16.1 g. More detailed results of MRI derived measurements for papillary muscle mass as compared to ex-vivo LV mass are presented in table 2. Ex-vivo LV mass was strongly correlated with MRI derived measurements of LV mass without ($r=0.91$; $p<0.0001$) (Figure 3a) and with inclusion of LV papillary muscle mass ($r=0.93$; $p<0.0001$) (Figure 3c). Bland-Altman analysis (Figure 3b and Figure 3d) showed a significant underestimation for CMR measurements excluding as well as including the papillary muscle in LV mass measurements. Including the papillary muscle in CMR LV mass measurements resulted in the least underestimation (-10.6 ± 7.1 g) with the lowest percentage

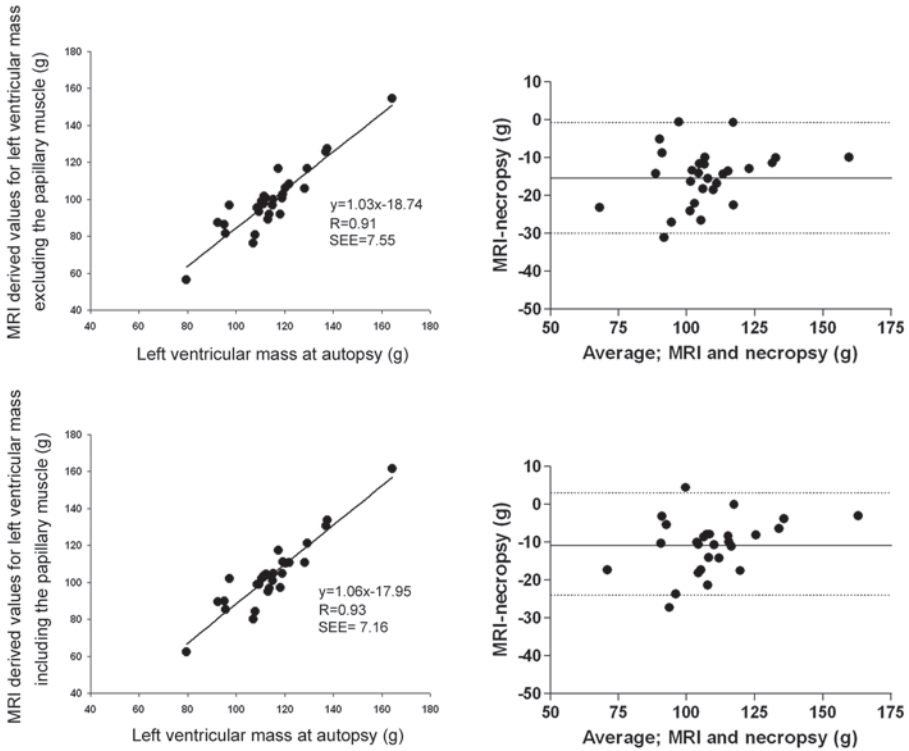


Figure 3 Correlation plot (a) and Bland Altman plot (b) of MRI LV mass versus LV mass obtained ex vivo without inclusion of the papillary muscle. Correlation plot(c) and Bland-Altman plot (d) of MRI LV mass versus LV mass obtained ex-vivo with inclusion of the papillary muscle. There is a significant bias for both measurements with less underestimation when the papillary muscles are included in the total LV mass (-10.6 ± 7.1 g versus: -15.1 ± 7.4 g). Dotted lines represent the 95% confidence interval. Results are obtained in the end diastolic phase.

Table 2. LV mass measurements including and excluding the papillary muscles compared to ex-vivo mass measurements

| | Pigs | |
|-----------------|------------------|------------------|
| | ED mass Pap+ (g) | ED mass Pap- (g) |
| Mean±SD | 103.8 ±18.2 | 99.2 ±18.0 |
| Correlation | 0.93 | 0.92 |
| R2 | 0.85 | 0.84 |
| Difference (g) | -10.6 ±7.1 | -15.1 ±7.4 |
| Variability (%) | 6% | 7% |
| P-value | <0.001 | <0.001 |

Mean ± standard deviation (SD) and mean difference ± SD of the difference between calculated LV mass and LV mass at autopsy are measured. Results of the paired t-test for comparison between calculated LV mass with ex-vivo LV mass (114.6 ±16.1 g).

variability (6.7%) when compared to the post mortem values. The computed LV mass values increased from 86.6 ±7.3% to 92.3 ± 6.2% of the true ex-vivo mass when papillary muscle was included.

Discussion

The results of this study demonstrate that left ventricle papillary muscle mass can be detected accurately using the automatic contour detection algorithm with an increase in analysis time of only 1 minute. The variability due to the contour detection method used was not different when compared to the intra- and interobserver variability of manual contour detection. Estimated LV mass shows the least underestimation when the papillary muscles were included in LV mass measurements compared to ex-vivo LV mass. To our knowledge this is the first report of algorithms for automated detection of the papillary muscle with accuracy that is comparable to manual tracing.

Automatic contouring programs often struggles with delineation of the papillary muscles[10]. This is mainly related to the complex anatomy and blurring of the boundaries by partial volume effects and motion artifacts. This may be one of the reasons why no previous studies on LV mass measurement by CMR included the

papillary muscle. Publications on papillary muscle mass use manual contour detection, which is time consuming and usually not applied for total LV mass [11]. In our study using modern imaging sequences and optimized contour detection algorithms the average analysis time was not significantly increased when the papillary muscles were additionally included.

The literature contains several publications where the difference between computed LV mass and ex-vivo LV mass was determined. Significant overestimation as well as underestimation has been reported. However, in most studies the difference between computed LV mass and LV mass at autopsy was significantly lower when the papillary muscle was included in LV mass measurements compared to the difference between masses when the papillary muscle was excluded from LV mass measurements [12-14]. Sievers et al. [11] reported small differences in ED volume and ES volume but no influence on ejection fraction and diagnostic accuracy for the presence or absence of heart disease was the same using either technique. Excluding the papillary muscle from analysis reduced measurement time from 25 +/- 4 min to 13 +/- 3 min. Other investigators reported a linear relationship between LV mass and papillary muscle mass [13] and that papillary muscles significantly affects LV ejection fraction and mass [15, 16]. The results from the present study indicate that anatomical structures such as the papillary muscles have a significant impact on mass measurements.

Nevertheless, we still found a significant underestimation for the computed LV mass compared to ex-vivo LV mass. The underestimation can be explained by different factors. First it is difficult to dissect the LV muscle from the total heart accurately and some right ventricular mass, aortic and mitral valve annulus may remain. Second, left ventricular trabeculations were not included in myocardial mass measurements as described in the methods and may account for a considerable amount of myocardial mass. Third some mass of the apex and mitral annulus may not be included in the LV mass analysis. To reduce the latter effect the software included the information of the long axis because the transition from the left atrium to the left ventricle and the apex are better discriminated and reduction in interstudy variability has been demonstrated. However due to a slice thickness of 8 mm partial volume effects cannot be excluded.

Study limitations

We did not measure interstudy reproducibility for manual contour detection or automatic contour detection of the LV papillary muscle. Therefore a direct comparison of the reproducibility between the two methods was not possible.

Conclusion

The automatic algorithm for detecting the papillary muscle was accurate with variabilities comparable to intra- and interobserver variabilities observed when using the manual contour detection. LV mass determination improved significantly when the papillary muscles were included in the LV mass measurements. Taken together these observations warrant the inclusion of automatic contour detection of papillary muscle mass in studies that involve the determination of LV mass.

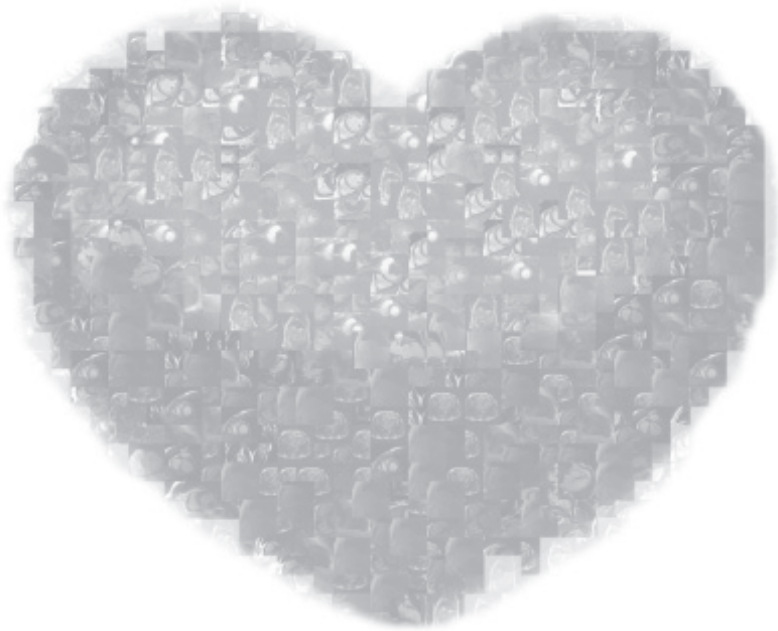
References

1. Katz J, Milliken MC, Stray-Gundersen J, et al. Estimation of human myocardial mass with MR imaging. *Radiology* 1988; 169: 495-498.
2. Stratemeier EJ, Thompson R, Brady TJ, et al. Ejection fraction determination by MR imaging: comparison with left ventricular angiography. *Radiology* 1986; 158: 775-777.
3. Semelka RC, Tomei E, Wagner S, et al. Normal left ventricular dimensions and function: interstudy reproducibility of measurements with cine MR imaging. *Radiology* 1990; 174: 763-768.
4. Semelka RC, Tomei E, Wagner S, et al. Interstudy reproducibility of dimensional and functional measurements between cine magnetic resonance studies in the morphologically abnormal left ventricle. *Am Heart J* 1990; 119: 1367-1373.
5. Bloomgarden DC, Fayad ZA, Ferrari VA, Chin B, Sutton MG, Axel L. Global cardiac function using fast breath-hold MRI: validation of new acquisition and analysis techniques. *Magn Reson Med* 1997; 37: 683-692.
6. Lorenz CH, Walker ES, Morgan VL, Klein SS, Graham TP, Jr. Normal human right and left ventricular mass, systolic function, and gender differences by cine magnetic resonance imaging. *J Cardiovasc Magn Reson* 1999; 1: 7-21.
7. Moon JC, Lorenz CH, Francis JM, Smith GC, Pennell DJ. Breath-hold FLASH and FISP cardiovascular MR imaging: left ventricular volume differences and reproducibility. *Radiology* 2002; 223: 789-797.

8. van Geuns RJ, Baks T, Gronenschild EH, et al. Automatic quantitative left ventricular analysis of cine MR images by using three-dimensional information for contour detection. *Radiology* 2006; 240: 215-221.
9. Bland JM, Altman DG. Statistical methods for assessing agreement between two methods of clinical measurement. *Lancet* 1986; 1: 307-310.
10. van der Geest RJ, Buller VG, Jansen E, et al. Comparison between manual and semiautomated analysis of left ventricular volume parameters from short-axis MR images. *J Comput Assist Tomogr* 1997; 21: 756-765.
11. Sievers B, Kirchberg S, Bakan A, Franken U, Trappe HJ. Impact of papillary muscles in ventricular volume and ejection fraction assessment by cardiovascular magnetic resonance. *J Cardiovasc Magn Reson* 2004; 6: 9-16.
12. Francois CJ, Fieno DS, Shors SM, Finn JP. Left ventricular mass: manual and automatic segmentation of true FISP and FLASH cine MR images in dogs and pigs. *Radiology* 2004; 230: 389-395.
13. Vogel-Claussen J, Finn JP, Gomes AS, et al. Left ventricular papillary muscle mass: relationship to left ventricular mass and volumes by magnetic resonance imaging. *J Comput Assist Tomogr* 2006; 30: 426-432.
14. Yamaoka O, Yabe T, Okada M, et al. Evaluation of left ventricular mass: comparison of ultrafast computed tomography, magnetic resonance imaging, and contrast left ventriculography. *Am Heart J* 1993; 126: 1372-1379.
15. Weinsaft JW, Cham MD, Janik M, et al. Left ventricular papillary muscles and trabeculae are significant determinants of cardiac MRI volumetric measurements: Effects on clinical standards in patients with advanced systolic dysfunction. *Int J Cardiol* 2007;
16. Papavassiliu T, Kuhl HP, Schroder M, et al. Effect of endocardial trabeculae on left ventricular measurements and measurement reproducibility at cardiovascular MR imaging. *Radiology* 2005; 236: 57-64.

Part **3**

Detection of ischemic heart disease



Chapter 5

Comparison of adenosine magnetic resonance perfusion imaging with invasive coronary flow reserve and fractional flow reserve in patients with suspected coronary artery disease

International Journal of Cardiology, Accepted

Sharon W Kirschbaum^{1,2}

Tirza Springeling^{1,2}

Alexia Rossi²

Eric Duckers¹

Juan Luis Gutiérrez-

Chico¹;

Eveline Regar¹

Pim J de Feyter²

Robert-Jan M van

Geuns^{1,2}.

1. Department of
Cardiology, Erasmus
University Medical
Center, Rotterdam, the
Netherlands

2. Department of
Radiology, Erasmus
University Medical
Center, Rotterdam, the
Netherlands

Fractional Flow Reserve (FFR) and Coronary Flow Reserve (CFR) have shown to be reliable to assess the functional severity of a coronary artery obstruction (1, 2), although both techniques have a different physiological background. These techniques are disadvantageous because they are invasive, expensive and albeit infrequently associated with complications and as a clinician one would rather have a non invasive test of myocardial ischemia.

Adenosine Cardiac Magnetic Resonance perfusion imaging (MRP) has emerged as a safe non invasive imaging technique to detect stress induced myocardial perfusion abnormalities(3). The purpose was to compare the ability of functional non-invasive MRP to detect evidence of myocardial ischemia with invasive CFR and FFR as standard of reference in patients with stable angina.

Symptomatic patients with suspected coronary artery disease and normal left ventricular ejection fraction who were referred for invasive coronary angiography (ICA) were asked to participate in this study. Exclusion criteria were (1)myocardial infarction, (2)previous revascularization, (3)pregnancy, (4)claustrophobia, (5)unstable coronary artery disease, (6)renal insufficiency (glomerular filtration rate of <60 ml/min/1,73 m²)or (7)arrhythmias. All patients underwent MRP and ICA within 4 weeks. The study protocol conforms to the ethical guidelines of the 1975 Declaration of Helsinki as reflected in a priori approval by the local Ethics Committee of the Erasmus Medical Centre in Rotterdam and all participating patients gave written informed consent to undergo MRP. ICA was part of routine clinical management and functional assessment was performed for stenosis visually $>30\%$ diameter using a wire which can simultaneously measure pressure and flow (ComboWire, Vulcano, Zaventem, Belgium). A significant reduction in CFR was defined as less than 2.0(4) and FFR less than 0.80(5). CMR images were acquired using a 1.5 Tesla MRI-scanner(GE Medical systems, Milwaukee, Wisconsin USA). Perfusion imaging was planned to cover the basal mid and apical part of the left ventricle. After rest perfusion vasodilatation was induced by adenosine(140ug/kg/min body weight over 3 minutes) a second bolus of gadolinium-diethyltriaminepentaacetic-acid was injected (0.05 mmol/kg at 3 ml/sec) and stress perfusion images were acquired. All MRP images were analysed using CAAS-MRV (version 3.2.1; Pie Medical Imaging, Maastricht, Netherlands). Mean signal intensity for each myocardial segment was registered over time and signal intensity–time curves were obtained, the foot point and the point of signal maximum were determined by the software using 5 consecutive points. The upslope

of the signal intensity was divided by the signal intensity of the left ventricular cavity at rest and during the hyperaemic phase. The magnetic resonance perfusion reserve index (MPRI) was calculated by dividing the corrected upslope of the stress examination by the corresponding segment's upslope of the rest examination.

Spearman's correlation was calculated to investigate the relationship between MPRI and FFR or CFR respectively. The area under the receiver operating characteristic (AUROC) curve was calculated to determine the 'best' thresholds of MPRI for the prediction of a $\text{FFR} \geq 0.80$ or a $\text{CFR} \geq 2.0$, following the method of maximizing the sum of sensitivity and specificity. Sensitivity, specificity, negative predic-

Table 1. Patient demographics

| | N=50 |
|----------------------------------------|---------|
| Age (years) | 64±10 |
| Men | 38 (76) |
| Risk factors | |
| Smoking | 10 (20) |
| Diabetes Mellitus | 9 (18) |
| Hypertension | 25 (50) |
| Hypercholesterolemia | 32 (64) |
| Family history | 22 (44) |
| Medication | |
| β – Blocker | 41 (82) |
| Statin | 46 (92) |
| ASA | 46 (92) |
| Pre test likelihood of CAD | |
| Low | 3 (6) |
| Intermediate | 34 (68) |
| High | 13 (26) |
| Left ventricular ejection fraction (%) | 64±6 |

Values are presented as number (%) or mean ± standard deviation. ASA, Acetylsalicylic Acid; CAD, Coronary Artery Disease.

tive value (NPV) and positive predictive value (PPV) were calculated to predict the ability of MPRI to identify myocardial ischemia in comparison with FFR or CFR. Statistical significance was accepted as $p < 0.05$. Fifty patients comprised the study group (table 1).

A total of 75 vessels were included in the analysis, 55%(42 of 75) in the left anterior descending artery, 23%(16 of 75) in the left circumflex artery and 23%(17 of 75) in the right coronary artery. Mean CFR was 2.1 ± 0.8 (range 1.1 to 4.5). Mean FFR was 0.80 ± 0.14 (range 0.37 to 1.0). MPRI correlated with CFR ($r = 0.58$, $p < 0.0001$) and was lower in flow limiting territories (CFR value < 2.0) compared to non flow limiting territories (CFR ≥ 2.0) (1.4 ± 0.4 vs. 2.0 ± 0.4 ; $p < 0.0001$; figure). The optimal cut off value for MPRI for the detection of a CFR < 2.0 was 1.9 (AUROC 0.85; 95% 0.76-0.94, $p < 0.0001$). Sensitivity, specificity, PPV and NPV for MPRI for the detection of functional relevant flow obstruction as define by an CFR < 2.0 were 97% (83-100), 65% (47-77), 71% (56-83) and 96%(78-100), respectively (table 2).

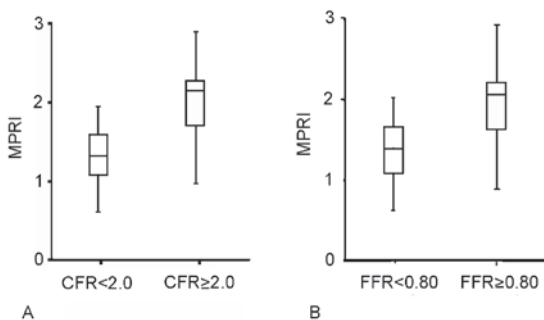


Figure. Graphic showing a box plot with the median, upper and lower quartile, upper and lower extreme of MPRI values with a CFR < 2.0 and CFR ≥ 2.0 (A) and a FFR < 0.80 and FFR ≥ 0.80 (B).

MPRI correlated with FFR ($r = 0.42$, $p < 0.05$) and was lower in territories with a FFR of < 0.80 as compared to a FFR ≥ 0.80 (1.4 ± 0.4 vs. 1.9 ± 0.5 ; $p < 0.0001$; figure). The optimal cut off value for MPRI for the detection of a stenosis with a FFR < 0.80 was 1.9, AUROC 0.83 (95% 0.74-0.92, $p < 0.0001$). Sensitivity, specificity, PPV and NPV for MPRI for the detection of coronary artery disease as define by an FFR < 0.80 were 97% (82-99), 60%(44-74), 65% (49-77) and 96% (79-99), respectively (table 3).

Our study showed that non invasive assessment of myocardial perfusion correlated both with FFR and CFR with equivalent diagnostic performance with a high sensitivity and NPV. Because of the high sensitivity and NPV, MRP is a reliable tool

Table 2. Diagnostic performance of MPRI per vessel analysis versus CFR<2

| | True positive | True negative | False positive | False negative | Sensitivity (%) | Specificity (%) | PPV (%) | NPV (%) | ACC (%) |
|----------|---------------|---------------|----------------|----------------|-----------------|-----------------|---------|---------|---------|
| MPRI<1.8 | 29 | 28 | 12 | 6 | 83 | 70 | 71 | 82 | 76 |
| MPRI<1.9 | 34 | 24 | 14 | 1 | 97 | 65 | 71 | 96 | 80 |
| MPRI<2.0 | 35 | 25 | 15 | 0 | 100 | 63 | 70 | 100 | 80 |
| MPRI<2.1 | 35 | 20 | 20 | 0 | 100 | 50 | 64 | 100 | 73 |

PPV, positive predictive value; NPV, negative predictive value; ACC, accuracy; MPRI, myocardial perfusion reserve index.

Table 3. Diagnostic performance of MRP per vessel analysis versus FFR<0.80

| | True positive | True negative | False positive | False negative | Sensitivity (%) | Specificity (%) | PPV (%) | NPV (%) | ACC (%) |
|----------|---------------|---------------|----------------|----------------|-----------------|-----------------|---------|---------|---------|
| MPRI<1.8 | 27 | 29 | 14 | 5 | 84 | 67 | 66 | 85 | 75 |
| MPRI<1.9 | 31 | 26 | 17 | 1 | 97 | 60 | 65 | 96 | 76 |
| MPRI<2.0 | 31 | 24 | 19 | 1 | 97 | 56 | 62 | 96 | 73 |
| MPRI<2.1 | 31 | 18 | 25 | 1 | 97 | 42 | 55 | 95 | 65 |

PPV, positive predictive value; NPV, negative predictive value; ACC, accuracy; MPRI, myocardial perfusion reserve index.

for the detection of hemodynamic significant coronary artery disease and can be used as a sensitive screening tool to exclude ischemia in the absence of the use of radiation and with the use of a safe contrast agent. The last several years MRP was compared to either FFR or CFR and diagnostic performance was diverse (6, 7). As results in literature varied, this study compared non invasive perfusion imaging with both FFR and CFR evaluating coronary physiology, however MRP did not compare favourably to either invasive technique where one may expect that MRP will better correspond to CFR because of the same physiological background. According to the result of the present study, a patient with a normal MPRI has a very low probability of having ischemia and maybe therefore MRP could fill in the diagnostic gap in the increasing elderly population with hypertension, hypertrophia and diabetes where shortness of breath may be related to microvascular disease. On the other hand MRP can not differentiate between epicardial or microvascular disease. This limits the application for decisions on treatment strategies and visualization of anatomy seems still necessary to identify atherosclerotic lesions which can be treated with revascularization therapies.

This study demonstrates that MRP compare favorable to either CFR or FFR and may be an attractive alternative to non invasively assess ischemia in patients with chest pain.

Acknowledgement

The authors of this manuscript have certified that they comply with the Principles of Ethical Publishing in the International Journal of Cardiology(8).

Literature

1. Pijls NH, De Bruyne B, Peels K, et al. Measurement of fractional flow reserve to assess the functional severity of coronary-artery stenoses. *N Engl J Med* 1996;334:1703-1708.
2. Uren NG, Melin JA, De Bruyne B, et al. Relation between myocardial blood flow and the severity of coronary-artery stenosis. *N Engl J Med* 1994;330:1782-1788.
3. Nandalur KR, Dwamena BA, Choudhri AF, Nandalur MR, Carlos RC. Diagnostic performance of stress cardiac magnetic resonance imaging in the detection of coronary artery disease: a meta-analysis. *J Am Coll Cardiol* 2007;50:1343-1353.

4. Chamuleau SA, Meuwissen M, van Eck-Smit BL, et al. Fractional flow reserve, absolute and relative coronary blood flow velocity reserve in relation to the results of technetium-99m sestamibi single-photon emission computed tomography in patients with two-vessel coronary artery disease. *J Am Coll Cardiol* 2001;37:1316-1322.
5. Tonino PA, De Bruyne B, Pijls NH, et al. Fractional flow reserve versus angiography for guiding percutaneous coronary intervention. *N Engl J Med* 2009;360:213-224.
6. Kurita T, Sakuma H, Onishi K, et al. Regional myocardial perfusion reserve determined using myocardial perfusion magnetic resonance imaging showed a direct correlation with coronary flow velocity reserve by Doppler flow wire. *Eur Heart J* 2009;30:444-452.
7. Nagel E, Klein C, Paetsch I, et al. Magnetic resonance perfusion measurements for the noninvasive detection of coronary artery disease. *Circulation* 2003;108:432-437.
8. Shewan LG, Coats AJ. Ethics in the authorship and publishing of scientific articles. *Int J Cardiol* 2010; 144: 1-2.

Chapter 6

Non-invasive diagnostic workup of patients with suspected stable angina by computed tomography coronary angiography and magnetic resonance perfusion imaging

Circulation Journal, accepted

Sharon W Kirschbaum^{1,2}

Koen Nieman^{1,2}

Tirza Springeling^{1,2}

Annick C Weustink^{1,2}

Steve Ramcharitar¹

Carlos van Mieghem¹

Alexia Rossi²

Eric Duckers¹

Patrick W. Serruys¹

Eric Boersma¹

Pim J de Feyter^{1,2}

Robert-Jan M van

Geuns^{1,2}.

1. Department of
Cardiology, Erasmus
University Medical
Center, Rotterdam, the
Netherlands

2. Department of
Radiology, Erasmus
University Medical
Center, Rotterdam, the
Netherlands

Abstract

Background To evaluate additional adenosine magnetic resonance perfusion (MRP) in diagnostic work up of patients with suspected stable angina with computed tomography coronary angiography (CTCA) as first in line diagnostic modality.

Methods and Results Two hundred and thirty symptomatic patients (male, 52%; age, 56 year) with suspected stable angina underwent CTCA. In patients with a stenosis of >50% as visually assessed, MRP was performed and quantitative myocardial perfusion reserve index (MPRI) was calculated. CFR using invasive coronary flow measurements served as standard of reference.

CTCA showed non-significant CAD in 151/230 (66%) patients and significant CAD in 79/230 patients (34%), of whom 50 subsequently underwent MRP and CFR. MRP showed reduced perfusion in 32 patients (64%), which was confirmed by CFR in 27 (84%). All 18 normal MRP (36%) were confirmed by CFR. The positive likelihood ratio of MRP for the presence of functional significant disease in patients with a lesion on CTCA was 4.49 (95%CI, 2.12-9.99). The negative likelihood ratio was 0.05 (95% CI, 0.01-0.34).

Conclusions CTCA as first in line diagnostic modality excluded coronary artery disease in a high percentage of patients referred for diagnostic work up of suspected stable angina. MRP had a significant contribution in the detection of functional significant lesions in patients with a positive CTCA.

Introduction

The use of computed tomography coronary angiography (CTCA) in the diagnostic work-up of suspected coronary artery disease (CAD) is rapidly expanding. While CTCA reliably excludes severe CAD, the technique cannot accurately measure the severity of coronary obstructions or assess their hemodynamical importance. Prior studies with invasive coronary angiography^{1,2} have indicated that an anatomical significant lesion does not always equate with functional significance. With the introduction of CTCA this problem has reoccurred as nearly 50% of the significant lesions on CTCA were not functional relevant^{3,4}. Recently adenosine magnetic resonance perfusion (MRP) has emerged as a safe technique to evaluate the functional significance of a stenosis⁵. We hypothesized that MRP can identify which patients with an abnormal CTCA require further invasive investigation. We therefore investigated the additive value of MRP in symptomatic patients where CTCA was applied as a first in line diagnostic tool and additional testing was indicated, using invasive coronary flow reserve (CFR) as standard of reference.

Methods

Study population.

Between September 2007 and February 2009 CTCA was part of the routine work-up of patients with stable chest complaints and suspected CAD. During this period most patients with a visually estimated obstruction of $\geq 50\%$ in at least one coronary vessel on CTCA were referred for coronary angiography at the discretion of the physician using the information of patient history, risk factors and additional non-invasive stress testing if performed. All referred consecutive patients were approached to undergo MRP and CFR measurements during invasive coronary angiography using a flow wire (Vulcano, Zaventem, Belgium). The pre-test probability for obstructive CAD was estimated using the Diamond and Forrester score based on the type of chest discomfort, age and gender, regarding $<20\%$ as low, 21-80% as intermediate, and $>80\%$ as high probability⁶. Exclusion criteria were (1) previous myocardial infarction, (2) previous percutaneous coronary intervention or coronary artery bypass grafting, (3) contraindications for magnetic resonance imaging (MRI), (4) possible pregnancy and/or breast feeding, (5) inability to breath hold for up to 15 seconds, (6) inability to

give reliable informed consent, (7) known claustrophobia, (8) unstable coronary artery disease, (9) known allergy to contrast material; (10) renal insufficiency with glomerular filtration rate of <60 ml/min/1,73 m²; (11) chronic obstructive pulmonary disease; (12) persistent arrhythmias. The institutional review board of the Erasmus Medical Centre in Rotterdam approved the study and all participating patients gave written informed consent.

CTCA

CTCA was performed with a 64-slice dual-source CTCA scanner (Siemens Definition, Forchheim, Germany). A 80-100 ml bolus of iopromide (Ultravist 370 mg/ml, Schering, AG, Berlin, Germany) was injected at a rate of 5.0-5.5 ml/s, followed by a 40 ml saline bolus chaser at an identical injection rate. Data acquisition was synchronized with contrast enhancement of the coronary arteries by means of a bolus tracking technique. A spiral CTCA scan was performed with the following parameters: tube voltage 120 kV, nominal tube current 380-412 mA/rot, rotation time 330ms, temporal resolution 83 ms, variable table feed of 0.20-0.34 depending on the heart rate, collimation 32 x 0.6 mm with double Z-axis sampling resulting in a 64-slice acquisition. Prospectively electrocardiogram-triggered tube modulation with selective tube output during the desired cardiac phase, mid-diastolic for heart rates <65 min and from end-systolic to mid-diastolic for higher heart rates, was used to reduce the radiation dose. The mean radiation dose was 13.4 ± 3.4 mSv, including preparation scans. The scan time varies between 5 and 10 seconds, depending on the table feed. All patients received nitroglycerin (0.4 mg/dose) sublingually, before scanning, no additional beta-blockers were used. The average heart rate during acquisition was 66 ± 12 min⁻¹. Using retrospective electrocardiogram-gating, 0.75-mm slices were reconstructed at 0.4-mm intervals during mid-diastole and/or end-systole depending on the tube modulation protocol, with a medium smooth kernel (B26f).

Axial source, multiplanar reformations and maximum intensity projections were used for qualitative assessment of the coronary arteries. Vessels were qualitatively scored as significantly stenosed ($\geq 50\%$ diameter narrowing) or not significantly stenosed ($<50\%$). Two experienced observers blinded by the MRP, CFR and clinical results of the patients analysed the CTCA based on consensus reading. Borderline lesions were considered significant. Additionally based on left or right dominance, the left ventricular segments (AHA model) were determined as being perfused by either the left or right coronary artery.

Cardiac magnetic resonance perfusion imaging

Scan protocol. A 1.5 Tesla scanner with an eight-element phased-array receiver coil was used for imaging (Signa CV/i, GE Medical systems, Milwaukee, Wisconsin USA). Repeated breath holds and gating to the electrocardiogram were applied to minimize the influence of cardiac and respiratory motion on data collection. Cine MRI was performed using a steady-state free-precession technique (FIESTA). Sequence details have been published before ⁷. To cover the entire ventricle 10-12 cine breath-hold short-axis images were acquired. After rest cine imaging, rest perfusion imaging was performed. During a breath hold, the extra vascular contrast media, gadolinium diethyltriaminepentaacetic acid (Magnevist, Schering, Germany) was injected via the intravenous catheter (0.05 mmol/kg at 3 ml/sec; Medrad). Its first pass was monitored using a presaturation scheme with a notched excitation followed by a segmented gradient echo/ echo-planar read-out with the following imaging parameters; field of view 32-36 x 32-36, rectangular field of view 0.75, repetition time 6.8 ms, echo time 2.0 ms, inversion time 150-175 ms, preparation pulse 90°, time to echo 1.2, train length 4, number of averages 0.75, bandwidth 125 kHz, flip angle 20, matrix 128/96, slice thickness 8 mm. Voxel size was 2,5-2,8 mm vs. 2,5-2,8 mm vs. 8 cm. The temporal resolution per slice of 120 ms allowed imaging of 3-5 slices per R-R interval. Perfusion imaging covered the basal mid and apical part of the left ventricle. Fifteen minutes after rest perfusion vasodilatation was induced by adenosine (140ug/kg/min body weight over 3 minutes) a second bolus of gadolinium diethyltriaminepentaacetic acid was injected via the intravenous catheter (0.05 mmol/kg at 3 ml/sec) and stress first pass perfusion images were acquired using the same pulse sequence and orientations used for rest perfusion. Approximately 10 minutes later delayed enhancement MRI was performed with an inversion recovery gradient echo sequence 10-20 minutes after gadolinium injection. Imaging parameters have been published previously ⁸. Slice locations of the delayed enhancement images were copied from the cine images.

CMR data analysis

All images were transferred to a Microsoft Windows™ based personal computer for analysis (CAAS-MRV, version 3.2.1; Pie Medical Imaging, Maastricht, The Netherlands). Left ventricular volumes and ejection fraction (EF) were analysed using the additional information of the long axis to limit the extent of volume at the base and the apex of the heart ⁷. Papillary muscles and trabeculations were considered as being part of the blood pool volume. A 16-segment model, excluding the apex, was used to analyse the myocardial wall in each patient.

For perfusion analysis mean signal intensity for each myocardial segment was registered over time, displayed as signal intensity–time curves. The maximum upslope of the signal intensity was determined by using 5 consecutive points on the curve, a straight-line model was used for a linear fit of the data. The maximum upslope of the signal intensity of the myocardial segment was divided by the maximum upslope of the signal intensity of the left ventricular cavity. This was calculated during rest and during the hyperaemic phase. The myocardial perfusion reserve index (MPRI) was calculated by division of the corrected upslope of the stress examination by the corresponding segment's corrected upslope value of the rest examination. A MPRI of 2,0 was used to define a functional important stenosis^{9,10}. The MRP scans were evaluated by an experienced observer blinded by the results of CTCA and CFR.

Intracoronary flow wire

All patients underwent ICA through the femoral artery using a 6 or 7 french guiding catheter. After injection of 2 mg isosorbide dinitrate, angiograms of the left and right coronary artery was acquired in multiple projections using standard techniques. In each patient CFR measurements were performed each lesion that appeared significant on CTCA. The intra-coronary flow wire was passed through the catheter to a position distal to the stenosis. Intra-coronary CFR measurements were performed in the resting state and during injection of adenosine (140 ug/kg/min) with continuous monitoring of symptoms, heart rate, blood pressure and electrocardiography. CFR was calculated as the ratio of the hyperaemic average peak velocity divided by the rest average peak velocity. The CFR was determined in an average of two stable consecutive beats at rest and during hyperaemic stress. In this study a significant reduction in CFR was defined as a CFR of less than 2.0 based on previous results¹¹.

All data were analysed in a random order with the investigator blinded to the clinical information and the previous results.

Statistical analysis

Continues variables were expressed as mean \pm standard deviation. Categorical variables were expressed as numbers and percentages. The diagnostic performance of MRP in patients with a positive CTCA for the detection of functional significant CAD as defined by coronary flow reserve is presented as sensitivity, specificity, positive predictive value, negative predictive value with the corre-

sponding 95% confidence intervals (CI), and positive and negative likelihood ratios (LRs) with corresponding 95% CI were calculated. All data analysis was performed with SPSS for Windows 15.0.0 (SPSS Inc., Chicago, Illinois).

Results

Patient cohort and CTCA results

Of the 260 patients with chest pain without a history of cardiovascular disease that visited our out-patient clinic, 230 underwent CTCA, while the others had clinical contraindications for CTCA. For the cohort of patients with CTCA the pre-test likelihood of CAD was low, intermediate and high in 15% (34 of 230), 62% (143 of 230) and 23% (53 of 230), respectively. The median interval between CTCA and CAG was 30 days (25th and 75th percentile, 16-46), without any interventions or events during that period for any of the patients. Baseline patient characteristics are presented in table 1. The average age was higher and male gender and a

Table 1. Patient demographics

| | CTCA \geq 50% N=79 | CTCA<50% N=151 | p-value |
|------------------------------------------|-------------------------|-------------------|---------|
| Age (years) | 62 \pm 7 | 55 \pm 9 | <0.05 |
| Men | 54(68) | 62(41) | <0.05 |
| Risk factors | | | |
| Smoking | 22(29) | 41(27) | 1.00 |
| Diabetes Mellitus | 12(15) | 15(10) | 0.15 |
| Hypertension | 39(49) | 66(44) | 0.72 |
| Hypercholesterolemia | 32(41) | 57(38) | 0.49 |
| Family history of ischemic heart disease | 28(35) | 69(45) | 0.25 |
| Pre test probability of CAD* | | | |
| Low (0-20%) | 11 (14) | 30(19) | 0.18 |
| Intermediate (21-80%) | 51(64) | 103(68) | 0.09 |
| High (81-100%) | 17(22) | 18(12) | <0.05 |

Values are presented as number (%) or mean \pm standard deviation.

CAD, coronary artery disease. *according to the Diamond and Forrester criteria²⁴.

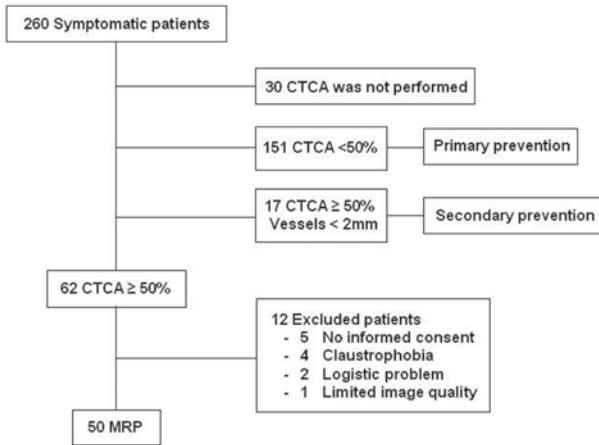


Figure 1. Flow diagram according to the STARD criteria; CTCA, computed tomography coronary angiography; MR, magnetic resonance imaging; CFR, coronary flow reserve.

primary prevention guidelines¹². Further follow-up of these patients was performed by a general practitioner. After 1 year, patients were contacted by telephone by the initial investigators. None of the patients without CAD on CTCA underwent revascularization in this 1 year follow-up period.

In 79 patients, a significant stenosis on CTCA was detected in 118 vessels, in 66 vessels in the left coronary artery, in 25 vessels in the left circumflex and in 27 vessels in the right coronary artery.

Of the 79 patients with significant stenosis on CTCA, 17 were not referred for CAG because all these patients had small vessel disease (visual estimated vessel diameter of < 2 mm) on CTCA and secondary prevention was started. Of the 62 patients referred for CAG after CTCA, 50 patients consented, and participated in this study and underwent CMR. Of the remainder, 4

high pre test probability was more prevalent in the patient group with significant CAD on CTCA.

CTCA showed no significant lesion in 151 (66%) patients and a significant lesion in 79 patients (34%). In patients without a lesion on CTCA life style changes were advised and medical therapy initiated following primary

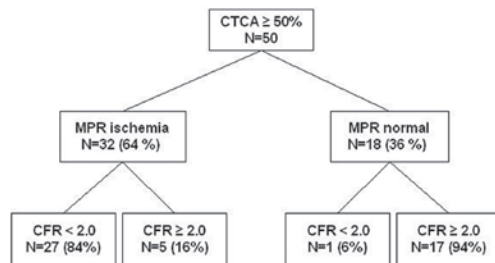


Figure 2. Flow chart describing the relationship between computed tomography coronary angiography (CTCA) adenosis magnetic resonance perfusion (MRP) and coronary flow reserve (CFR). This flow chart illustrates the additional value for MRP in patients with obstructive coronary artery disease on CTCA.

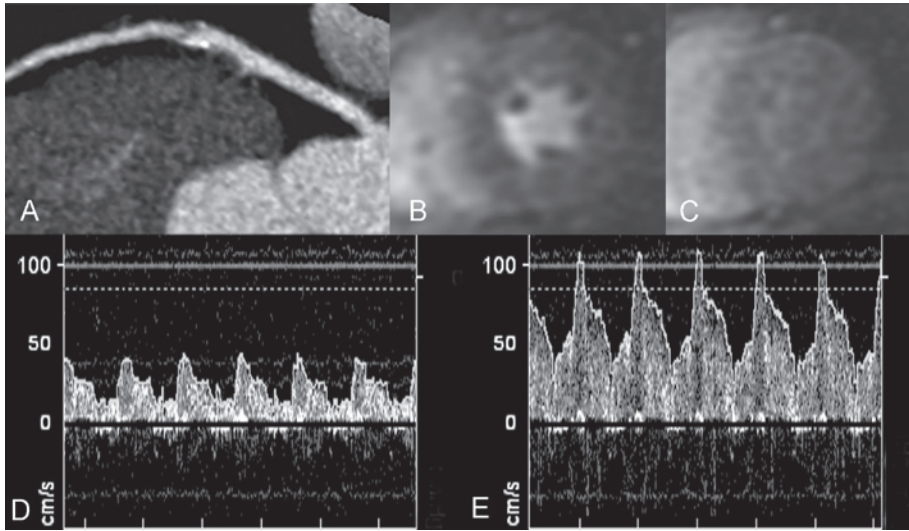


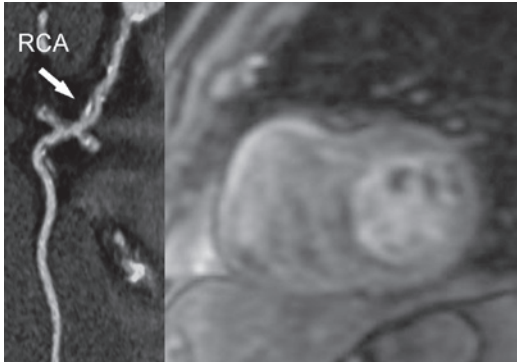
Figure 3. In the left upper corner (A) a CTCA image was shown with a significant lesion of the mid-LAD; (B, C) MR perfusion image during adenosine stress (B) and during rest (C) with normal perfusion of the myocardium in the perfusion territory of the LAD, the MPRI in this region was 2.3. In the bottom of the figure is a CFR image of the flow during rest (D, on the left side) and during adenosine stress (E, on the right side). The CFR in this patient was 2.6.

had contraindications to MRI (all claustrophobic), 5 refused to be enrolled, in 1 patient the MPRI could not be determined because of the limited image quality due to triggering problems and two patients could not be enrolled due to logistic reasons (figure 1). Despite the fact that none had a known history of myocardial infarction, five patients showed delayed myocardial enhancement suggestive of prior ischemic injury. None of these infarcts were in the region of the vessel with a stenosis on CTCA and thus did not influence the MPRI.

Diagnostic performance of MRP

Mean left ventricular ejection fraction was $64 \pm 6\%$, end-diastolic volume index was $80 \pm 16 \text{ ml/m}^2$, end-systolic volume index was $29 \pm 9 \text{ ml/m}^2$. In 17 (34%) patients MRP correctly ruled out functional significant CAD, i.e. the CFR was ≥ 2 (figure 2 and 3). In 1 patient MRP showed no significant perfusion defect while CFR was < 2.0 . Of the patients with a positive MRP scan ($n=32$), 27 patients had a $\text{CFR} < 2$, indicating coronary insufficiency. For five patients with a perfusion deficit on MRP the CFR was within normal limits (Figure 4).

Pre-test probability of a reduced CFR in patients with a positive CTCA was 54% (27/50). The post test probability after MRP was 84%. The positive likelihood ratio for the presence of functional significant disease was 4.49 (95%CI, 2.12-9.99). The negative likelihood ratio was 0.05 (95% CI, 0.01-0.34). Sensitivity, specificity, positive and negative predictive value for MRP for the detection of a reduced



CFR in patients with a positive CTCA scan were 96%(79-99), 78%(61-95), 84%(71-98) and 95%(72-99).

Figure 4. Patient with a significant lesion in the RCA on CTCA (left) and a perfusion defect in the inferoseptal wall on MRP (right), the CFR in this patient was 1.9.

Discussion

We demonstrated that in patients referred for evaluation of chest pain suspected for CAD an initial normal CTCA occurred in the majority (66%) of the patients, ruling out obstructive coronary artery disease in a fast and reliable manner. In the patients with an abnormal CTCA scan MRP correctly excluded the presence of a functionally significant lesion in 34% of the patients, thereby avoiding referral for invasive coronary evaluation. An abnormal MRP resulted in an increase of the presence of functional significant coronary artery disease from 54% to 84% with an positive likelihood ratio of 4.49.

CTCA as first line diagnostic test

Whether CTCA or functional testing should be employed first in patients with chest pain is still under investigation. In this study MRP was added to CTCA, which served as the first in line diagnostic modality. Argument in favour of CTCA is the high negative predictive value which allows reliable exclusion of disease with excellent long-term outcome¹³. At the current time few medical centers have the facilities or resources to perform MRP on a routine basis and MRP is a complex technique not very suited as a first in line test in a general population as it takes almost an hour for an experienced team to acquired a full protocol

including stress and rest perfusion imaging, functional imaging and delayed enhancement. Also post processing for quantitative analysis can be cumbersome and the associated costs currently inhibit the widespread use of MRP as a first in line diagnostic test. CTCA is a faster test, with interpretable results in nearly all patients it is less expensive as compared to MRP and a strategy based on CTCA first is further enforced as faster scanners with lower radiation dose are now available .

MRP as functional test

Magnetic resonance imaging is one of several imaging techniques available to detect inducible myocardial hypoperfusion ¹⁴, which includes, single photon emission computed tomography (SPECT), positron emission tomography (PET) or echocardiography. Advantages of MRP are the high spatial resolution, the absence of ionising radiation, the absent need for an acoustic window, the possibility to combine the stress-test with sensitive infarct imaging and reproducible evaluation of ventricular function. Also a normal MRP is associated with an excellent long term survival ¹⁵. MRP, as for most non-invasive perfusion imaging techniques provides information about the blood supply to the myocardium, which is affected by epicardial and microvasculature disease. Microvascular perfusion can be reduced in patients with hypertension ¹⁶, diabetes ¹⁷ or obesity ¹⁸ which also may cause chest pain. Based on this knowledge we compared non-invasive MRP to invasive CFR measurements, which is similarly affected by both the epicardial vessels as well as the microvasculature.

Combined use of CTCA and MRP

Our study confirmed the acknowledged long known poor correlation between anatomy and function in particular for stenoses of intermediate severity ^{1,2}. Despite the presence of obstructive CAD on CTCA, 36% showed no inducible perfusion abnormality on MRP, and 47% had a normal CFR. Poor correlation between anatomy and function has similarly been demonstrated for CFR or FFR versus QCA ¹⁹, as well as SPECT and FFR versus CTCA ^{3, 11, 20} and recently of CTCA was compared with MRP ²¹. In this study of van Werkhoven et al. a normal perfusion was observed in 33% of the patients with significant obstructive CAD on CTCA. Furthermore comparing CTCA with invasive fractional flow reserve measurements demonstrated that a significant lesion on CTCA was not functionally relevant in approximately 50% of the patients ³, also in our population no functionally significant lesion was detected in 45% of patients with significant obstruc-

tive CAD on CTCA. Based on this knowledge revascularization decisions have to be based both on anatomical and functional information. Using the combined approach 27 of 32 (84%) patients with a positive CTCA and MRP were confirmed by the reference standard, which is a post test probability sufficient to warrant invasive coronary angiography. A negative rule out could be obtained in 151 of 230 (66%) patients with one test and 22 (10%) underwent both tests without having functional coronary artery disease. These numbers strongly support the proposed algorithm with CTCA as first in line diagnostic test followed by MRP in patients with a positive CTCA. This strategy has to be confirmed with larger studies with longer follow-up and cost-effectiveness analysis.

Study limitations

This study has limitations. First, in patients with a negative CTCA scan MRP was not performed. However, it is known that patients with suspected CAD and no or minimal coronary arteriosclerosis on CTCA may be safely deferred^{22,23}. Also we did not observe any revascularization in patients where CTCA was negative. A second limitation was that in 17 patients with a positive CTCA the routine clinical workup did not support invasive analysis because of small vessel disease and could therefore not be part of this study. None of these patients did have major cardiac events or invasive test during 12 months follow-up, confirming the original conservative strategy of the treating physician.

Conclusion

Given the previously discussed findings and the consistently high negative predictive value from CTCA in different patient populations we can conclude that in patients with chest pain suspected for CAD a combined approach using anatomy and a function may best identify the patients who will most likely benefit from further invasive coronary angiography, in a fast and effective manner.

References

1. Tobis J, Azarbal B, Slavin L. Assessment of intermediate severity coronary lesions in the catheterization laboratory. *Journal of the American College of Cardiology*. 2007; 49: 839-848.
2. White CW, Wright CB, Doty DB, Hiratza LF, Eastham CL, Harrison DG, et al. Does visual interpretation of the coronary arteriogram predict the physiologic importance of a coronary stenosis? *The New England journal of medicine*. 1984; 310: 819-824.
3. Meijboom WB, Van Mieghem CA, van Pelt N, Weustink A, Pugliese F, Mollet NR, et al. Comprehensive assessment of coronary artery stenoses: computed tomography coronary angiography versus conventional coronary angiography and correlation with fractional flow reserve in patients with stable angina. *Journal of the American College of Cardiology*. 2008; 52: 636-643.
4. Schuijf JD, Wijns W, Jukema JW, Atsma DE, de Roos A, Lamb HJ, et al. Relationship between noninvasive coronary angiography with multi-slice computed tomography and myocardial perfusion imaging. *Journal of the American College of Cardiology*. 2006; 48: 2508-2514.
5. Karamitsos TD, Arnold JR, Pegg TJ, Cheng AS, van Gaal WJ, Francis JM, et al. Tolerance and safety of adenosine stress perfusion cardiovascular magnetic resonance imaging in patients with severe coronary artery disease. *The international journal of cardiovascular imaging*. 2009; 25: 277-283.
6. Gibbons RJ, Balady GJ, Bricker JT, Chaitman BR, Fletcher GF, Froelicher VF, et al. ACC/AHA 2002 guideline update for exercise testing: summary article. A report of the American College of Cardiology/American Heart Association Task Force on Practice Guidelines (Committee to Update the 1997 Exercise Testing Guidelines). *Journal of the American College of Cardiology*. 2002; 40: 1531-1540.
7. Kirschbaum SW, Baks T, Gronenschild EH, Aben JP, Weustink AC, Wielopolski PA, et al. Addition of the long-axis information to short-axis contours reduces interstudy variability of left-ventricular analysis in cardiac magnetic resonance studies. *Invest Radiol*. 2008; 43: 1-6.
8. Kirschbaum SW, Baks T, van den Ent M, Sianos G, Krestin GP, Serruys PW, et al. Evaluation of left ventricular function three years after percutaneous recanalization of chronic total coronary occlusions. *The American journal of cardiology*. 2008; 101: 179-185.
9. Costa MA, Shoemaker S, Futamatsu H, Klassen C, Angiolillo DJ, Nguyen M, et al. Quantitative magnetic resonance perfusion imaging detects anatomic and physiologic coronary artery disease as measured by coronary angiography and fractional flow reserve. *Journal of the American College of Cardiology*. 2007; 50: 514-522.
10. Futamatsu H, Wilke N, Klassen C, Shoemaker S, Angiolillo DJ, Siuciak A, et al. Evaluation of cardiac magnetic resonance imaging parameters to detect anatomically and hemodynamically significant coronary artery disease. *American heart journal*. 2007; 154: 298-305.

11. Uren NG, Melin JA, De Bruyne B, Wijns W, Baudhuin T, Camici PG. Relation between myocardial blood flow and the severity of coronary-artery stenosis. *The New England journal of medicine*. 1994; 330: 1782-1788.
12. Graham I, Atar D, Borch-Johnsen K, Boysen G, Burell G, Cifkova R, et al. European guidelines on cardiovascular disease prevention in clinical practice: full text. Fourth Joint Task Force of the European Society of Cardiology and other societies on cardiovascular disease prevention in clinical practice (constituted by representatives of nine societies and by invited experts). *Eur J Cardiovasc Prev Rehabil*. 2007; 14 Suppl 2: S1-113.
13. Ostrom MP, Gopal A, Ahmadi N, Nasir K, Yang E, Kakadiaris I, et al. Mortality incidence and the severity of coronary atherosclerosis assessed by computed tomography angiography. *Journal of the American College of Cardiology*. 2008; 52: 1335-1343.
14. Schwitter J, Wacker CM, van Rossum AC, Lombardi M, Al-Saadi N, Ahlstrom H, et al. MR-IMPACT: comparison of perfusion-cardiac magnetic resonance with single-photon emission computed tomography for the detection of coronary artery disease in a multicentre, multivendor, randomized trial. *European heart journal*. 2008; 29: 480-489.
15. Jahnke C, Nagel E, Gebker R, Kokocinski T, Kelle S, Manka R, et al. Prognostic value of cardiac magnetic resonance stress tests: adenosine stress perfusion and dobutamine stress wall motion imaging. *Circulation*. 2007; 115: 1769-1776.
16. Rodriguez-Porcel M, Zhu XY, Chade AR, Amores-Arriaga B, Caplice NM, Ritman EL, et al. Functional and structural remodeling of the myocardial microvasculature in early experimental hypertension. *American journal of physiology*. 2006; 290: H978-984.
17. Iltis I, Kober F, Dalmaso C, Cozzone PJ, Bernard M. Noninvasive characterization of myocardial blood flow in diabetic, hypertensive, and diabetic-hypertensive rats using spin-labeling MRI. *Microcirculation*. 2005; 12: 607-614.
18. de Jongh RT, Serne EH, RG IJ, de Vries G, Stehouwer CD. Impaired microvascular function in obesity: implications for obesity-associated microangiopathy, hypertension, and insulin resistance. *Circulation*. 2004; 109: 2529-2535.
19. Pijls NH, De Bruyne B, Peels K, Van Der Voort PH, Bonnier HJ, Bartunek JKJJ, et al. Measurement of fractional flow reserve to assess the functional severity of coronary-artery stenoses. *The New England journal of medicine*. 1996; 334: 1703-1708.
20. Doucette JW, Corl PD, Payne HM, Flynn AE, Goto M, Nassi M, et al. Validation of a Doppler guide wire for intravascular measurement of coronary artery flow velocity. *Circulation*. 1992; 85: 1899-1911.
21. Van Werkhoven JM, Heijenbrok MW, Schuijf JD, Jukema JW, Van der Wall EE, Schreur JH, et al. Combined Non-Invasive Anatomic and Functional assessment with MSCT and MRI for the Detection of Significant Coronary Artery Disease in Patients with an Intermediate Pre-Test Likelihood. *Heart (British Cardiac Society)*. 2009;

22. Gilard M, Le Gal G, Cornily JC, Vinsonneau U, Joret C, Pennec PY, et al. Midterm prognosis of patients with suspected coronary artery disease and normal multislice computed tomographic findings: a prospective management outcome study. *Archives of internal medicine*. 2007; 167: 1686-1689.
23. Min JK, Shaw LJ, Devereux RB, Okin PM, Weinsaft JW, Russo DJ, et al. Prognostic value of multidetector coronary computed tomographic angiography for prediction of all-cause mortality. *Journal of the American College of Cardiology*. 2007; 50: 1161-1170.
24. Diamond GA, Forrester JS. Analysis of probability as an aid in the clinical diagnosis of coronary-artery disease. *The New England journal of medicine*. 1979; 300: 1350-1358.

Chapter 7

Contractile reserve in segments with non-transmural infarction in chronic dysfunctional myocardium using low dose dobutamine CMR

Journal of the american college of cardiology
Cardiovasc Imaging. 2010 Jun;3(6):614-22

Sharon W Kirschbaum^{1,2}
Alexia Rossi MD²
Ron T van Domburg¹
Katerina Gruszczynska²
Gabriel P. Krestin²
Patrick W Serruys¹
Dirk J Duncker¹
Pim J de Feyter^{1,2}
Robert-Jan M van
Geuns^{1,2}

1. Department of
Cardiology, Erasmus
University Medical
Center, Rotterdam, the
Netherlands

2. Department of
Radiology, Erasmus
University Medical
Center, Rotterdam, the
Netherlands

Abstract

Objectives To quantify contractile reserve of chronic dysfunctional myocardium in particular in segments with intermediate (25% to 75%) transmural extent of infarction (TEI), using low dose dobutamine magnetic resonance imaging (MRI) in patients with a chronic total coronary occlusion (CTO).

Background Recovery of dysfunctional segments with intermediate TEI after PCI is variable and difficult to predict and may be related to contractility of the unenhanced rim.

Methods Fifty-one patients (mean age 60 ± 9 , 76% male) with a CTO underwent MRI at baseline and 35 patients at follow-up to quantify segmental wall thickening (SWT) at rest and during 5 and 10-mcg/kg/min dobutamine and at follow-up. Delayed-enhancement MRI was performed to quantify TEI. Dysfunctional segments were stratified according to TEI, end diastolic wall thickness (EDWT) or unenhanced rim thickness and SWT was quantified. Segments with an intermediate TEI were further stratified according to baseline SWT of the unenhanced rim (SWT_{UR}) (<45% and >45%) and SWT was quantified. For each parameter odds ratio and diagnostic performance for the prediction of contractile reserve was calculated.

Results Significant contractile reserve was present in dysfunctional segments with EDWT >6 mm, unenhanced rim thickness >3 mm or TEI of <25%, only TEI had significant relation with contractile reserve (OR 0.98; 95%CI 0.96-0.99; $p=0.02$). In segments with intermediate TEI ($n=58$) mean SWT did not improve significantly. However segments with SWT_{UR} <45% showed contractile reserve and improved at follow-up while segments with SWT_{UR} >45% were unchanged. SWT_{UR} had a significant relation with contractile reserve (OR 0.98; 95%CI 0.97-0.99; $p=0.02$).

Conclusions MR quantification of transmural extent of infarcted myocardium allows to assess the potential of dysfunctional segments to improve in function during dobutamine of most segments. However in segments with intermediate TEI, measurement of baseline contractility of the epicardial rim better identifies which segments maintain contractile reserve.

Introduction

Chronic dysfunctional myocardium can result either from previous myocardial infarction or from hibernating myocardium due to an obstructive atherosclerotic lesion (1). Contrast enhanced magnetic resonance imaging (MRI) can identify infarcted myocardium. In patients with chronic dysfunctional myocardium the likelihood of recovery of segments without infarction is high while segments with complete transmural infarction do not recover after revascularization. However, the likelihood of recovery after revascularization of segments with transmural extent of infarction (TEI) between 25-75% is highly variable (2,3). Contractile reserve using low dose dobutamine can also be used to predict recovery of function after revascularization (4-9) and is described to be a useful addition to delayed enhancement MRI (10). Surprisingly the relation between quantitative contractile reserve and TEI in patients with chronic dysfunctional myocardium has not been investigated thus far.

In this study we quantified contractile reserve in myocardial segments stratified according to (i) the TEI, (ii) end-diastolic wall thickness (EDWT) and (iii) thickness of the unenhanced rim in patients with chronic dysfunctional myocardium due to a chronic total occlusion (CTO) during low dose dobutamine and compared this with SWT at follow-up. We paid particular attention to the evaluation of segments with an intermediate transmural extent of infarction between 25-75%. In this group we investigated the influence of baseline contractility of the epicardial viable rim on contractile reserve and improvement in function after revascularization of the total segment.

Methods

Patient population

Seventy patients with a CTO who were referred for percutaneous coronary intervention were prospectively recruited for enrolment in this study. Eight patients (11%) refused to participate. A CTO was classified as a complete occlusion for more than 3 months as obtained from either the clinical history of prolonged anginal chest pain or myocardial infarction or the date of the diagnostic angiogram before revascularization. Exclusion criteria were acute myocardial infarction within the last three months; atrial fibrillation; inability to lie flat; and contraindications for magnetic resonance studies. In 11 patients (16%) MRI could not be successfully completed, due to claustrophobia (n=8), obesity (n=2), and allergic re-

Table 1. Baseline patient characteristics (n=51)

| | |
|--------------------------------|---------|
| Age (years) | 60±9 |
| Men | 39 (76) |
| Smoking | 10 (20) |
| Diabetes Mellitus | 10 (20) |
| Hypertension | 29 (57) |
| Hypercholesterolemia | 39 (76) |
| Family history | 23 (45) |
| Baseline Ejection fraction (%) | 50±11 |
| ACE inhibitor | 17 (33) |
| β - Blocker | 44 (86) |
| Statin | 42 (82) |
| ASA | 44(86) |

Values are presented as number (%) or mean ± standard deviation.
ACE= angiotensin-converting enzyme; ASA= acetylsalicylic acid.

action to the contrast agent (n=1). Ultimately, 51 patients were studied. Of these patients 78% had a positive exercise test the remaining 22% had progressive anginal symptoms. Of those 51 patients, 35 patients underwent successful revascularization of their CTO followed by a second MRI-scan at 6,2±0,5 months after the procedure. Baseline parameters of all 51 patients are presented in table 1.

The institutional review board of the Erasmus Medical Center approved the study and all patients gave written informed consent.

MRI-protocol

MR images were acquired using a 1.5 Tesla scanner with a eight-element cardiac phased-array receiver coil placed over the thorax (Signa CV/i, GE Medical systems, Milwaukee, Wisconsin USA). Cine MRI was performed using a steady-state free-precession technique (FIESTA). Imaging parameters were; field of view 36-40 x 28-32 cm; matrix size was 224 x 196; repetition time, 3.4 ms; echo time, 1.5 ms; flip angle, 45 degrees; 12 views per segment and slice thickness was 8.0 mm with a 2.0 mm slice gap. The two- and four-chamber end diastolic images at end expiration provided the reference images to obtain 10-12 cine breath-hold short-axis images to cover the entire left ventricle.

Dobutamine was infused at 5 and 10-mcg/kg/min for 5 minutes at each dosage using an intravenous catheter, which was placed in the antecubital vein. Functional imaging was repeated using the same long-axis imaging planes as at rest. For the short axis we used 3 slices; basal, mid-ventricular and apical. During the test the patients were monitored using continuous ECG leads and blood pressure was measured every 3 minutes.

Delayed enhancement imaging was performed with a gated breath hold T1 weighted-inversion recovery gradient-echo sequence 20 minutes after infusion of Gadoliniumdiethyltriaminepentaacetic acid (0.2 mmol/kg intravenously, Magnevist, Schering, Germany). Imaging parameters were; repetition time 6.3, echo time 1.5, flip angle 20°, inversion pulse of 180°, matrix 192 x 160, number of averages 1-2, inversion time 180-280 ms (adjusted to null the signal of the remote myocardium). The slice locations of the delayed enhanced images were copied from the cine-images.

Definitions and data analysis

The images were analysed using the CAAS-MRV program (version 3.1; Pie Medical Imaging, Maastricht, The Netherlands). Papillary muscles and trabeculations were considered as being part of the blood pool volume. A 16 segment-model, excluding the apex, was used to analyse the myocardial wall in each patient (11). Segmental wall thickening of the full wall (SWT_{FW}) was assessed quantitatively at rest, during 5 - and 10-mcg/kg/min dobutamine and at follow-up and was con-

sidered dysfunctional if wall thickening was less than 45% (12). Contractile reserve was present if SWT_{FW} increased $>10\%$ after administration of either 5 or 10 mcg/kg/min dobutamine. SWT_{FW} was analyzed in dysfunctional segments in the perfusion territory of a CTO before and $6,2\pm 0,5$ months after revascularization. Segments were stratified according to TEI, end diastolic wall thickness (EDWT) and the thickness of the unenhanced rim and SWT_{FW} was determined according to these parameters for each segment. The diagnostic angiogram was visually scored by two experience observers. The place of occlusion and left or right

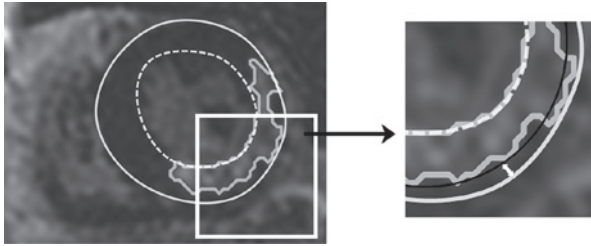


Figure 1. Unenhanced rim. Example of the epicardial viable unenhanced rim, which was defined as the mean wall thickness (mm) of the unenhanced area of a segment. The unenhanced rim was calculated using the following formula $((100 - \text{hyperenhanced area}) * \text{EDWT}) / 100$. The functionality of the epicardial viable unenhanced rim was related to the outcome parameter.

$<25\%$, $25-50\%$, $50-75\%$ and $>75\%$ infarct transmuralty per segment. EDWT was divided into 3 groups; <6 mm (6), $6-8$ mm and >8 mm. The thickness of the unenhanced rim (figure 1) was defined as the mean wall thickness of the non-enhanced area of a segment and was also divided into 3 groups; <3 mm (13), $3-6$ mm, and >6 mm. Segmental wall thickening of only the unenhanced rim (SWT_{UR}) was measured quantitatively in segments with an intermediate TEI (between $25-75\%$) and divided into two groups: dysfunctional (SWT_{UR} : $<45\%$) and normokinetic (SWT_{UR} : $>45\%$). For SWT_{UR} the increase in wall thickness in the end systolic phase as compared to the end diastolic phase was assigned to the thickness of the unenhanced rim as we assume that scar tissue does not contract and expressed as a percentage of the unenhanced rim (figure 2).

Statistical analysis

Data are presented as mean \pm standard deviation. Dysfunctional segments were either stratified into the TEI, or the EDWT or the thickness of the unenhanced rim. To investigate the differences of SWT during rest, dobutamine and follow-up for

dominance was established and the LV segments were correlated to vessel anatomy. The TEI was analyzed quantitatively by dividing the hyper enhanced area using computer assisted tracings by the total area in each segment and expressed as a percentage. TEI was divided into 4 groups;

TEI, EDWT and the unenhanced rim, variance analysis with repeated measurements was used. Post hoc analysis was performed using Tukey student range method. The change in hemodynamic parameters during infusion of dobutamine and the contractile reserve in dysfunctional segments with an intermediate extent of infarction were also tested using analysis of variance followed by Tukey student range method. To investigate whether these parameters were related with dobutamine, multivariable logistic regression analyses were used. All analyses were adjusted for demographics (age, gender, BMI), clinical factors (hypertension, diabetes, hypercholesterolemia, smoking, family history of cardiac disease) and medications (beta-blocker, aspirin, ACE-inhibitor and statin). The goodness of fit of the model was calculated by the chi-square test. Interaction

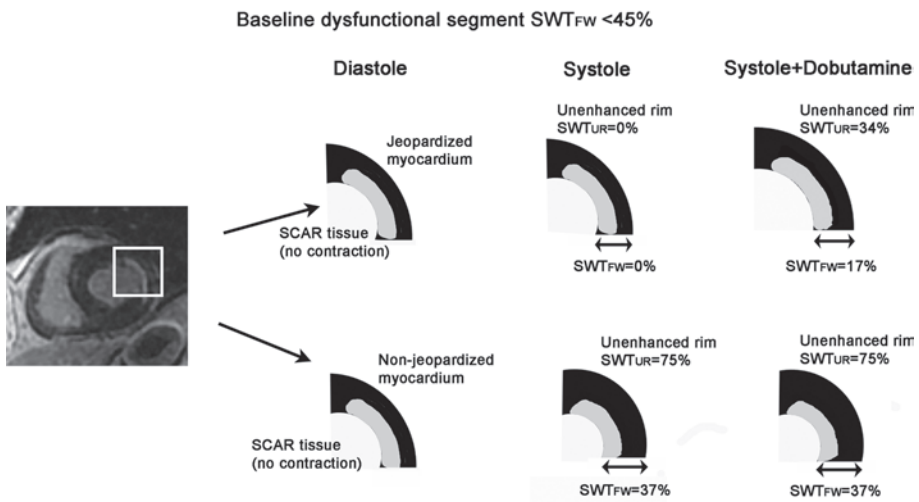


Figure 2. Theoretical model. In dysfunctional segments with a TEI of 50% SWTFW improves during dobutamine if jeopardized dysfunctional myocardium is present (upper row) and thus if SWTur is <45%. In this situation we may expect a benefit of revascularization on myocardial function. SWTFW will not improve during dobutamine if SWTur is normokinetic (lower row) and thus no jeopardized myocardium is present. In this situation we may expect no benefit of revascularization on myocardial function. We assume that infarct tissue does not contract.

terms were included in the models to investigate confounding between these parameters. The Area under the Receiver Operator Curve (AUROC) was calculated and the diagnostic performance for EDWT (cut-off 6 mm (6)), TEI (cut-off 50% (3)), unenhanced rim thickness (cut-off 3 mm (13)) and SWTur (cut-off 45%) to predict the presence of contractile reserve were calculated. All data analysis was performed with SPSS for Windows 15.0.0 (SPSS Inc., Chicago, Illinois).

Results

Patient population

In 22 (43%) patients the CTO was located in the left anterior descending coronary artery, in 9 (18%) patients in the left circumflex coronary artery and in 20 (39%) patients in the right coronary artery. Of the 51 patients that were included in the study, 45 (88%) patients had an infarct of which 43 (84%) patients in the perfusion territory of the CTO. All images were of sufficient quality for analysis. Administration of dobutamine was well tolerated by all patients, no serious side effects occurred. All hemodynamic parameters that were measured increased slightly but consistently during infusion of dobutamine (table 2). Of those 51 patients 35 patients underwent successful revascularization of their CTO, 16 (46%) of the left anterior descending coronary artery, in 7 (20%) patients in the left circumflex coronary artery and in 12 (34%) patients in the right coronary artery these patients underwent a follow-up MRI scan. In one patient new hyper enhancement occurred in the anteroseptal wall. The new infarct mass was 9 gram.

Segmental analysis

Table 2. Hemodynamic data of 51 patients before PCI.

| | Rest | 5 mcg/kg/min dobutamine | 10 mcg/kg/min dobutamine |
|---------------------------|---------|----------------------------|-----------------------------|
| Systolic BP (mm Hg) | 133±19 | 140±20 | 138±17 |
| Diastolic BP (mm Hg) | 76±11 | 73±11 | 72±9 |
| Heart rate (bpm) | 66±10 | 70±10 | 73±11*† |
| Ejection fraction (%) | 50±13 | 57±15* | 60±14*† |
| EDVi (ml/m ²) | 93±26 | 83±29 | 83±27 |
| ESVi (ml/m ²) | 48±24 | 38±24 | 36±23* |
| Cardiac output (l/min) | 5.7±1.0 | 6.1±1.9 | 6.8±1.6 |
| Stroke volume (ml) | 87±22 | 88±32 | 95±26 |

Data are presented as mean±standard deviation

BP = blood pressure

bpm = beats per minute

EDVi = end diastolic volume index

ESVi = end systolic volume index

*p<0.05 vs baseline †p<0.05 vs 5 mcg/kg/min

All segments Two hundred seventy nine segments were in the perfusion territory of the CTO. Mean SWT of all CTO perfused segments (normokinetic + dysfunctional segments) was $36\pm 34\%$ at baseline and increased to $43\pm 41\%$ during 5 mcg/kg/min and $44\pm 42\%$ during 10 mcg/kg/min of dobutamine (both $p < 0.001$ vs. baseline). SWT of remote segments amounted $78\pm 27\%$ at baseline, $71\pm 42\%$ during 5 mcg/kg/min and $82\pm 41\%$ during 10 mcg/kg/min ($p = 0.20$).

Dysfunctional segments Of the CTO perfused segments, 163 segments (60%) were dysfunctional (figure 3). During low dose dobutamine stress, 92 (56%) of the dysfunctional segments at baseline conditions manifested a difference in contractile reserve of more than 10% after 10-mcg/kg/min dobutamine. Mean SWT of all dysfunctional CTO perfused segments increased from $16\pm 19\%$ at baseline to $30\pm 34\%$ during 5-mcg/kg/min dobutamine and to $31\pm 34\%$ during 10-mcg/kg/min dobutamine (both $p < 0.0001$ vs. baseline).

Contractile reserve in dysfunctional segments and SWT at follow-up

Segments were stratified using 3 parameters; TEI, the EDWT or the thickness of

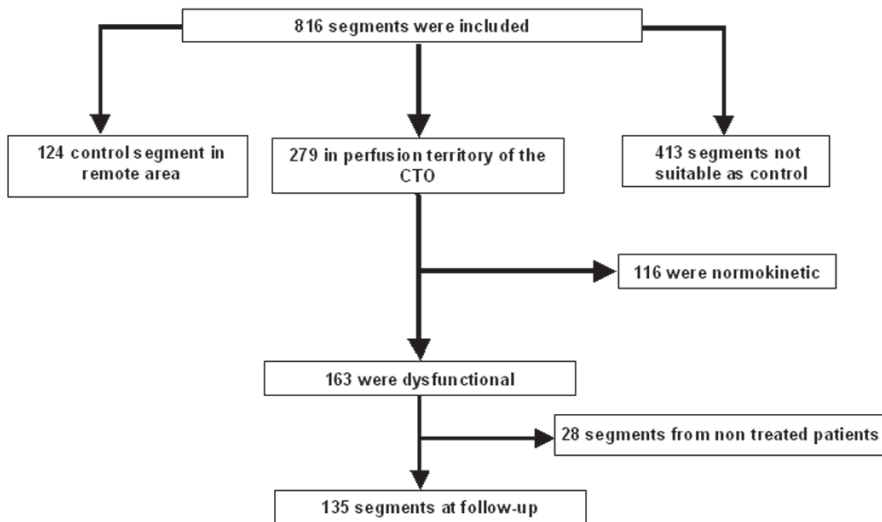


Figure 3. Flow of segments through the study. To better describe the flow of segments through the study we present this figure. Twenty percent (163/819) of the segments that were included were dysfunctional and contractile reserve was determined. Eighty three percent (135/163) of these dysfunctional segments were reperfused. TEI, transmural extent of infarction; CTO, chronic total occlusion.

Table 3. Segmental analyses of 51 patients before PCI

| | | N | Rest (%) | 5 mcg/kg/min dobutamine (%) | 10 mcg/kg/min dobutamine (%) |
|------------------------|-------|----|----------|--------------------------------|---------------------------------|
| TEI (%) | <25 | 79 | 19±18 | 36±38* | 33±34* |
| | 25-50 | 48 | 16±19 | 29±29 | 34±30* |
| | 50-75 | 27 | 10±21 | 15±28 | 24±28 |
| | >75 | 9 | 5±12 | 9±13 | 5±20 |
| EDWT (mm) | <6 | 22 | 14±24 | 23±26 | 23±29 |
| | 6-8 | 68 | 16±18 | 35±39* | 33±36* |
| | >8 | 73 | 18±18 | 28±32* | 29±30* |
| Unenhanced rim (mm) | <3 | 28 | 8±14 | 3±15 | 7±18 |
| | 3-6 | 56 | 16±20 | 31±32* | 33±36* |
| | >6 | 79 | 18±18 | 32±36* | 31±32* |
| Remote | | 69 | 78±27 | 71±42 | 82±41*† |

TEI = transmural extent of infarction
EDWT = end diastolic wall thickness

*p<0.05 vs baseline
†p<0.05 vs 5 mcg/kg/min

Table 4. Frequency of segments with contractile reserve

| | | Rest-5 mcg/kg/min dobutamine | Rest-10 mcg/kg/min dobutamine |
|---------------------|-------|---------------------------------|----------------------------------|
| TEI (%) | <25 | 72%(57/79) | 68% (54/79) |
| | 25-50 | 48%(23/48) | 54%(26/48) |
| | 50-75 | 26%(7/27) | 41%(11/27) |
| | >75 | 11% (1/9) | 0% (0/9) |
| EDWT (mm) | <6 | 45% (10/22) | 41% (9/22) |
| | 6-8 | 50% (34/68) | 51% (35/68) |
| | >8 | 62%(45/73) | 66%(48/73) |
| Unenhanced rim (mm) | <3 | 36% (10/28) | 32% (9/28) |
| | 3-6 | 46%(26/56) | 54%(30/56) |
| | >6 | 61%(48/79) | 58%(46/79) |

TEI = transmural extent of infarction
EDWT = end diastolic wall thickness

Table 5 Multivariate logistic regression analysis and the predictive value for the presence of contractile reserve.

| | OR (95%CI) | P-value | Sensitivity (%) | Specificity (%) | PPV (%) | NPV (%) |
|-----------------------------|---------------------|---------|--------------------|--------------------|------------|------------|
| TEI | 0.98 (0.96-0.99) | 0.02 | 85(77-91) | 42(31-56) | 70(62-78) | 53(35-70) |
| Unenhanced rim thickness | 1.13 (0.97-1.32) | 0.12 | 88(79-93) | 27(16-41) | 69(61-77) | 54(34-72) |
| EDWT | 1.00 (0.83-1.23) | 0.93 | 88(79-93) | 16(8-29) | 66(58-74) | 41(21-63) |

Mean values (95% confidence interval); PPV, positive predictive value; NPV, negative predictive value.

the unenhanced rim. For each of these parameters SWT at rest and during infusion of dobutamine was calculated according to the group definition and presented in (table 3). Mean SWT increased significantly during 5mcg/kg/min dobutamine in segments with an EDWT >6 mm, unenhanced rim of >3 mm or if TEI<25%. For segments with TEI between 25-50%, SWT only improved during a higher dose of 10-mcg/kg/min dobutamine. SWT during dobutamine infusion remained significantly lower for all segments in the area distal to the CTO as compared to segments in the remote area. The frequency of segments with contractile reserve is presented in table 4.

Interaction terms between EDWT, TEI and unenhanced rim turned to be far from significant. Multivariate logistic regression analysis including baseline characteristics showed that TEI was the only parameter that could predict contractile reserve (OR 0.98; 95%CI 0.96-0.99; p=0.02 and AUROC of 0.66; 95%CI 0.57-0.75; p=0.001). Unenhanced rim thickness and EDWT could not predict contractile reserve (AUC 0.63; 95% CI 0.54-0.72; p=0.009 and 0.52; 95% CI 0.42-0.61; p=0.74 respectively)(table 5). Adding TEI to the multivariate model including demographic and clinical factors and medication improved the chi square value of the model significantly (from 29 to 34, p<0.01). Sensitivity, specificity, PPV and NPV were given in table 5.

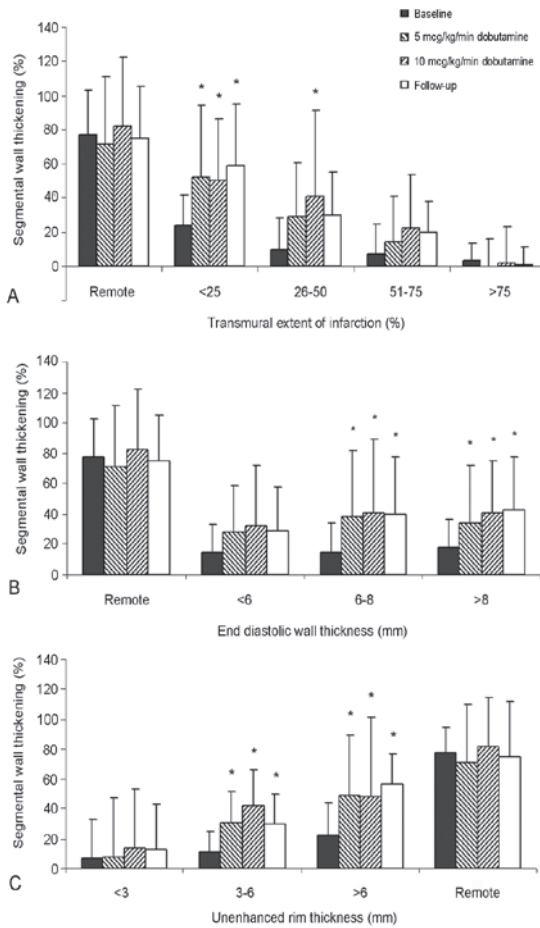


Figure 4. Segmental wall thickening before and after revascularization

Segmental wall thickening before revascularization at rest during 5- and 10-mcg/kg/min dobutamine and at follow-up in segments stratified according to the (a) TEI and (b) EDWT and the (c) thickness of the unenhanced rim. Mean SWT increased significantly during dobutamine and at follow-up in segments with an EDWT >6 mm or and unenhanced rim of >3 mm. For TEI, SWT increased during dobutamine when TEI<50% however segments with a TEI between 25-50% did not increase significantly at follow-up.

*p<0.05 vs. baseline; TEI, transmural extent of infarction; EDWT, end diastolic wall thickness.

In the subgroup of 35 patients that underwent PCI, SWT was calculated before and after PCI according to the same group definition as described above and presented in figure 4abc. SWT before PCI was significantly different as compared to SWT at follow-up. Importantly SWT during dobutamine before revascularization was not statistically different as compared to SWT at follow-up.

Segments with intermediate TEI

In 35 patients that underwent PCI, 58 segments had a TEI between 25-75%. Contractile reserve was present in 71% (41/58) of the segments and 61% (36/58) of the segments improved after revascularization. Of the segments that show contractile reserve (n=41) 34 improved after revascularization (83%). This in contrast to segments without contractile reserve (17/58) where only some of the segments improved at follow-up (2/17; 12%).

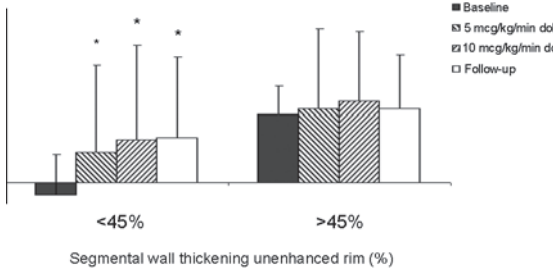


Figure 5. Contractile reserve in segments with an intermediate transmural extent of infarction. In segments with an intermediate transmural extent of infarction (TEI between 25-75%) it is difficult to determine which segment will respond after dobutamine or will improve at follow-up. Therefore we divided the dysfunctional segments (SWT<45%); in this group into SWT_{UR} <45% and SWT_{UR} >45%. Contractile reserve was present in segments with SWT_{UR}<45%. No contractile reserve was present if SWT_{UR} was normal (SWT_{UR} >45%). *p<0.05 vs. baseline; SWT_{UR}, segmental wall thickening unenhanced rim.

To discriminate which of the segments with an intermediate TEI will show contractile reserve and will improve after revascularization we used another parameter, SWT_{UR}. In segments with SWT_{UR} of >45% (n=13) mean SWT_{FW} at rest did not change significantly during 5 mcg/kg/min dobutamine (p=0.66), 10 mcg/kg/min dobutamine (p=0.22) and at follow-up (p=0.44). Seven of the 13 segments (54%) did not show contractile reserve and 69% (9/13) of the segments did not improve after PCI.

In segments with SWT_{UR} <45% (n=45), mean SWT_{FW} at rest increased significantly during 5 mcg/kg/min (p<0.05), 10 mcg/kg/min (p<0.01) and at follow-up (p<0.0001)(figure 5). In contrast to segments with an intermediate TEI and SWT_{UR}>45%, intermediate segments with an SWT_{UR}<45% frequently show contractile reserve (34/45; 74%) and improvement after PCI (31/45; 67%).

Multivariate logistic regression analysis for each viability parameter including baseline characteristics was performed to investigate the importance of all viability parameters. This demonstrated the importance of SWT_{UR} as it was the only parameter in segments with an intermediate TEI with a significant relation with the outcome parameter (OR 0.98; 95%CI 0.97-0.99; p=0.02 and AUROC of 0.70; 95%CI 0.58-0.82; p=0.003) (table 6). Addition of SWT_{UR} to the model improved the chi square value of the model significantly (from 9 to 14, p<0.01). Sensitivity, specificity, PPV and NPV of SWT_{UR} for the prediction of contractile reserve were as follows, 79%(63-89), 52%(33-79), 69%(54-81) and 64%(42-81).

Table 6 Multivariate logistic regression analysis and area under the ROC analysis for segment with an intermediate TEI.

| | OR (95% CI) | P-value | AUROC (95% CI) | P-value |
|--------------------------|-------------------|---------|------------------|---------|
| SWTur | 0.98 (0.97-0.99) | 0.02 | 0.70 (0.58-0.82) | 0.003 |
| EDWT | 0.91 (0.68-1.22) | 0.55 | 0.45 (0.32-0.59) | 0.49 |
| TEI | 0.99 (0.94 -1.03) | 0.56 | 0.51 (0.42-0.69) | 0.40 |
| Unenhanced rim thickness | 0.99 (0.67-1.46) | 0.99 | 0.51 (0.37-0.64) | 0.07 |

TEI = transmural extent of infarction; EDWT = end diastolic wall thickness

SWTur = segmental wall thickening unenhanced rim; AUROC = area under the receiver operator curve.

Discussion

In our study we demonstrated that dysfunctional myocardial segments in the territory of a CTO improved significantly during dobutamine and at follow-up if EDWT>6 mm, TEI<25% or if the thickness of the epicardial unenhanced rim was >3 mm. However only TEI could predict contractile reserve. This study furthermore showed that the functionality of the epicardial viable rim allows refined assessment of contractile reserve and the change in SWT at follow-up for segments with a TEI between 25-75%.

Low dose dobutamine improves cellular energetics and contractile function in hypoperfused myocardium (14). Subsequently the test simulates the effect of revascularization with a high accuracy (15-17), whereas TEI is less accurate for prediction of improvement in function especially in segments with an intermediate extent of infarction(10). Kim et al (2) reported that the likelihood of recovery was inversely related to TEI, yet, the likelihood of recovery following revascularization was less predictable in segments with a TEI between 25-75% and only 25% of the segments recovered after revascularization in this subgroup (2). The number of dysfunctional segments with a TEI of 25-75% is substantial and additional parameters seem necessary for accurate prediction of improvement. The TEI is a relative value that omits the thickness of

a segment. The amount of contractile reserve will probably be less in segments with an EDWT of 3 mm with 50% TEI as compared to a segment with the same infarct transmurality and an EDWT of 8 mm. It may be therefore interesting to measure the thickness of the epicardial viable unenhanced rim. Secondly the amount of rest function of the epicardial-unenhanced rim is important for its contribution to regional wall thickening after revascularization. The relative contribution to SWT_{FW} of restoring function of an akinetic epicardial unenhanced area is more than restoring function of a normal contracting epicardial unenhanced area.

These more complex analyses can easily be assessed by current post processing techniques allow quantification of the CMR images, which provide more refined and accurate assessment of the extent of scar tissue, the extent and functionality of the epicardial viable tissue and the presence of contractile reserve of dysfunctional myocardial segments.

We confirmed findings of other studies, which showed that the presence of a small-unenhanced rim was associated with a higher probability of non-viable tissue as assessed by PET-studies (13,18). In our study the presence of an unenhanced rim thickness of < 3 mm is associated with absence of contractile reserve and absence of change in SWT after PCI.

Furthermore this study shows that if SWT_{UR} is more than 45% in case of intermediate TEI no contractile reserve and no change in SWT after PCI was present. On the other hand if systolic wall thickening was less than 45% in these segments, contractile reserve could be elicited by low dose dobutamine and SWT changed significantly at follow-up. This concept has been further explained and illustrated (figure 2). Theoretically if 50% of a dysfunctional segment ($SWT_{FW} < 45\%$) in the perfusion territory of a CTO is marked by the contrast agent and therefore considered as scar tissue and the remaining 50% of that segments is viable but akinetic or hypokinetic, contractility will increase during dobutamine infusion and SWT will change after PCI. If the remaining non-enhanced part in a segment with the same TEI of 50% is not dysfunctional ($SWT_{UR} > 45\%$), total wall thickening will still be classified as dysfunctional (below 45%) although no contractile reserve and no change in SWT after PCI will be present. This theoretical model assumes that scar tissue does not contract and that therefore the SWT of the segments should be ascribed to the contractility of the unenhanced rim

both at baseline and during low dose dobutamine infusion. Our study provides evidence for the additional value of quantitative determination of rest function of the unenhanced rim to assess the presence of viable tissue.

Study limitations

Due to the limited number of patients we could only perform segmental wise analysis in this paper where interaction between individual segments of a patient can be present.

Conclusion

MR quantification of infarcted myocardium provides precise delineation of the TEI and the unenhanced rim and allows assessing the potential of dysfunctional segments to show contractile reserve. However TEI fails to predict contractile reserve in the intermediate segments, in these segments wall thickening at rest of the unenhanced rim can be used to determine the presence of contractile reserve of the total segment.

References

1. Rahimtoola SH. Chronic myocardial hibernation. *Circulation* 1994;89:1907-8.
2. Kim RJ, Wu E, Rafael A, et al. The use of contrast-enhanced magnetic resonance imaging to identify reversible myocardial dysfunction. *N Engl J Med* 2000;343:1445-53.
3. Kaandorp TA, Bax JJ, Schuijf JD, et al. Head-to-head comparison between contrast-enhanced magnetic resonance imaging and dobutamine magnetic resonance imaging in men with ischemic cardiomyopathy. *Am J Cardiol* 2004;93:1461-4.
4. Dendale P, Franken PR, Holman E, Avenarius J, van der Wall EE, de Roos A. Validation of low-dose dobutamine magnetic resonance imaging for assessment of myocardial viability after infarction by serial imaging. *Am J Cardiol* 1998;82:375-7.
5. Arnese M, Cornel JH, Salustri A, et al. Prediction of improvement of regional left ventricular function after surgical revascularization. A comparison of low-dose dobutamine echocardiography with 201Tl single-photon emission computed tomography. *Circulation* 1995;91:2748-52.
6. Baer FM, Theissen P, Schneider CA, et al. Dobutamine magnetic resonance imaging predicts contractile recovery of chronically dysfunctional myocardium after successful revascularization. *J Am Coll Cardiol* 1998;31:1040-8.

7. Trent RJ, Waiter GD, Hillis GS, McKiddie FI, Redpath TW, Walton S. Dobutamine magnetic resonance imaging as a predictor of myocardial functional recovery after revascularisation. *Heart* 2000;83:40-6.
8. Sandstede JJ, Bertsch G, Beer M, et al. Detection of myocardial viability by low-dose dobutamine Cine MR imaging. *Magn Reson Imaging* 1999;17:1437-43.
9. Bove CM, DiMaria JM, Voros S, Conaway MR, Kramer CM. Dobutamine response and myocardial infarct transmuralty: functional improvement after coronary artery bypass grafting--initial experience. *Radiology* 2006;240:835-41.
10. Wellnhofer E, Olariu A, Klein C, et al. Magnetic resonance low-dose dobutamine test is superior to SCAR quantification for the prediction of functional recovery. *Circulation* 2004;109:2172-4.
11. Cerqueira MD, Weissman NJ, Dilsizian V, et al. Standardized myocardial segmentation and nomenclature for tomographic imaging of the heart: a statement for healthcare professionals from the Cardiac Imaging Committee of the Council on Clinical Cardiology of the American Heart Association. *Circulation* 2002;105:539-42.
12. Holman ER, Buller VG, de Roos A, et al. Detection and quantification of dysfunctional myocardium by magnetic resonance imaging. A new three-dimensional method for quantitative wall-thickening analysis. *Circulation* 1997;95:924-31.
13. Kuhl HP, van der Weerd A, Beek A, Visser F, Hanrath P, van Rossum A. Relation of end-diastolic wall thickness and the residual rim of viable myocardium by magnetic resonance imaging to myocardial viability assessed by fluorine-18 deoxyglucose positron emission tomography. *Am J Cardiol* 2006;97:452-7.
14. Yi KD, Downey HF, Bian X, Fu M, Mallet RT. Dobutamine enhances both contractile function and energy reserves in hypoperfused canine right ventricle. *Am J Physiol Heart Circ Physiol* 2000;279:H2975-85.
15. Nelson C, McCrohon J, Khafagi F, Rose S, Leano R, Marwick TH. Impact of scar thickness on the assessment of viability using dobutamine echocardiography and thallium single-photon emission computed tomography: a comparison with contrast-enhanced magnetic resonance imaging. *J Am Coll Cardiol* 2004;43:1248-56.
16. Sayad DE, Willett DL, Hundley WG, Grayburn PA, Peshock RM. Dobutamine magnetic resonance imaging with myocardial tagging quantitatively predicts improvement in regional function after revascularization. *Am J Cardiol* 1998;82:1149-51, A10.
17. Baer FM, Theissen P, Crnac J, et al. Head to head comparison of dobutamine-transoesophageal echocardiography and dobutamine-magnetic resonance imaging for the prediction of left ventricular functional recovery in patients with chronic coronary artery disease. *Eur Heart J* 2000;21:981-91.
18. Knuesel PR, Nanz D, Wyss C, et al. Characterization of dysfunctional myocardium by positron emission tomography and magnetic resonance: relation to functional outcome after revascularization. *Circulation* 2003;108:1095-100.

Part **4**

Magnetic resonance imaging guided management of ischemic heart disease



Chapter 8

Combining magnetic resonance viability variables better predicts improvement of myocardial function prior to percutaneous coronary intervention

International Journal of Cardiology, accepted

Sharon W. Kirschbaum^{1,2}

Alexia Rossi^{1,2}

Eric Boersma¹

Tirza Springeling^{1,2}

Martin van de Ent¹

Gabriel P Krestin²

Patrick W Serruys¹

Dirk J Duncker¹

Pim J de Feyter^{1,2}

Robert-Jan M van

Geuns^{1,2}

1. Department of
Cardiology, Erasmus
University Medical
Center, Rotterdam, the
Netherlands

2. Department of
Radiology, Erasmus
University Medical
Center, Rotterdam, the
Netherlands

Abstract

Objectives To optimise the predictive value of cardiac magnetic resonance imaging (MRI) for improvement of myocardial dysfunction prior to percutaneous coronary intervention (PCI).

Methods We performed cardiac MRI in 72 patients (male 87%, age 60 year) before and 6 months after successful PCI (43/72) or unsuccessful PCI (29/72) of a chronic total coronary occlusion (CTO). Before PCI, 5 viability parameters were evaluated: transmural extent of infarction (TEI), contractile reserve during dobutamine, end diastolic wall thickness, unenhanced rim thickness and segmental wall thickening of the unenhanced rim (SWTur). Multivariate analysis was performed and based on the regression coefficient (RC) a predictive score was constructed. Diagnostic performance to predict improvement in myocardial function for each parameter and for the viability score was determined.

Results The predictive value of a combination of contractile reserve, SWTur and TEI was incremental to TEI alone (AUROC 0.91 vs. 0.77; $p < 0.001$). A viability score of ≥ 5 based on contractile reserve (RC=4), SWTur (RC=1) and TEI (RC=2) was 91% sensitive and 84% specific in predicting improvement of myocardial function.

Conclusion Combining viability parameters results in a better prediction of improvement of dysfunctional myocardial segments after successful PCI.

Introduction

Myocardial dysfunction is frequently due to coronary artery stenosis in the western world. This can either be due to akinesia in transmural infarcted regions or be the results from hibernation of the myocardium as a result of chronic reduced flow. Hibernating myocardium may improve after restoration of coronary blood flow [1]. The improvement of myocardial function and the rate of recovery are related to the extent of myocardial infarction [2-4].

Contrast enhanced cardiac magnetic resonance imaging (MRI) is able to detect myocardial infarction [5, 6] and can predict improvement of depressed myocardial function after revascularization [7, 8]. However the diagnostic accuracy of contrast enhanced MRI as well as wall thickness [9, 10], contractile reserve [9, 11] and thickness of the unenhanced rim [12] is moderate. Moderate diagnostic performance of contrast enhanced MRI is caused by the limited predictive value of this technique in segments with an intermediate transmural extent of infarction [2, 4]. Initial attempts to combine viability parameters suggest an improvement in diagnostic accuracy [11, 13]. A structured analysis investigating the optimal combination of these 5 viability parameters has not yet been performed. The aim of the present study was to improve the diagnostic accuracy of pre-treatment MRI using combined viability assessment. We therefore studied a patient group scheduled for percutaneous coronary intervention (PCI) of a chronic total coronary occlusion (CTO) which represents the best in-vivo model of hibernation if present.

Methods

Patient population

Patients were recruited from April 2006 to February 2009. Patients scheduled for PCI of a CTO of a native coronary artery were prospectively selected for enrolment in this study. Sixty four percent of the patients had a positive exercise test and the remaining 36% had progressive anginal symptoms. All patients underwent a diagnostic angiogram. Inclusion criteria were (1) CTO, (2) sinus rhythm, (3) abnormalities in wall motion in the perfusion territory of the CTO on contrast ventriculography or echocardiography. Exclusion criteria were (1) myocardial infarction within the last three months; (2) atrial fibrillation; (3) contraindications

for magnetic resonance studies, (4) inability to give reliable informed consent, (5) known allergy to gadolinium based contrast material, (6) unstable coronary artery disease.

Inclusion flow chart is presented in figure 1 and baseline patient characteristics are presented in table 1. All successfully treated patients received drug eluting

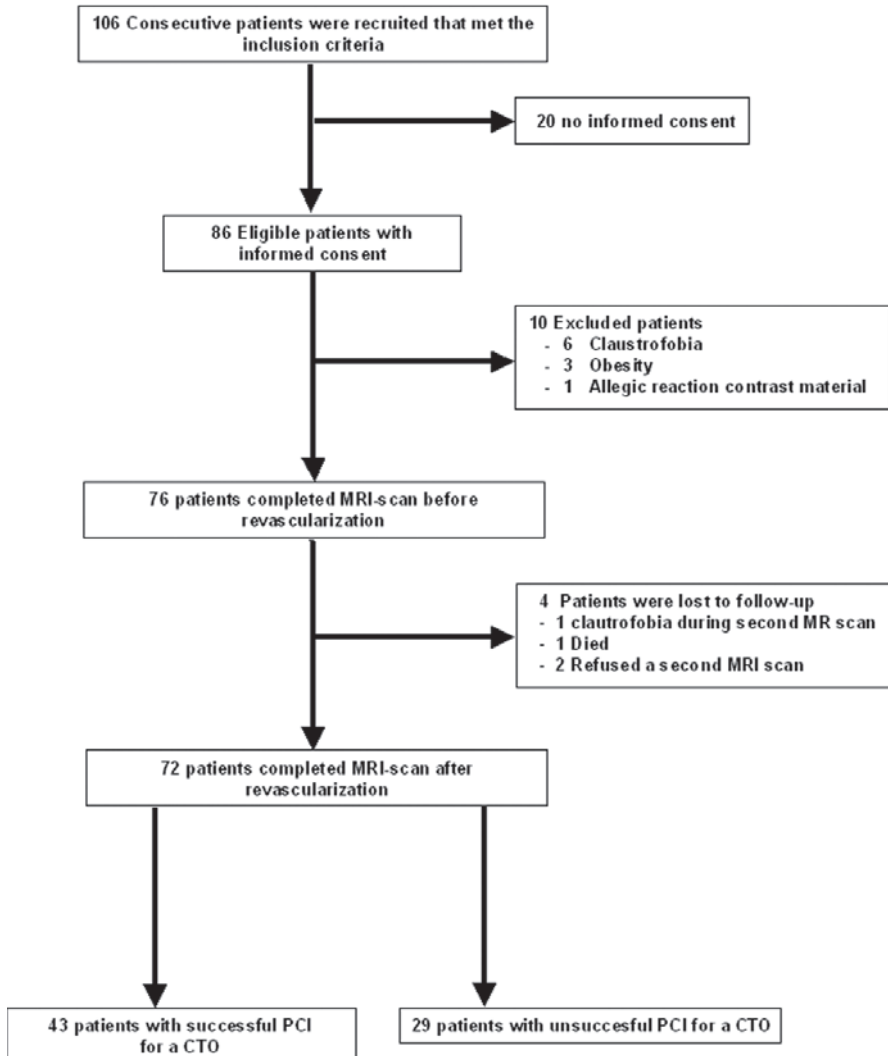


Figure 1. Flow of patients through the study; PCI, percutaneous coronary intervention; MRI, magnetic resonance imaging; CTO, chronic total coronary occlusion.

stents. A successful PCI was defined as restoration of Thrombolysis In Myocardial Infarction (TIMI) grade 3 flow using a drug eluting stent. The study protocol conforms to the ethical guidelines of the 1975 Declaration of Helsinki as reflected in a priori approval by the institutional review board of the Erasmus Medical Center in Rotterdam and all participating patients gave written informed consent.

Table 1. Baseline patient characteristics

| | Successful PCI N=43 | Unsuccessful PCI N=29 | P-value |
|-------------------------------------------|------------------------|--------------------------|---------|
| Age (years) | 60±10 | 61±10 | 0.32 |
| Men | 34(79) | 28(93) | 0.18 |
| Previous MI | 23(53) | 6(21) | 0.006 |
| MI on DE-MRI | 36(84) | 25(86) | 1.00 |
| TEI<25% | 9(21) | 6(21) | 0.77 |
| TEI between 25-75% | 20(47) | 15(52) | 0.63 |
| TEI>75% | 7(16) | 4(13) | 1.00 |
| 1-vessel disease | 29(67) | 24(82) | 0.15 |
| 2-vessel disease | 10(23) | 4(14) | 0.32 |
| 3-vessel disease | 4(9) | 1(3) | 0.64 |
| Previous PCI | 10(23) | 8(28) | 0.79 |
| Smoking | 9(21) | 7(24) | 0.78 |
| Diabetes Mellitus | 9(21) | 8(17) | 0.58 |
| Hypertension | 18(42) | 15(50) | 0.79 |
| Hypercholesterolemia | 34(79) | 24(80) | 0.75 |
| Family history | 20(47) | 13(43) | 0.61 |
| Baseline Ejection fraction (%) | 50±11 | 46±16 | 0.30 |
| End diastolic volume (ml/m ²) | 93±27 | 98±38 | 0.46 |
| End systolic volume (ml/m ²) | 48±24 | 58±41 | 0.21 |
| Infarct size on DE-MRI (g) | 17±15 | 14±17 | 0.51 |
| ACE inhibitor | 19(44) | 15(50) | 0.80 |
| β - Blocker | 39(91) | 28(93) | 0.64 |
| Statin | 39(91) | 27(90) | 1.00 |
| ASA | 39(91) | 28(93) | 1.00 |

Values are presented as number (%) or mean ± standard deviation. PCI, Percutaneous Coronary Intervention; DE-MRI, Delayed enhancement-cardiovascular magnetic resonance; MI, myocardial infarction; ACE, Angiotensin-converting enzyme; ASA, acetylsalicylic acid.

MRI-protocol

A 1.5 Tesla scanner with a dedicated eight-element phased-array receiver coil was used for imaging (Signa CV/i, GE Medical systems, Milwaukee, Wisconsin USA). Cine MRI was performed using a steady-state free-precession technique (FIESTA). Imaging parameters were reported previously [4]. Dobutamine was infused at 5 and 10-mcg/kg/min for 5 minutes at each dosage using an intravenous catheter, which was placed in the antecubital vein. Functional imaging was repeated using the same imaging planes as at rest. During the test the patients were monitored using electrocardiogram leads and blood pressure was measured at every 3 minutes interval. Criteria for ending the dobutamine-MRI examination were (1) development of a new wall motion abnormality, (2) fall of systolic blood pressure of >40 mm HG, (3) marked hypertension >240/120 mm Hg, (4) severe chest pain, (5) ventricular arrhythmias or new atrial arrhythmias, (6) intolerable side effects of dobutamine. Delayed enhancement imaging was performed with a gated breath hold T1-inversion recovery gradient-echo sequence 20 minutes after infusion of Gadoliniumdiethyltriaminepentaacetic acid (0.2 mmol/kg intravenously, Magnevist, Schering, Germany). Imaging parameters were reported previously [4]. The same slice locations and planning of the cine images were used for the acquisition of the delayed enhanced images.

Definitions and data analysis

All conventional angiograms before PCI were evaluated by two experienced observers. According to the place of occlusion and left or right dominance, the left ventricular segments were determined as being perfused by an occluded or a non-occluded vessel. A CTO was classified as a complete occlusion for more than 3 months as obtained from either the clinical history of prolonged anginal chest pain or the date of the diagnostic angiogram before PCI. All images were automatically analyzed using CAAS-MRV (version 3.2.1; Pie Medical Imaging, Maastricht, The Netherlands) [14]. Manual corrections were performed afterwards where necessary. Papillary muscles and trabeculations were considered as being part of the blood pool volume. A 17 segment-model was used to analyse the myocardial wall in each patient [15]. The 17th segment was excluded from analysis for the reason that wall thickening analysis was not possible as on short axis images no left ventricular cavity is visible. Segmental wall thickening (SWT) was defined as a percent increase of LV wall thickness during systole as compared to diastole. To study the effect of PCI on SWT, dysfunctional segments in the perfusion territory of a CTO were analysed. Myocardial segments were considered

dysfunctional if wall thickening was less than 45% [2, 16]. The predictive value of the different viability parameters were calculated with an improvement in SWT >10% after revascularization as standard for viability. Five viability indexes were evaluated before PCI; (1) end diastolic wall thickness (EDWT) [9] (2) contractile reserve during low dose dobutamine (LDD), at either 5-mcg/kg/min or 10-mcg/kg/min dose; (3) unenhanced rim thickness [12]; (4) SWT of the unenhanced rim (SWTUR) and (5) TEI. The unenhanced rim thickness was determined by subtracting the hyperenhanced area from the total area of a given segment. This area was expressed as a percentage of the total segmental area and multiplied by the EDWT. For SWTUR the increase in wall thickness in the end systolic phase as compared to the end diastolic phase was assigned to the thickness of the unenhanced rim as we assume that scar tissue does not contract and expressed as a percentage of the unenhanced rim. The TEI was quantified by dividing the hyperenhanced area by the total area and expressed as a percentage. For the hyperenhanced area the minimum and maximum signal intensity of the myocardium was used and a cut-off value was visually detected for each patient individually matching the hyperenhanced area visual estimated by the observer. Using this cut-off value for hyperenhancement, contours were automatically traced. We evaluated these 5 indexes in dysfunctional myocardial segments. To compose the viability score we performed multivariate regression analysis to determine which parameter had additive predictive value. The optimal cut-off value of each individual parameter was calculated separately and the parameters were then used as binary variables. If a parameter was considered viable and reaches a certain threshold the regression coefficient (RC) was added to the sum of the viability score. The viability score was calculated as the sum of the RC of the parameters which were considered viable. All MRI data were analysed quantitatively in a random order with the investigator blinded to the clinical information and the previous results.

Statistical analysis

Continuous data are expressed as mean values \pm one standard deviation (SD), whereas dichotomous data are expressed as numbers and percentages. Differences in baseline characteristics between patients with successful PCI and non-successful PCI were evaluated using chi-square tests, Fisher's exact tests, and unpaired Student's t-tests, as appropriate. Changes in left ventricular volumes and function were evaluated by two-way analysis of variance with repeated measures over time, followed by paired Student's t-tests. Improvement was defined

as an absolute change (from baseline to 6 months follow-up) in SWT of at least 10%. We applied Bonferroni's correction to adjust for the inflation of the type I error with multiple testing.

Univariable logistic regression (LR) analyses were applied to assess the power of viability parameters for the prediction of improvement in myocardial function. Results are presented as odds ratios (ORs) with corresponding 95% confidence intervals (CIs), which refers to 10 units for TEI, SWTur and LDD. Then, receiver operator characteristic (ROC) curve analyses were performed to determine the 'best' thresholds of relevant predictors, following the method of maximizing the sum of sensitivity and specificity. We present the observed area under the ROC curves (AUROC) for each of these predictors.

Subsequently, multivariable LR analyses were conducted. All variables that were significantly associated with improvement entered this multivariable stage with their values categorized at the optimal cut-off value. A backward deletion process was performed, until all variables in the model had a $p < 0.05$. The RC of the variables that composed the final model were used to construct a 'viability score'. Again ROC curve analyses were applied to determine the 'best' threshold of this score for the prediction of improvement of myocardial function.

We used the segment and not the patient as unit of our analyses. We realized that potential correlation existed between the multiple segments that were derived from the same patient. Therefore, general estimating equation (GEE) analyses were applied to construct the LR models.

We performed extensive internal validation of our results by bootstrap analyses [17, 18]. A total of 1,000 replications of the dataset were obtained by random sampling segments (with replacement), with the patient as cluster. All statistical tests were two sided, and a p -value < 0.05 was considered statistically significant.

Additionally a per patient analysis on diagnostic accuracy was performed using both TEI and the viability score. The test was considered positive for viability when $> 50\%$ of the segments in the revascularised area were viable according to the TEI or the viability score.

Results

Patient population

Of 106 consecutively approached patient, 72 patients completed the study protocol. The median time interval between baseline MRI and PCI was 18 days (25th and 75th percentile, 6-31), clinical evidence of myocardial infarction did not occur during this time interval. Follow-up MRI scan was performed at a median time interval of 183 days (25th and 75th percentile, 181-190) after PCI. PCI of the CTO was successful in 43 patients and unsuccessful in 29 patients. Nineteen patients (14 with successful and 5 with unsuccessful PCI of a CTO) underwent PCI of another vessel during the same procedure.

In patients with successful PCI, the CTO was located in 19 (44%) patients in the left anterior descending artery, in 10 (23%) patients in the left circumflex artery and in 14 (33%) patients in the right coronary artery. In patients without successful PCI the CTO was located in 10(37%) patients in the left anterior descending artery, in 6 (20%) in the left circumflex artery and in 13 (43%) patients in the right coronary artery. Nineteen patients underwent PCI of another vessel during the same procedure, 14 patients in the group with successful PCI and 5 patients in the group with unsuccessful PCI of their CTO ($p=0.12$). All patients with successful PCI for their CTO were symptom free at follow-up. Administration of dobutamine was well tolerated by all patients, no serious side effects occurred. Blood pressure and heart rate increased slightly but consistently during infusion of dobutamine. In two patients (7%) in the group with unsuccessful PCI new hyper enhancement occurred at follow-up (new infarct mass 2.1 and 3.6 gram).

All 1136 segments were available for analysis. Three hundred thirty six segments were in the perfusion territory of the CTO of which 255 segments were dysfunctional (159 segments in the patient group that underwent successful PCI and 96 segments in the patient group with unsuccessful PCI).

Left ventricular function and volumes

EF increased significantly in patients that underwent successful PCI (from 50 ± 11 to $54\pm 12\%$; $p<0.001$). End diastolic volume index was unchanged (from 93 ± 27 to 88 ± 34 ml/m²; $p=0.21$) and end systolic volume index decreased (from 48 ± 24 to 43 ± 29 ml/m²; $p=0.02$). In patients with unsuccessful PCI, EF (46 ± 16 to $47\pm 13\%$;

$p=0.41$), end diastolic volume index (98 ± 38 ml/m² to 92 ± 35 ml/m²; $p=0.08$) and end systolic volume index (58 ± 41 ml/m² to 52 ± 35 ml/m²; $p=0.16$) remained unchanged.

Mean SWT of dysfunctional segments in the perfusion territory of the CTO improved significantly in patients after successful PCI ($16\pm 19\%$ to $39\pm 35\%$; $p<0.0001$). In patients with unsuccessful PCI mean SWT remained unchanged at follow-up ($19\pm 21\%$ to $21\pm 25\%$; $p=0.54$). Both patient groups showed significant contractile reserve before PCI (figure 2).

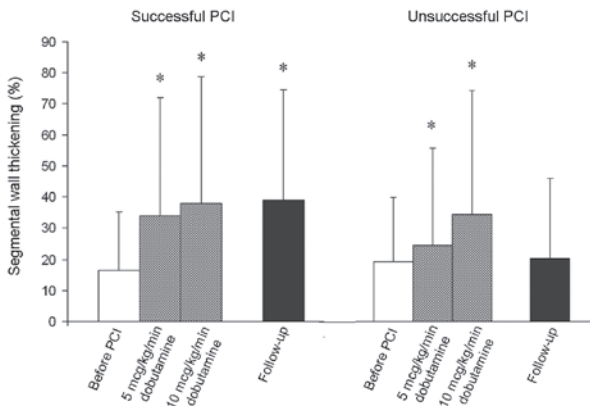


Figure 2. In patients with successful percutaneous coronary intervention (PCI), segmental wall thickening (SWT) improved significantly during dobutamine and at follow-up as compared to SWT before PCI. In patients without successful PCI, SWT improved significantly during dobutamine but not at follow-up as compared to baseline. * $p<0.05$ vs. before PCI.

Single assessment of myocardial viability and regional functional recovery

The optimal cut-off value and the AUROC for all parameters for the prediction of improvement are presented in table 2. All viability parameters had significant predictive value according to the univariate logistic regression analysis (table 3). Sensitivity, specificity, positive predictive value (PPV) and negative predictive value (NPV) for all viability parameters to predict functional improvement of dysfunctional segments after PCI are presented in table 4. The sensitivity, specificity, PPV and NPV of TEI for the prediction of improvement in function after PCI was 89(81-94)%, 48(36-64)%, 79(70-85)% and 67(51-82)%. LDD was a better predictor for functional improvement after PCI with sensitivity, specificity, PPV and NPV of 93(86-97)%, 77(63-87)%, 89(82-94)% and 85(71-93)%.

The analysis per segment was confirmed by bootstrap analysis. The mean and the standard deviation for the sensitivity and specificity are presented in table 5.

Table 2. Receiver operator characteristic curve analysis for each viability parameter

| | Cut-off value | AUROC (95% Confidence interval for AUROC) |
|-------------------------------|---------------|----------------------------------------------|
| LDD (%) | 7 | 0.86(0.80 to 0.93) |
| TEI (%) | 50 | 0.77(0.69-0.85) |
| EDWT (mm) | 6 | 0.62 (0.52 to 0.72) |
| Unenhanced rim thickness (mm) | 3 | 0.76 (0.68 to 0.84) |
| SWTUR (%) | 45 | 0.62(0.53 to 0.72) |

LDD, contractile reserve during low dose dobutamine; TEI, transmural extent of infarction; EDWT, end diastolic wall thickness; SWTur, Segmental wall thickening of the unenhanced rim

Table 3. Logistic univariate and multivariate regression analysis of the contribution of different viability parameters for improvement in SWT.

| | OR | 95% Confidence Interval for OR | P-value |
|--------------------------|------|--------------------------------|----------|
| Univariate | | | |
| LDD | 1.82 | (1.49-2.22) | P<0.0001 |
| TEI | 0.68 | (0.58-0.79) | P<0.0001 |
| EDWT | 1.3 | (1.1-1.7) | P=0.0063 |
| Unenhanced rim thickness | 1.4 | (1.2-1.5) | P<0.0001 |
| SWTur | 0.85 | (0.76-0.95) | P=0.0052 |
| Multivariate | | | |
| LDD | 1.06 | (1.02-1.09) | P<0.0001 |
| TEI | 0.96 | (0.94-0.97) | P<0.0001 |
| SWTur | 0.98 | (0.97-0.99) | P=0.0029 |

LDD, contractile reserve during low dose dobutamine; TEI, transmural extent of infarction; EDWT, end diastolic wall thickness; SWTur, Segmental wall thickening of the unenhanced rim; OR, odds ratio. The odds ratio refers to 10 units for TEI, SWTur and LDD.

Combined assessment of myocardial viability and regional functional recovery

Multivariate analysis including all 5 different viability parameters showed that EDWT and the thickness of the unenhanced rim did not have incremental predictive value. TEI, SWTur and LDD had incremental predictive value (table 3). For the viability score we added the RC without decimal to the sum of the score. Receiver operator characteristic curve analysis demonstrated an optimal thresh-

Table 4. Diagnostic performance of each viability index for the prediction of improvement in SWT.

| | RC | OR | Sig. | Sensitivity (%) | Specificity (%) | PPV (%) | NPV (%) |
|---------------------------------|----|------------|-------|-----------------|-----------------|-----------|-----------|
| LDD (>7%) | 4 | 46(17-123) | 0.000 | 93(86-97) | 77(63-87) | 89(82-94) | 85(71-93) |
| TEI (<50%) | 2 | 8(4-18) | 0.000 | 89(81-94) | 48(36-64) | 79(70-85) | 67(51-82) |
| EDWT (>6mm) | 1 | 4(2-10) | 0.003 | 92(84-96) | 27(16-41) | 72(64-79) | 61(39-80) |
| Unenhanced rim thickness (>3mm) | 3 | 15(6-42) | 0.000 | 94(88-98) | 48(34-62) | 79(71-85) | 81(62-92) |
| SWTUR (<45%) | 1 | 4(2-8) | 0.003 | 88(80-93) | 33(21-47) | 73(64-80) | 56(38-74) |
| Score (5) | | 52(19-140) | 0.000 | 92(84-96) | 83(69-91) | 92(84-96) | 83(69-91) |

LDD, contractile reserve during low dose dobutamine; TEI, transmural extent of infarction; EDWT, end diastolic wall thickness; SWTur, Segmental wall thickening of the unenhanced rim; PPV, positive predictive value; NPV, negative predictive value; RC, regression coefficient; OR, odds ratio; 95% confidence interval is presented between brackets.

old for the viability score of 5.0 for the prediction of improvement in SWT with an AUROC of 0.91 (95%CI 0.86-0.95) (figure 3). Sensitivity, specificity, PPV and NPV for this cut-off value were 92(84-96)%, 83(69-91)%, 92(84-96)% and 83(69-91)% respectively. SWT improved significantly in segments with a viability score of ≥ 5.0 ($16 \pm 20\%$ to $49 \pm 30\%$; $p < 0.0001$) and remained unchanged in segments with a viability score of < 5.0 ($18 \pm 16\%$ to $18 \pm 23\%$; $p = 1.00$) (figure 4). In segments with a viability score of ≥ 5.0 , 92% of the segments improved. In segments with a viability score of < 5.0 only 17% of the segments showed an improvement of SWT.

Myocardial viability assessment in segments with an intermediate transmural extent of infarction

In segments with an intermediate TEI (1-75%)($n = 110$), 85 segments were classified as viable using delayed enhancement imaging (TEI $< 50\%$) of which 61(72%) improved. Twenty-five segments were classified as not viable (TEI $> 50\%$) of which still 11 segments (44%) improved. Using the viability score with a

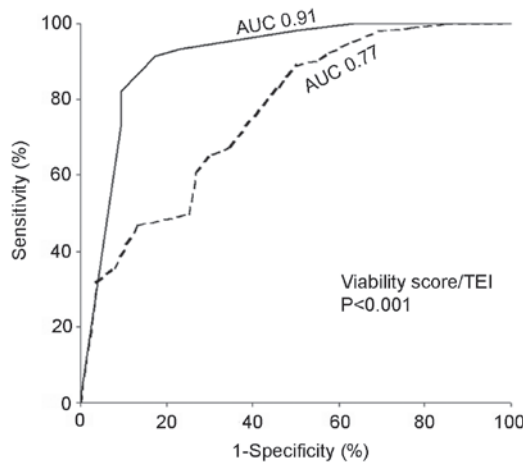


Figure 3. Viability score (solid line) was compared to the more widely used transmural extent of infarction using delayed enhancement imaging (dotted line) alone. AUROC was significantly higher ($P<0.001$) for viability score as compared to TEI alone.

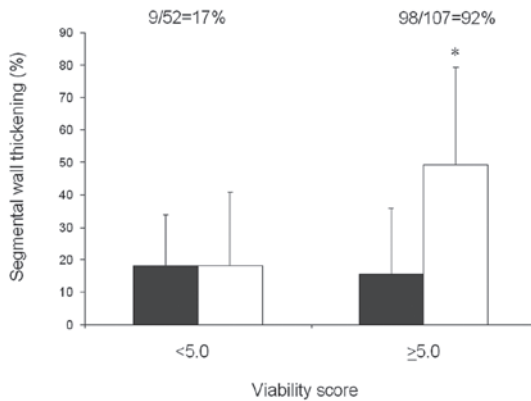


Figure 4. Ninety-two percent of the segments with a viability score of ≥ 5 showed improvement of segmental wall thickening (SWT) $>10\%$ after percutaneous coronary intervention (PCI) and mean SWT improved significantly in these segments. Only seventeen percent of the segments with viability score of <5 showed improvement of SWT $>10\%$ and mean SWT did not improve. For example if a segment shows contractile reserve, has a TEI of $<50\%$ and $SWT_{ur}>45\%$ than the viability score is; $4+2+0=6$ which is > 5 . SWT is expected to improve which can be predicted with a sensitivity of 91%, specificity of 84% PPV of 93% and NPV of 83%. Black bars = SWT before PCI and white bars = SWT at 6 months follow-up.

cut-off value of 5.0, 70 segments were classified as viable of which 64 segments (91%) improved. Forty segments were classified as being not viable of which only 8 improved (20%).

Table 5. Sensitivity and specificity after bootstrap analysis

| | Sensitivity (%) | | Specificity (%) | |
|---------------------------------|-----------------|-----|-----------------|------|
| | Mean | SD | Mean | SD |
| LDD (>7%) | 90.0 | 3.6 | 81 | 11.4 |
| TEI (<50%) | 92.3 | 3.6 | 45.0 | 13.8 |
| EDWT (>6mm) | 92.6 | 3.6 | 27.7 | 11.3 |
| Unenhanced rim thickness (>3mm) | 96.3 | 2.9 | 43.2 | 13.8 |
| SWTUR (<45%) | 87.2 | 4.1 | 40.2 | 11.9 |

LDD, Contractile reserve during low dose dobutamine; TEI, transmural extent of infarction; EDWT, end diastolic wall thickness; SWTur, Segmental wall thickening of the unenhanced rim; SD, standard deviation

Per patient analysis

Using the TEI for viability assessment, 42%(5/12) of the patients that did not show improvement in myocardial function at 6 months follow-up were considered viable before revascularization and underwent percutaneous revascularization. These false positives were reduced to 8% (1/12) using the viability score. Sensitivity, specificity, PPV and NPV for the prediction of improvement in the revascularised area for TEI were 97(84-99)%, 58(32-81)%, 86(71-94)% , 88(53-98)% and for the viability score were 97(84-99)%, 92(65-99)%, 97(84-99)% and 92(65-99)% respectively.

Discussion

In our study we demonstrated that successful recanalization with PCI in patients with a CTO improved myocardial function of CTO related segments that were dysfunctional. We further demonstrated that the combination of multiple MRI derived viability parameters including dobutamine contractile reserve assessment, TEI (non viable necrotic tissue) and SWT of normal remaining myocardium was a better predictor of improvement of dysfunctional segments

prior to PCI for CTO than the single widely used parameter of TEI. Lastly we demonstrated that the use of multiple MRI derived viability parameters better identified patients who would benefit from PCI compared to the use of the single MRI derived variable. This would allow better use of limited resource and offers more effective management of patients with a CTO.

MRI using delayed enhancement of infarcted myocardial tissue after administration of gadolinium is helpful to assess viability of systolic dysfunctional hibernating left ventricular myocardium. Depended on the TEI, dysfunctional myocardium still maintains the capability to recover function after revascularization with CABG or PCI [11, 19]. Recovery was predicted for 78% of the myocardial segments if the myocardium was fully viable (TEI=0%) while almost no recovery may be expected if the TEI was almost transmural (>75% infarction of a myocardial segment) [7]. Similar results in improvement of dysfunctional myocardium were obtained using delayed enhancement MRI in patients with a recanalization of a CTO with PCI [2]. The likelihood of recovery was much less predictable if intermediate TEI (between 1-75%) was present [9, 12, 13]. Recently we introduced SWTur and investigated the relation of this parameter but also of TEI, EDWT and thickness of the unenhanced rim with contractile reserve by low dose dobutamine. TEI and SWTur had significant predictive value [20].

In the present study, recovery of function after revascularization was the outcome parameter and therefore it was also possible to investigate the predictive value of contractile reserve during dobutamine. Contractile reserve was a better predictor of myocardial improvement [9, 11, 21-23] because, unlike the other parameters, it directly unmasks the potential of the presence of contractile reserve of dysfunctional non infarcted myocardium. Using a combination of 3 viability parameters improved the prediction of viability in particular for segments with an intermediate TEI. Important to realize is that the majority (68%) of all dysfunctional segments in our study had an intermediate TEI. This is feasible in clinical practice because the versatility of current MRI allows viability assessment of multiple MRI variables that can be obtained from one MRI session. Combination of various MRI viability parameters is also useful in other patient groups [13, 24] representing different aspects of viability such as the presence of contractile reserve, extent of infarction, segmental wall thickening of epicardial non infarcted rim of myocardium which incorporated into a simple score each with a weighted factor was a reliable predictor of improvement of dysfunctional myocardium prior to recanalization of CTO.

Limitations

Sustained recanalization at follow-up was not confirmed by coronary angiography but no clinical evidence of recurrent ischemia was reported and all patients received a drug eluting stent with acknowledged low restenosis rate [3, 25]. The recovery of myocardial function was assessed at 6 months and the established improvement may have been underestimated because it has been shown that the myocardial function may continue to further improve after 6 months up to a period of 3 years [4].

Conclusion

Combined viability analysis using the viability score was a better predictor than the most widely used transmural extent of infarction. This may be useful for the selection of patients where improvement of myocardial function by PCI of a CTO is desired.

Acknowledgement

The authors of this manuscript have certified that they comply with the Principles of Ethical Publishing in the International Journal of Cardiology [26].

References

1. Cwajg JM, Cwajg E, Nagueh SF, et al. End-diastolic wall thickness as a predictor of recovery of function in myocardial hibernation: relation to rest-redistribution T1-201 tomography and dobutamine stress echocardiography. *J Am Coll Cardiol* 2000;35:1152-1161.
2. Baks T, van Geuns RJ, Duncker DJ, et al. Prediction of left ventricular function after drug-eluting stent implantation for chronic total coronary occlusions. *J Am Coll Cardiol* 2006;47:721-725.
3. Haas F, Augustin N, Holper K, et al. Time course and extent of improvement of dysfunctioning myocardium in patients with coronary artery disease and severely depressed left ventricular function after revascularization: correlation with positron emission tomographic findings. *J Am Coll Cardiol* 2000;36:1927-1934.

4. Kirschbaum SW, Baks T, van den Ent M, et al. Evaluation of left ventricular function three years after percutaneous recanalization of chronic total coronary occlusions. *Am J Cardiol* 2008;101:179-185.
5. Mayr A, Klug G, Schocke M, et al. Late microvascular obstruction after acute myocardial infarction: Relation with cardiac and inflammatory markers. *Int J Cardiol*.
6. Thiele H, Schuster A, Erbs S, et al. Cardiac magnetic resonance imaging at 3 and 15 months after application of circulating progenitor cells in recanalised chronic total occlusions. *Int J Cardiol* 2009;135:287-295.
7. Kim RJ, Wu E, Rafael A, et al. The use of contrast-enhanced magnetic resonance imaging to identify reversible myocardial dysfunction. *N Engl J Med* 2000;343:1445-1453.
8. Kuhl HP, Lipke CS, Krombach GA, et al. Assessment of reversible myocardial dysfunction in chronic ischaemic heart disease: comparison of contrast-enhanced cardiovascular magnetic resonance and a combined positron emission tomography-single photon emission computed tomography imaging protocol. *Eur Heart J* 2006;27:846-853.
9. Baer FM, Theissen P, Schneider CA, et al. Dobutamine magnetic resonance imaging predicts contractile recovery of chronically dysfunctional myocardium after successful revascularization. *J Am Coll Cardiol* 1998;31:1040-1048.
10. Schmidt M, Voth E, Schneider CA, et al. F-18-FDG uptake is a reliable predictor of functional recovery of akinetic but viable infarct regions as defined by magnetic resonance imaging before and after revascularization. *Magn Reson Imaging* 2004;22:229-236.
11. Wellnhofer E, Olariu A, Klein C, et al. Magnetic resonance low-dose dobutamine test is superior to SCAR quantification for the prediction of functional recovery. *Circulation* 2004;109:2172-2174.
12. Ichikawa Y, Sakuma H, Suzawa N, et al. Late gadolinium-enhanced magnetic resonance imaging in acute and chronic myocardial infarction. Improved prediction of regional myocardial contraction in the chronic state by measuring thickness of nonenhanced myocardium. *J Am Coll Cardiol* 2005;45:901-909.
13. Bodi V, Sanchis J, Lopez-Lereu MP, et al. Usefulness of a comprehensive cardiovascular magnetic resonance imaging assessment for predicting recovery of left ventricular wall motion in the setting of myocardial stunning. *J Am Coll Cardiol* 2005;46:1747-1752.
14. Kirschbaum SW, Baks T, Gronenschild EH, et al. Addition of the long-axis information to short-axis contours reduces interstudy variability of left-ventricular analysis in cardiac magnetic resonance studies. *Invest Radiol* 2008;43:1-6.
15. Cerqueira MD, Weissman NJ, Dilsizian V, et al. Standardized myocardial segmentation and nomenclature for tomographic imaging of the heart: a statement for healthcare professionals from the Cardiac Imaging Committee of the Council on Clinical Cardiology of the American Heart Association. *Circulation* 2002;105:539-542.

16. Holman ER, Buller VG, de Roos A, et al. Detection and quantification of dysfunctional myocardium by magnetic resonance imaging. A new three-dimensional method for quantitative wall-thickening analysis. *Circulation* 1997;95:924-931.
17. Efron B, Tibshirani RJ. *An introduction to the bootstrap*; 1993.
18. Zhou XH, Obuchowski NA, McClish DK. *Statistical methods in diagnostic medicine*; 2002.
19. Selvanayagam JB, Kardos A, Francis JM, et al. Value of delayed-enhancement cardiovascular magnetic resonance imaging in predicting myocardial viability after surgical revascularization. *Circulation* 2004;110:1535-1541.
20. Kirschbaum SW, Rossi A, van Domburg RT, et al. Contractile reserve in segments with nontransmural infarction in chronic dysfunctional myocardium using low-dose dobutamine CMR. *JACC Cardiovasc Imaging*;3:614-622.
21. Baer FM, Theissen P, Crnac J, et al. Head to head comparison of dobutamine-transoesophageal echocardiography and dobutamine-magnetic resonance imaging for the prediction of left ventricular functional recovery in patients with chronic coronary artery disease. *Eur Heart J* 2000;21:981-991.
22. Cornel JH, Bax JJ, Elhendy A, et al. Biphasic response to dobutamine predicts improvement of global left ventricular function after surgical revascularization in patients with stable coronary artery disease: implications of time course of recovery on diagnostic accuracy. *J Am Coll Cardiol* 1998;31:1002-1010.
23. Trent RJ, Waiter GD, Hillis GS, McKiddie FI, Redpath TW, Walton S. Dobutamine magnetic resonance imaging as a predictor of myocardial functional recovery after revascularisation. *Heart* 2000;83:40-46.
24. Plein S, Greenwood JP, Ridgway JP, Cranny G, Ball SG, Sivananthan MU. Assessment of non-ST-segment elevation acute coronary syndromes with cardiac magnetic resonance imaging. *J Am Coll Cardiol* 2004;44:2173-2181.
25. Hoye A, Tanabe K, Lemos PA, et al. Significant reduction in restenosis after the use of sirolimus-eluting stents in the treatment of chronic total occlusions. *J Am Coll Cardiol* 2004;43:1954-1958.
26. Shewan LG, Coats AJ. Ethics in the authorship and publishing of scientific articles. *Int J Cardiol* 2010;144:1-2.

Chapter 9

Evaluation of left ventricular function 3 years after percutaneous recanalisation of chronic total coronary occlusions

American journal of cardiology. 2008 Jan 15;101(2):179-85.

Sharon W Kirschbaum^{1,2}

Timo Baks^{1,2}

Martin van den Ent¹

George Sianos¹

Gabriel P Krestin²

Patrick W Serruys¹

Pim J de Feyter^{1,2}

Robert-Jan M van Geuns^{1,2}

Erasmus University
Medical Center,
Rotterdam,
the Netherlands

1. Department of
Cardiology,

2. Department of
Radiology,

Abstract

We investigated early and late effects of percutaneous revascularization for chronic total coronary occlusion (CTO) on left ventricular (LV) function and volumes. Magnetic resonance imaging was performed in 21 patients before, at 5 months, and at 3 years after recanalisation. Global LV function and volumes and segmental wall thickening (SWT) were quantified on cine-images. Two viability indexes were used; the transmural extent of infarction (TEI) on delayed contrast enhancement images and end-diastolic wall thickness at baseline (EDWT). A significant decrease in mean end-diastolic volume index (86 ± 14 ml/m² to 78 ± 15 ml/m²; $p=0.02$) and mean end-systolic volume index (35 ± 13 ml/m² to 30 ± 13 ml/m²; $p=0.03$) was observed three years after recanalisation. Mean ejection fraction tended to improve ($60 \pm 9\%$ to $63 \pm 11\%$; $p=0.11$). SWT significantly increased at 5 month follow-up ($p<0.001$) and an additional improvement was found at 3 years ($p=0.04$) follow-up in segments with TEI of $<25\%$. In segments with TEI between 25% and 75%, SWT remained unchanged at 5-month follow-up ($p=0.89$), but improved after 5 months ($p=0.04$). SWT remained unchanged in segments with transmural scars. For segmental functional recovery, TEI was a better predictor than EDWT (odds ratio 5.6, CI: 1.5-21.1; $p=0.01$ versus 2.5, CI: 0.7-8.3; $p=0.14$). In conclusion, a positive effect on LV remodeling and ejection fraction is observed up to three years after recanalisation. Both early and late improvement of regional LV function is observed in the perfusion territory of CTO and is related to the transmural extent of infarction on pre-treatment MRI.

Introduction

Chronic total coronary occlusions (CTO) are observed in up to 30-35% of the patients with suspected or known coronary artery disease that underwent a diagnostic coronary artery catheterization¹. Myocardium in the perfusion territory of a CTO can be either functionally normal or can be dysfunctional and viable or dysfunctional and non viable. Dysfunctional but viable myocardium may recover function after percutaneous coronary intervention for CTO²⁻⁴. It is currently unknown in what time span recovery of dysfunctional but viable myocardium can be seen. Several studies observed the beneficial effect of treatment of a CTO on left ventricular (LV) function with a follow-up time of approximately 6 months⁵⁻⁸. These early observations suggest that the time span of functional recovery of dysfunctional but viable myocardium may extent beyond 6 months but no data is available in patients with a recanalised CTO^{9,10}. In the present study we evaluated patients with dysfunctional myocardium due to CTO, early (5 months) and late (3 years) after percutaneous revascularization.

Materials and methods

Patients scheduled for percutaneous revascularization of a CTO of a native coronary artery were prospectively studied, of these patients 75% had a positive exercise test the remaining 25% had progressive anginal symptoms. All successful treated patients received a drug eluting stent. Forty-seven patients were included in this study. In 34 patients, percutaneous coronary intervention was successful. Follow-up at 3 years was obtained in 21 patients; 1 patient died, 1 patient had a defibrillator implanted, 1 patient gained too much weight to fit into the scanner, and 10 patients refused re-investigation.

In these patients MRI was performed at 16 ± 16 days before percutaneous coronary intervention and 5 ± 1 month and 2.7 ± 0.3 years after percutaneous coronary intervention. Fifty percent of the patients underwent a diagnostic heart catheterization at 3 years follow-up. One patient had a >50% in stent restenosis on the angiogram, however fractional flow reserve measurements were negative (0.89). More patient characteristics are listed in table 1. Exclusion criteria were any of the contraindications for magnetic resonance studies (pacemakers, claustrophobia, cochlea implants). The institutional review board of the Erasmus

Table 1. Baseline patient characteristics

| Subject | Age | Sex | Chronic total occlusion | Prior Myocardial infarct | Ejection fraction (%) | Eind diastolisch volume (ml) | Eind systolisch volume (ml) | Hyper-tension | Smoke | Diabetes | Hyper-Cholesterolemia | Family History | ACE-inhibitor | B-blokker | statin | ASA |
|---------|-----|-----|-------------------------|--------------------------|-----------------------|------------------------------|-----------------------------|---------------|-------|----------|-----------------------|----------------|---------------|-----------|--------|-----|
| 1 | 36 | M | LAD | + | 47 | 113 | 59 | 0 | 0 | 0 | 0 | 0 | + | + | + | + |
| 2 | 46 | M | RCA | + | 48 | 94 | 49 | 0 | 0 | + | + | + | 0 | + | + | + |
| 3 | 51 | M | RCA | 0 | 59 | 88 | 36 | + | + | 0 | + | + | 0 | + | + | + |
| 4 | 53 | M | RCA | + | 58 | 92 | 39 | 0 | + | 0 | + | 0 | 0 | + | + | + |
| 5 | 58 | M | LAD | + | 65 | 85 | 30 | + | + | 0 | + | 0 | 0 | + | + | + |
| 6 | 61 | M | LAD | + | 68 | 85 | 27 | + | 0 | 0 | 0 | + | + | 0 | + | + |
| 7 | 61 | M | RCA | 0 | 69 | 91 | 28 | 0 | 0 | 0 | + | + | 0 | + | + | + |
| 8 | 62 | M | RCA | 0 | 81 | 65 | 13 | 0 | 0 | + | 0 | 0 | 0 | + | + | + |
| 9 | 62 | M | LAD | 0 | 67 | 79 | 26 | 0 | 0 | 0 | + | + | 0 | + | + | + |
| 10 | 63 | M | LAD | + | 53 | 103 | 48 | + | 0 | + | + | 0 | 0 | 0 | + | + |
| 11 | 64 | M | RCA | + | 46 | 110 | 59 | 0 | 0 | 0 | 0 | 0 | + | 0 | + | + |
| 12 | 66 | M | RCA | 0 | 67 | 72 | 23 | 0 | 0 | 0 | + | + | + | + | + | + |
| 13 | 66 | F | LAD | + | 59 | 94 | 39 | + | 0 | 0 | + | 0 | + | + | + | + |
| 14 | 69 | M | RCA | + | 62 | 88 | 34 | + | 0 | 0 | + | + | 0 | + | + | + |
| 15 | 70 | M | LCX | + | 50 | 102 | 51 | 0 | + | 0 | 0 | + | 0 | 0 | + | + |
| 16 | 71 | F | RCA | 0 | 70 | 58 | 17 | + | 0 | 0 | + | + | 0 | 0 | + | + |

| | | | | | | | | | | | | | | | | | | | | | |
|----|----|---|-----|---|----|----|----|---|---|---|---|---|---|---|---|---|---|---|---|---|---|
| 17 | 72 | M | RCA | + | 49 | 84 | 43 | 0 | + | 0 | 0 | 0 | 0 | 0 | 0 | 0 | 0 | 0 | + | 0 | + |
| 18 | 76 | F | LAD | 0 | 64 | 81 | 29 | + | + | 0 | 0 | 0 | + | + | 0 | 0 | 0 | + | 0 | + | + |
| 19 | 76 | M | LCX | + | 56 | 89 | 39 | 0 | 0 | 0 | 0 | + | + | 0 | 0 | 0 | 0 | 0 | + | + | + |
| 20 | 77 | M | LAD | 0 | 59 | 72 | 30 | 0 | 0 | 0 | 0 | + | + | 0 | 0 | 0 | 0 | + | + | + | + |
| 21 | 79 | M | LAD | 0 | 72 | 64 | 18 | + | 0 | 0 | 0 | 0 | 0 | 0 | 0 | 0 | 0 | + | + | + | + |

+ = Yes; 0 = No; ACE = angiotensin-converting enzyme; ASA = acetylsalicylic acid

Medical Center approved the study and each subject gave written informed consent.

Magnetic resonance images were acquired using a 1.5 Tesla scanner. Patients were positioned in the supine position with a cardiac 4 or 8-element phased-array receiver coil placed over the thorax (Signa CV/i, GE Medical systems, Milwaukee, Wisconsin USA). Repeated breath holds and gating to the electrocardiogram were applied to minimize the influence of cardiac and respiratory motion on data collection. Cine MRI was performed using a steady-state free-precession technique (FIESTA). Imaging parameters were; field of view 36-40 x 28-32 cm; matrix size was 224 x 196; repetition time, 3.4 ms; echo time, 1.5 ms; flip angle, 45 degrees; 12 views per segment and slice thickness was 8.0 mm with a 2.0 mm slice gap. Using standard techniques to identify the major cardiac axes, two-chamber and four chamber cine magnetic resonance images were obtained. The 2- and 4-chamber end diastolic images at end expiration provided the reference images to obtain a series of short axis views. This resulted in 10-12 cine breath-hold short-axis images to cover the entire left ventricle.

Delayed enhancement imaging was performed with a gated breath hold T1-inversion recovery gradient-echo sequence 20 minutes after infusion of Gadoliniumdiethyltriaminepentaacetic acid (0.2 mmol/kg intravenously, Magnevist, Schering, Germany). Imaging parameters were; repetition time 6.3 ms, echo time 1.5 ms, flip angle 20°, inversion pulse of 180°, matrix 192 x 160, number of averages 1-2, inversion time 180-280 ms (adjusted to null the signal of the

remote myocardium). The slice locations of the delayed enhanced images were copied from the cine-images.

All conventional angiograms before revascularization were evaluated by two experienced observers (TB and RvG). Collateral function was scored using the Rentrop classification¹¹. The CTO was classified as a complete occlusion for >6 weeks as obtained from the clinical history of prolonged anginal chest pain, myocardial infarction or the date of the diagnostic angiogram before revascularization. LV function was calculated using a dedicated software package (Mass, Medis, the Netherlands). Papillary muscles and trabeculations were considered as being part of the blood pool volume. A 16 segment-model, excluding the apex¹², was used to analyze the myocardial wall in each patient. Segmental wall thickening (SWT) was defined as a percent increase of LV wall thickness during systole compared to diastole. Myocardial segments were considered dysfunctional if wall thickening was less than 45%¹³. To study changes in wall thickening over time, the perfused territories of the CTO region were analyzed at baseline and 5 months and 3 years after recanalisation.

Two viability indexes were evaluated: 1) end diastolic wall thickness (EDWT)¹⁴ and 2) the transmural extent of infarction (TEI) at baseline⁷. Delayed enhancement images for the TEI were analyzed by experienced observers (TB and RvG), blinded for the clinical data, and the decision was made based on consensus. The TEI was calculated on a 5-point scale and defined as: 1=0%, 2=1-25%, 3=26-50%, 4=51-75% and 5=76-100%.

Data are presented as mean +/- standard deviation. The change in LV function and volume indexes and the changes in SWT in viable segments (<25% TEI), possible (26% to 75% TEI), non-viable segments (>75%), and remote segments between baseline and follow-up were tested using the Students-t-test. All test were done two sided and a p-value of <0.05 was considered to indicate statistical significance. We analyzed separately the usefulness of the viability indexes evaluated before revascularization. We calculated sensitivity, specificity, positive predictive value and negative predictive value for predicting segmental improvement. A logistic regression model was used to investigate the power of the two viability indexes for predicting segmental improvement of more than 10%.

Results

The patient population consisted of 21 patients. In 11 patients the CTO was located in the left anterior descending, in 8 patients in the right coronary artery and in 2 patients in the circumflex artery. All images were good for analysis. Mean duration of occlusion was 7 ± 5 months. At follow-up, medication was similar to baseline except for clopidogrel, which was discontinued after 6 months.

A total of 336 myocardial segments were available for analysis of which 106 segments were in the perfusion territory of a CTO. Of these 106 segments, abnormal contractile function (wall thickening of $<45\%$) was present in 49 (46%) segments: 24 (49%) in the anterior area, 4 (8%) in the lateral area, and 21 (43%) in the inferior area. Of the 49 dysfunctional segments in the perfusion territory of a CTO, 21 (43%) had a TEI of $<25\%$, 25 (50%) had TEI of 25-75% and 3 (6%) had a TEI of $>75\%$. In this study 19 segments had delayed enhancement before revascularization while SWT was normal. Albeit most of them had TEI of $<25\%$ (53%). EDWT was measured in these 49 dysfunctional segments at baseline: 11 segments had baseline EDWT of $<7\text{mm}$, 23 segments had EDWT between 7 and 9 mm and 15 segments had EDWT of more $>9\text{mm}$. A significant decrease in mean end-diastolic volume index ($86 \pm 14\text{ ml/m}^2$ to $78 \pm 15\text{ ml/m}^2$; $p=0.02$) and mean end-systolic volume index ($35 \pm 13\text{ ml/m}^2$ to $30 \pm 13\text{ ml/m}^2$; $p=0.03$) was observed 3 years after recanalisation. Mean ejection fraction tended to improve ($60 \pm 9\%$ to $63 \pm 11\%$; $p=0.11$)(Figure 1). At 3 years follow-up 15 (71%) patients had normal ejection fraction, 13 (62%) normal end diastolic volume and 14 (67%) normal end

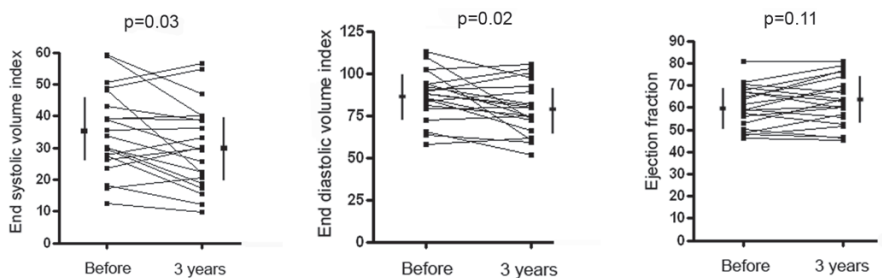


Figure 1

The change in left ventricular volume indexes and ejection fraction between baseline, and 3 years follow-up measured with magnetic resonance imaging (MRI). The mean ejection fraction remained unchanged, but end-systolic and end-diastolic volume indexes decreased significantly. (Normal values for EF, EDV and ESV are $63 \pm 4\%$; $162 \pm 28\text{ml}$ and $60 \pm 11\text{ml}$, respectively)

systolic volume values. SWT improved more than 10% in 27 (55%) of the dysfunctional segments. Twenty-one (43%) segments developed normal wall thickening while 12 (24%) segments had a further deterioration of wall thickening after 3 years of follow-up (Figure 2).

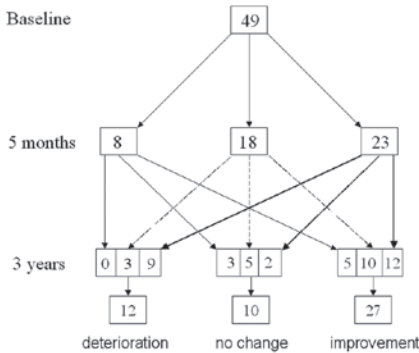


Figure 2

Functional changes for dysfunctional segments over time, numbers of the segments are given and related to the segments before. Segments were categorized into a deterioration of wall thickening of at least 10%, no change in wall thickening or an improvement of wall thickening of at least 10% at 5 months and at 3 years.

improvement after 3 years (to $67\pm 48\%$; $p=0.04$). In segments with TEI between the 25% and 75%, SWT remained unchanged at 5 month follow-up ($22\pm 18\%$ to $22\pm 22\%$; $p=0.89$). Interestingly, after 3 years of follow-up SWT improved significantly in these segments (to $39\pm 43\%$; $p=0.04$). In segments with transmural scars (TEI > 75%), SWT remained unchanged at early ($4\pm 33\%$ to $-9\pm 16\%$; $p=0.54$) and late follow-up (to $13\pm 40\%$; $p=0.42$) (Figure 3a).

When the individual segments were stratified into EDWT at baseline, segments with EDWT of <7 mm SWT remained unchanged at early ($5\pm 17\%$ to $8\pm 28\%$; $p=0.77$) and late follow-up (to $15\pm 33\%$; $p=0.55$). In segments with EDWT between 7 and 9 mm, SWT showed no improvement after 5 months ($25\pm 16\%$ to $33\pm 27\%$; $p=0.17$) but showed a remarkable improvement after follow-up duration of three years (to $51\pm 46\%$; $p=0.05$). Segments with an EDWT of more than 9 mm SWT showed a marked improvement after 5 months ($18\pm 26\%$ to $44\pm 26\%$;

Mean SWT of all dysfunctional segments increased from $19\pm 21\%$ at baseline to $31\pm 30\%$ at 5 months follow-up and $47\pm 46\%$ at 3 year follow-up. However, SWT of the revascularised dysfunctional segments was significantly lower compared to remote segments ($47\pm 46\%$ versus $82\pm 36\%$; $p<0.001$). In segments with TEI of <25%, mean SWT increased significantly at 5 month follow-up ($18\pm 24\%$ to $47\pm 28\%$; $p<0.001$) with a considerable further im-

$p=0.002$), and tended to improve further after 3 years of follow-up (to 64 ± 44 ; $p=0.08$) (Figure 3b).

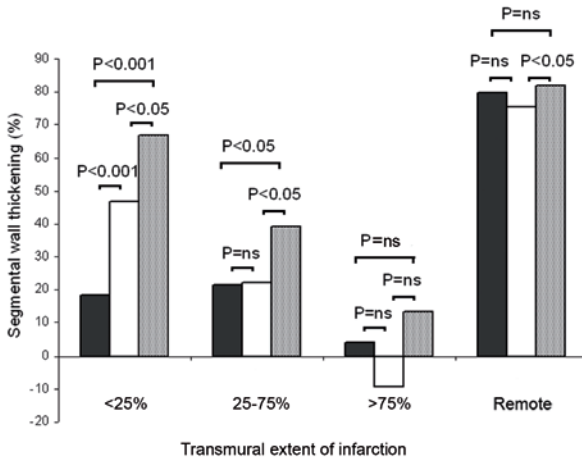


Figure 3a

Improvement of SWT is related to the transmural extent of infarction. Solid bars = SWT before stent implantation; Open bars = 5 months after revascularization; Dotted bars = 3 years after stent implantation. * $P < 0.05$

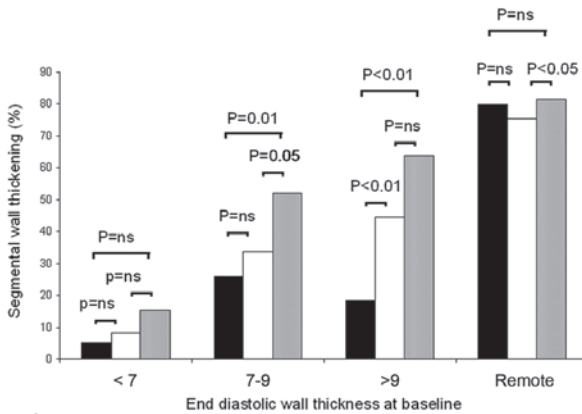


Figure 3b

Improvement in SWT is related to the EDWT at baseline. Solid bars = SWT before stent implantation; Open bars = 5 months after revascularization; Dotted bars = 3 years after stent implantation. * $P < 0.05$

Sensitivity, specificity, and positive and negative predictive values of viability indexes for predicting improvement of >10% of SWT are demonstrated in table 2. Univariate logistic regression analysis for predicting SWT at 3 years was performed. For each level increase in TEI the odds ratio was 0.63 (95%CI; 0.40-0.98; $p < 0.05$). When the cut of value of 25% TEI was chosen, the odds ratio was 5.63 (95%CI; 1.50-21.12; $p = 0.01$). The odds ratio for each increase of 1 mm in EDWT was 1.34 (95%CI; 0.92-1.96; $p = 0.13$). When we used a cut of value of 7 mm for EDWT, the odds ratio was 2.5 (95% CI; 0.74-8.31; $p = 0.14$). Multiple regression analysis showed no additive predictive value for EDWT in addition to TEI ($p = 0.63$).

Table 2. Viability indexes analyzed before revascularization for predicting improvement in segmental wall thickening at 3 years (improvement of > 10%).

| | Sensitivity | Specificity | Positive predictive value | Negative predictive value |
|--------------------------------------|-------------|-------------|---------------------------|---------------------------|
| Transmural extent of infarction <25% | 64% | 81% | 82% | 63% |
| End diastolic wall thickness 7 mm | 84% | 35% | 71% | 55% |
| End diastolic wall thickness 8 mm | 63% | 53% | 68% | 48% |
| End diastolic wall thickness 9 mm | 37% | 79% | 73% | 44% |

Discussion

We report in this paper that SWT improves in dysfunctional but viable segments 5 months after CTO recanalisation with an even further improvement after 3 years of follow-up. Secondly, a reduction in remodelling is observed up to three years after recanalisation as demonstrated by decreased end diastolic volume and end systolic volume. Third, improvement in regional function is related to the extent of myocardial fibrosis and can be predicted by DE-MRI before revascularisation.

Several authors have studied the effect of revascularisation for CTO on global and regional LV function^{5-8,15,16}. In general, a positive effect on regional wall mo-

tion was observed and ejection fraction tended to improve at approximately 6 months follow-up. Long-term follow-up studies registered clinical endpoints¹⁷⁻¹⁹. These non-randomised studies demonstrated a significant reduction in mortality and need for surgical revascularisations. One randomised study, the TOSCA-2 trial showed improvement in LV ejection fraction and remodelling in patients that underwent either optimal medical therapy or those that received percutaneous coronary intervention of the total occluded infarct related vessel shortly after the acute myocardial infarct¹⁶. However no difference between the 2 treatment strategies was found. The positive effect in both groups can be ascribed due to the stunning of the tissue early after the acute myocardial infarct, which will improve²⁰. In our group with a more chronic situation recovery of function or reduction in remodelling can be related to hibernating in the targeted area, which can only improve after revascularisation. Moreover in the TOSCA-2 trial no assessment of myocardial viability was made before revascularisation and viability is expected to be low where most of the patients presented with ST-elevated infarctions without trombolysis treatment, which resulted in high levels of serum markers.

No previous study with pre-treatment viability assessment on LV function after recanalisation of a CTO was performed with a follow-up of more than 6 months. Several authors described additional improvement in LV function after the general accepted 6 months follow-up period, but this was described in patients with surgical revascularisation for coronary artery disease^{21,22}.

The recovery time of dysfunctional myocardium is related to the extent of damage on cellular level²³ that depends on different factors, including the duration of ischemia and the severity of ischemia²⁴. Biopsies taken of hibernating myocardium showed defects in nearly all cells. The center of the cell loses its sarcomeres and myofibrils, the perinuclear area is absent of contractile material and cellular debris occurred in the enlarged extracellular space^{23,25}. In a study of 19 patients with dysfunctional myocardium, myocardial biopsies showed that there was a relationship between the extent of the structural changes and the rate of recovery²⁶. Significant recovery could already be noted 1 week after revascularization when the dysfunctional myocardium displayed no or little structural changes. In addition, when the structural changes were widespread the recovery was delayed and the extent of recovery remained incomplete at 6 months.

In the present study, improvement of SWT was observed beyond the 6 month period in segments with more extensive myocardial abnormalities (EDWT between 7 and 9, or TEI between 25-75%) suggesting that the restoration of flow after revascularisation may lead to late recovery of segments that did not or incompletely recover after 5 or 6 months. On the contrary, dysfunctional segments with less abnormalities (EDWT >9, or TEI <25%) showed early improvement of function, possibly representing (chronic) stunned areas with less or no structural cellular changes.

In the present study 2 previously described viability indexes were measured and the predictive value for possible systolic functional recovery was tested^{7,27}. The TEI performed well in predicting functional recovery with good sensitivity and specificity. The predictive value of EDWT was rather low for all cut of values tested. This is also illustrated by the high odds ratio for TEI but not significant univariate analysis for EDWT. The optimal cut-off value for EDWT was 7 mm in our study which is higher compared to the commonly used threshold for viability of >5.5 mm defined by MRI²⁸. This value has been chosen in the early 90's when conventional gradient echo techniques were used while nowadays steady-state free-precession techniques are the standard, which results in a higher contrast and a higher signal to noise ratio²⁹.

Several limitations of the present study should be mentioned. 1) The present study did not have a control group without an intervention; thus treatment effect on LV function, volumes and SWT cannot directly be ascribed due to the revascularization procedure but may be related to conservative therapy. 2) Angiograms at follow-up were only performed in 50% of the patients, but no clinical evidence of recurrent ischemia was reported and all patients received a drug eluting stent with low reported restenosis rates³⁰. 3) Functional follow up was only assessed at 5 months and 3 years.

References

1. Kahn JK. Angiographic suitability for catheter revascularization of total coronary occlusions in patients from a community hospital setting. *Am Heart J* 1993;126:561-564.
2. Ruygrok PN, De Jaegere PP, Verploegh JJ, Van Domburg RT, De Feyter PJ. Immediate outcome following coronary angioplasty. A contemporary single centre audit. *Eur Heart J* 1995;16 Suppl L:24-29.
3. Flameng W, Schwarz F, Hehrlein FW. Intraoperative evaluation of the functional significance of coronary collateral vessels in patients with coronary artery disease. *Am J Cardiol* 1978;42:187-192.
4. Stone GW, Reifart NJ, Moussa I, Hoyer A, Cox DA, Colombo A, Baim DS, Teirstein PS, Strauss BH, Selmon M, Mintz GS, Katoh O, Mitsudo K, Suzuki T, Tamai H, Grube E, Cannon LA, Kandzari DE, Reisman M, Schwartz RS, Bailey S, Dangas G, Mehran R, Abizaid A, Moses JW, Leon MB, Serruys PW. Percutaneous recanalization of chronically occluded coronary arteries: a consensus document: part II. *Circulation* 2005;112:2530-2537.
5. Danchin N, Angioi M, Cador R, Tricoche O, Dibon O, Juilliere Y, Cuilliere M, Cherrier F. Effect of late percutaneous angioplastic recanalization of total coronary artery occlusion on left ventricular remodeling, ejection fraction, and regional wall motion. *Am J Cardiol* 1996;78:729-735.
6. Dzavik V, Carere RG, Mancini GB, Cohen EA, Catellier D, Anderson TE, Barbeau G, Lazzam C, Title LM, Berger PB, Labinaz M, Teo KK, Buller CE. Predictors of improvement in left ventricular function after percutaneous revascularization of occluded coronary arteries: a report from the Total Occlusion Study of Canada (TOSCA). *Am Heart J* 2001;142:301-308.
7. Baks T, van Geuns RJ, Duncker DJ, Cademartiri F, Mollet NR, Krestin GP, Serruys PW, de Feyter PJ. Prediction of left ventricular function after drug-eluting stent implantation for chronic total coronary occlusions. *J Am Coll Cardiol* 2006;47:721-725.
8. Rambaldi R, Hamburger JN, Geleijnse ML, Poldermans D, Kimman GJ, Aiazian AA, Fioretti PM, Ten Cate FJ, Roelandt JR, Serruys PW. Early recovery of wall motion abnormalities after recanalization of chronic totally occluded coronary arteries: a dobutamine echocardiographic, prospective, single-center experience. *Am Heart J* 1998;136:831-836.
9. Cohen M, Charney R, Hershman R, Fuster V, Gorlin R. Reversal of chronic ischemic myocardial dysfunction after transluminal coronary angioplasty. *J Am Coll Cardiol* 1988;12:1193-1198.
10. Bax JJ, Schinkel AF, Boersma E, Rizzello V, Elhendy A, Maat A, Roelandt JR, van der Wall EE, Poldermans D. Early versus delayed revascularization in patients with ischemic cardiomyopathy and substantial viability: impact on outcome. *Circulation* 2003;108 Suppl 1:II39-42.
11. Rentrop KP, Cohen M, Blanke H, Phillips RA. Changes in collateral channel filling immediately after controlled coronary artery occlusion by an angioplasty balloon in human subjects. *J Am Coll Cardiol* 1985;5:587-592.

12. Cerqueira MD, Weissman NJ, Dilsizian V, Jacobs AK, Kaul S, Laskey WK, Pennell DJ, Rumberger JA, Ryan T, Verani MS. Standardized myocardial segmentation and nomenclature for tomographic imaging of the heart: a statement for healthcare professionals from the Cardiac Imaging Committee of the Council on Clinical Cardiology of the American Heart Association. *Circulation* 2002;105:539-542.
13. Holman ER, Buller VG, de Roos A, van der Geest RJ, Baur LH, van der Laarse A, Bruschke AV, Reiber JH, van der Wall EE. Detection and quantification of dysfunctional myocardium by magnetic resonance imaging. A new three-dimensional method for quantitative wall-thickening analysis. *Circulation* 1997;95:924-931.
14. Biagini E, Galema TW, Schinkel AF, Vletter WB, Roelandt JR, Ten Cate FJ. Myocardial wall thickness predicts recovery of contractile function after primary coronary intervention for acute myocardial infarction. *J Am Coll Cardiol* 2004;43:1489-1493.
15. Melchior JP, Doriot PA, Chatelain P, Meier B, Urban P, Finci L, Rutishauser W. Improvement of left ventricular contraction and relaxation synchronism after recanalization of chronic total coronary occlusion by angioplasty. *J Am Coll Cardiol* 1987;9:763-768.
16. Dzavik V, Buller CE, Lamas GA, Rankin JM, Mancini GB, Cantor WJ, Carere RJ, Ross JR, Atchison D, Forman S, Thomas B, Buszman P, Vozzi C, Glanz A, Cohen EA, Meciari P, Devlin G, Mascette A, Sopko G, Knatterud GL, Hochman JS. Randomized trial of percutaneous coronary intervention for subacute infarct-related coronary artery occlusion to achieve long-term patency and improve ventricular function: the Total Occlusion Study of Canada (TOSCA)-2 trial. *Circulation* 2006;114:2449-2457.
17. Suero JA, Marso SP, Jones PG, Laster SB, Huber KC, Giorgi LV, Johnson WL, Rutherford BD. Procedural outcomes and long-term survival among patients undergoing percutaneous coronary intervention of a chronic total occlusion in native coronary arteries: a 20-year experience. *J Am Coll Cardiol* 2001;38:409-414.
18. Olivari Z, Rubartelli P, Piscione F, Etti F, Fontanelli A, Salemm L, Giachero C, Di Mario C, Gabrielli G, Spedicato L, Bedogni F. Immediate results and one-year clinical outcome after percutaneous coronary interventions in chronic total occlusions: data from a multicenter, prospective, observational study (TOAST-GISE). *J Am Coll Cardiol* 2003;41:1672-1678.
19. Ivanhoe RJ, Weintraub WS, Douglas JS, Jr., Lembo NJ, Furman M, Gershony G, Cohen CL, King SB, 3rd. Percutaneous transluminal coronary angioplasty of chronic total occlusions. Primary success, restenosis, and long-term clinical follow-up. *Circulation* 1992;85:106-115.
20. Baks T, van Geuns RJ, Biagini E, Wielopolski P, Mollet NR, Cademartiri F, Boersma E, van der Giessen WJ, Krestin GP, Duncker DJ, Serruys PW, de Feyter PJ. Recovery of left ventricular function after primary angioplasty for acute myocardial infarction. *Eur Heart J* 2005;26:1070-1077.

21. Cornel JH, Bax JJ, Elhendy A, Maat AP, Kimman GJ, Geleijnse ML, Rambaldi R, Boersma E, Fioretti PM. Biphasic response to dobutamine predicts improvement of global left ventricular function after surgical revascularization in patients with stable coronary artery disease: implications of time course of recovery on diagnostic accuracy. *J Am Coll Cardiol* 1998;31:1002-1010.
22. Alfieri O, La Canna G, Giubbini R, Pardini A, Zogno M, Fucci C. Recovery of myocardial function. The ultimate target of coronary revascularization. *Eur J Cardiothorac Surg* 1993;7:325-330; discussion 330.
23. Haas F, Jennen L, Heinzmann U, Augustin N, Wottke M, Schwaiger M, Lange R. Ischemically compromised myocardium displays different time-courses of functional recovery: correlation with morphological alterations? *Eur J Cardiothorac Surg* 2001;20:290-298.
24. Bax JJ, Visser FC, Poldermans D, Elhendy A, Cornel JH, Boersma E, van Lingen A, Fioretti PM, Visser CA. Time course of functional recovery of stunned and hibernating segments after surgical revascularization. *Circulation* 2001;104:314-318.
25. Canty JM, Jr., Fallavollita JA. Hibernating myocardium. *J Nucl Cardiol* 2005;12:104-119.
26. Vanoverschelde JL, Depre C, Gerber BL, Borgers M, Wijns W, Robert A, Dion R, Melin JA. Time course of functional recovery after coronary artery bypass graft surgery in patients with chronic left ventricular ischemic dysfunction. *Am J Cardiol* 2000;85:1432-1439.
27. Baer FM, Voth E, Schneider CA, Theissen P, Schicha H, Sechtem U. Comparison of low-dose dobutamine-gradient-echo magnetic resonance imaging and positron emission tomography with [18F]fluorodeoxyglucose in patients with chronic coronary artery disease. A functional and morphological approach to the detection of residual myocardial viability. *Circulation* 1995;91:1006-1015.
28. Baer FM, Smolarz K, Theissen P, Voth E, Schicha H, Sechtem U. Regional ^{99m}Tc-methoxyisobutylisonitrile-uptake at rest in patients with myocardial infarcts: comparison with morphological and functional parameters obtained from gradient-echo magnetic resonance imaging. *Eur Heart J* 1994;15:97-107.
29. Thiele H, Nagel E, Paetsch I, Schnackenburg B, Bornstedt A, Kouwenhoven M, Wahl A, Schuler G, Fleck E. Functional cardiac MR imaging with steady-state free precession (SSFP) significantly improves endocardial border delineation without contrast agents. *J Magn Reson Imaging* 2001;14:362-367.
30. Hoyer A, Tanabe K, Lemos PA, Aoki J, Saia F, Arampatzis C, Degertekin M, Hofma SH, Sianos G, McFadden E, van der Giessen WJ, Smits PC, de Feyter PJ, van Domburg RT, Serruys PW. Significant reduction in restenosis after the use of sirolimus-eluting stents in the treatment of chronic total occlusions. *J Am Coll Cardiol* 2004;43:1954-1958.

Chapter 10

Complete percutaneous revascularization for multivessel disease in patients with impaired left ventricular function. Pre- and post procedural evaluation by cardiac magnetic resonance imaging

Journal of the american college of cardiology
Cardiovasc Interv. 2010 Apr;3(4):392-400

Sharon W Kirschbaum^{1,2}

Tirza Springeling^{1,2}

Eric Boersma¹

Adriaan Moelker²

Wim J van der Giessen¹

Patrick W Serruys¹

Pim de Feyter^{1,2}

Robert-Jan M van Geuns^{1,2}

1. Department of
Cardiology, Erasmus
Medical Center,
Rotterdam, the
Netherlands

2. Department of
Radiology, Erasmus
Medical Center,
Rotterdam, the
Netherlands

Abstract

Objectives To investigate the effect of complete, incomplete and unsuccessful revascularization by percutaneous coronary intervention (PCI) on left ventricular ejection fraction (EF) in patients with multivessel disease and impaired left ventricular function and assessed the diagnostic accuracy of cardiac magnetic resonance imaging (CMR) for improvement in EF.

Background The effect of PCI for multivessel coronary artery disease on long-term myocardial function and the predictive value of CMR on global function are incompletely investigated.

Methods CMR was performed in patients with multivessel disease before and 6 month after complete revascularization (n=34), incomplete revascularization (n=22) or in patients without successful revascularization (n=15). For the prediction of recovery of EF, wall thickening was quantified on cine images at rest and during 5- and 10 mcg/kg/min dobutamine. The transmural extent of infarction was quantified on delayed enhancement CMR.

Results EF improved significantly after complete revascularization (46 ± 12 to $51\pm 13\%$; $p<0.0001$) but did not change after incomplete (49 ± 11 to $49\pm 10\%$; $p=0.88$) or unsuccessful revascularization (49 ± 13 to $47\pm 13\%$; $p=0.11$). Sensitivity, specificity, positive and negative predictive value for the prediction of improvement in EF of $>4\%$ after PCI were 100%, 75%, 74% and 100% for dobutamine-CMR and 70%, 77%, 70% and 77%, for delayed enhancement-CMR respectively.

Conclusions Complete revascularization for multivessel coronary artery disease improves EF whereas EF did not change in patients after incomplete or unsuccessful revascularization. Improvement in EF can be predicted by performing CMR before PCI.

Introduction

Coronary atherosclerosis is the most common cause of heart failure in the western world (1). Several studies have shown that a coronary artery bypass graft for multivessel coronary atherosclerosis improved ejection fraction (EF) in the presence of viable tissue (2-4). Nowadays, percutaneous coronary intervention (PCI) is increasingly used as revascularization strategy instead of coronary artery bypass graft because both therapies have the same outcome in terms of survival and rates of myocardial infarction, as long as the extent of disease is not too extensive (Syntax score <33) (5). Due to extensive disease or depressed left ventricular systolic dysfunction which is thought to be irreversible PCI may result in incomplete revascularization, which has a significantly lower event free survival as compared to complete revascularization (6,7). The majority of events is due to repeated interventions but also a lower survival rate is associated with incomplete revascularization which is not fully understood. We hypothesised that complete revascularization in patients with multivessel disease and depressed EF does better improve EF as compared to incomplete revascularization.

In this study we evaluated the effect of complete, incomplete or unsuccessful revascularization by PCI on EF in patients with multivessel coronary artery disease and left ventricular dysfunction and whether improvement in EF after successful PCI can be predicted by performing cardiac magnetic resonance imaging (CMR) before PCI.

Materials and methods

Patient population

Patients with multivessel coronary artery disease and left ventricular wall motion abnormalities who were referred for PCI, based on the discretion of the physician using the information of patient history, risk factors and additional non-invasive stress testing if performed were prospectively approached for enrolment in this study. Inclusion criteria were (1) significant stenosis in at least two vessels, (2) sinus rhythm and (3) abnormalities in wall motion on contrast ventriculography or echocardiography. Exclusion criteria were (1) myocardial infarction within the last three months; (2) atrial fibrillation; (3) contraindications for magnetic resonance studies, (4) inability to give reliable informed consent, (5) known allergy to gadolinium based contrast material, (6) unstable coronary artery disease.

The institutional review board of the Erasmus Medical Center in Rotterdam approved the study and all patients gave written informed consent.

CMR-protocol

A 1.5 Tesla scanner with a dedicated eight-element phased-array receiver coil was used for imaging (Signa CV/i, GE Medical systems, Milwaukee, Wisconsin USA). Cine CMR was performed using a steady-state free-precession technique (FIESTA). Pulse sequence details have been published previously (8). To cover the entire ventricle, 10 to 12 short axis slices were planned on the four and two chamber view (gap 2 mm). Dobutamine was infused at 5 and 10-mcg/kg/min for 5 minutes at each dosage using an intravenous catheter, which was placed in the antecubital vein. Functional imaging was repeated during dobutamine infusion using the same long axis imaging planes as at rest, for the short axis only 3 slices were acquired. The 3 slices covered the basal mid and apical part of the left ventricle. During the test the patients were monitored using ECG leads for rhythm control and blood pressure was measured at every 3 minutes interval. Criteria for ending the dobutamine-CMR examination were (1) development of a new wall motion abnormality, (2) fall of systolic blood pressure of >40 mm Hg, (3) marked hypertension >240/120 mm Hg, (4) severe chest pain, (5) ventricular arrhythmias or new atrial arrhythmias or (6) intolerable side effects of dobutamine.

Delayed enhancement (DE)-CMR was performed 20 minutes after infusion of Gadoliniumdiethyltriaminepentaacetic acid (0.2 mmol/kg intravenously, Mag-

nevist, Schering, Germany). A gated breath hold T1-inversion recovery gradient-echo sequence was used as described previously (8). The slice locations of the delayed enhanced images were copied from the cine-images.

Definitions and data analysis

All conventional angiograms before PCI were evaluated by two observers and lesions were scored visually (<50%, 50-99% or 100%). A stenosis was considered significant if the diameter stenosis was >50%. Multivessel disease was defined as the presence of a significant lesion in at least 2 epicardial vessels in different perfusion territories. A chronic total occlusion (CTO) was classified as a complete occlusion for more than 3 months as obtained from either the clinical history of prolonged anginal chest pain or the date of the diagnostic angiogram before PCI. Revascularization was defined as complete when all significant stenosis defined on conventional angiogram were successfully treated. Revascularization was defined incomplete when not all significant lesions but at least one was successfully treated. Revascularization was defined unsuccessful when all significant lesions remained untreated. All CMR-images were transferred to a Microsoft Windows™ based personal computer for analysis using CAAS-MRV (version 3.2.1; Pie Medical Imaging, Maastricht, The Netherlands). This software uses the additional information of the long axis to limit the extent of volumes at the base and apex of the heart. The ejection fraction was determined by subtracting end systolic endocardial volume from the end diastolic endocardial volume and divide this number by the end diastolic endocardial volume. Papillary muscles and trabeculations were considered as being part of the blood pool volume. A 17 segment-model, excluding the apex, was used to analyse the myocardial wall in each patient. According to the place of the stenosis and left or right dominance, the left ventricular segments were determined as being perfused by a vessel with a significant lesion or a vessel with a non-significant lesion (9). Segmental wall thickening was defined as a percent increase of left ventricular wall thickness during systole compared to diastole. We studied the effect of revascularization on global function and regional function. To study the effect of revascularization on regional myocardial function, segments in the perfusion territory of a significant lesion (related to anatomy on conventional angiogram) were analysed. Myocardial segments were considered dysfunctional if wall thickening was less than 45% (10,11). Two viability indexes were evaluated before revascularization; (1) quantitative contractile reserve during dobutamine-CMR and (2) TEI which was calculated by dividing the hyper enhanced area by the

total area in 16 segments and expressed as a percentage. The TEI was divided into 5 groups; 0%, 1-25%, 25-50%, 50-75% and >75% infarct transmuralty per segment and segmental wall thickening was quantified for each group. A cut off value of TEI <25% was used to predict functional recovery after revascularization (10,12,13). For quantitative contractile reserve during dobutamine-CMR a cut off value of 7% was used (Kirschbaum MD, unpublished data that are under review, 2009). The percentage dysfunctional but viable segments per patient were defined as the sum of all-dysfunctional but viable segments divided by the total number of segments (N=16). The angiograms and the CMR data were analyzed in a random order with the investigator blinded to the clinical information and the previous results.

Biochemistry

Troponin T was measured 6 hours after the procedure. If troponin T was above the upper limit of normal (0,02 ug/l) serial blood samples were taken every 6 hours until maximum troponin T was identified. According to the guidelines (European Society of Cardiology American College of Cardiology/ American Heart Association) a diagnosis of an enzymatic periprocedural infarction was made if troponin T was greater than 3 times the upper limit of normal (14). Troponin T was quantified with electro Chemi Luminescence Immuno Assay (ECLIA) on a Elecsys type 2010 (Roche Diagnostics, Almere, The Netherlands).

Statistical analysis

Continuous data are expressed as mean values \pm one standard deviation (SD), whereas dichotomous data are expressed as numbers and percentages. Differences in baseline characteristics between patients undergoing complete, incomplete or unsuccessful revascularization were evaluated using chi-square tests, Fisher's exact tests, one-way ANOVA, or Kruskal-Wallis test where appropriate. The number of segments per patient perfused by a significant lesion was tested with one way ANOVA. Post hoc analysis was performed using Bonferroni correction. The changes in left ventricular EF and volumes within each group were tested with paired student's t test. The change in global functional parameters between groups was tested with analysis of variance or the unpaired student's t-test. The relationship between the amount of viability per patient and the change in left ventricular EF was analysed with linear regression analysis. We present the observed area under the ROC curves for both predictors. Differences in sensitivity and specificity between contrasting dobutamine-CMR and DE-CMR

were evaluated by Mc Nemar tests with exact methods. All tests were performed two sided and a p-value of <0.05 was considered statistically significant. All analysis were performed with SPSS 15.0.1 (SPSS Inc, Chicago, Illinois).

Results

Patient population

Between June 2006 and January 2008, 118 patients who met the inclusion criteria were prospectively selected of which 28 patients refused to participate. Of the 90 patients that were included 71 patients completed the study protocol. Inclusion flow chart is presented in figure 1. The mean time interval between baseline CMR and PCI was 36 ± 36 days, clinical evidence of myocardial infarction did not occur during his time interval. In 71 patients a second CMR scan was repeated at a mean of 7 ± 1 month after PCI. All treated patients received drug-eluting stents. Baseline patient characteristics are presented in table 1. Thirty-four patients underwent complete revascularization by PCI. The left anterior descending artery was treated in 34 patients, left circumflex artery in 23 patients, right coronary artery in 18 patients, the main stem in 3 patients, first diagonal branch in 6 patients, second diagonal branch in 2 patients and the marginal obtuses in 3 patients. A total of 989 vessels and 94 lesions underwent PCI with drug eluting stent implantation. Average of 1.9 drug eluting stents per vessel and 4.1 drug eluting stents per patient were implanted with an average stent length of 21.3 mm per patient. NYHA classification improved from 2.6 ± 1.1 before revascularization to 1.1 ± 0.4 at 6 months follow-up.

In patients with incomplete revascularization ($n=22$), left anterior descending artery was treated in 8 patients, the first diagonal branch in 1 patient, the left circumflex artery in 4 patients, the marginal obtuses in 1 patient and the right coronary artery in 10 patients. Average of 2.8 drug eluting stents were implanted per vessel with an average stent length of 22.1 mm. NYHA classification was 2.6 ± 0.7 before and changed to 1.4 ± 0.5 at 6 months follow-up. In 15 patients, PCI was not successful mainly due to the presence of a chronic total coronary occlusion and in some patients CABG was already rejected as an treatment option due to co-morbidity; these patients were only medically treated. NYHA classification changed from 2.8 ± 0.8 at baseline and changed to 2.1 ± 1.1 at 6 months follow-up. Administration of low dose dobutamine during CMR imaging was well toler-

Table 1 Baseline patient characteristics.

| | Complete PCI N=34 | Incomplete PCI N=22 | Unsuccessful PCI N=15 | P-value |
|---------------------------------------------------------|-------------------------|---------------------------|-----------------------------|---------|
| Age (years) | 62±9 | 64±10 | 62±9 | 0.54 |
| Men | 28(82) | 14(64) | 12(80) | 0.57 |
| Previous MI | 16(47) | 9(41) | 6(40) | 0.77 |
| MI on DE-CMR | 29(85) | 17(77) | 12(80) | 0.71 |
| Previous PCI | 6(18) | 6(22) | 7(47) | 0.10 |
| Risk Factors for coronary artery disease | | | | |
| Smoking | 6(18) | 4(18) | 3(20) | 0.86 |
| Diabetes Mellitus | 6(18) | 2(9) | 2(13) | 0.87 |
| Hypertension | 14(41) | 10(45) | 7(47) | 0.86 |
| Hypercholesterolemia | 28(82) | 14(64) | 15(100) | 0.50 |
| Family history | 17(50) | 9(41) | 9(60) | 0.52 |
| Medications | | | | |
| ACE inhibitor | 14(41) | 10(45) | 7(47) | 0.86 |
| β - Blocker | 30(88) | 20(91) | 15(100) | 0.47 |
| Statin | 33(97) | 20(91) | 14(93) | 0.54 |
| ASA | 33(97) | 20(91) | 15(100) | 0.44 |
| Baseline ejection fraction (%) | | | | |
| Baseline end systolic volume index (ml/m ²) | 56±34 | 52±23 | 47±23 | 0.10 |
| Infarct size on DE-CMR (g) | 24±21 | 19±22 | 25±21 | 0.30 |
| 2-vessel disease on CAG | 25(74) | 15(69) | 10(67) | 0.56 |
| Vessel with stenosis>50% | | | | |
| LAD | 34(38) | 18(38) | 9(25) | 0.04 |
| LCX | 23(26) | 10(21) | 6(17) | 0.23 |
| RCA | 18(20) | 14(29) | 10(28) | 0.98 |
| Main stem | 3(3) | 0 | 0 | 0.30 |
| Intermediate branch | 0 | 2(4) | 2(6) | 0.64 |

| | | | | |
|-----------------------------|----------|-----------|-----------|------|
| MO | 3(3) | 3(6) | 3(8) | 0.60 |
| Diagonal 1 | 6(7) | 1(2) | 4(11) | 0.11 |
| Diagonal 2 | 2(2) | 0 | 0 | 0.70 |
| Total | 89 | 48 | 36 | |
| Significant lesions/patient | 2.6 | 2.2 | 2.4 | 0.17 |
| Chronic total occlusion | 20(59) | 19(86) | 10(67) | 0.04 |
| Syntax score | 22.2±9.6 | 22.0±13.0 | 24.0±14.1 | 0.90 |

Values are presented as number (%) or mean ± standard deviation.

ACE= angiotensin-converting enzyme; ASA= acetylsalicylic acid; PCI, Percutaneous Coronary Intervention; MI, Myocardial infarction; CAG, coronary angiography; LAD, left anterior descending artery; LCX, left circumflex artery; RCA, right coronary artery; MO, marginal obtuses.

ated by all patients, no serious side effects occurred. All patients with delayed enhancement showed a distribution pattern extending from the endocardium, typical for ischemic heart disease.

Myocardial injury by DE-CMR and serum markers

DE-CMR before PCI showed pre-existing myocardial damage in 85% (29/34) in the patients that underwent complete revascularization, in 77% (17/22) of the patients with incomplete revascularization and in 87% (13/15) of the patients with an unsuccessful revascularization ($P=0.97$). Mean infarct mass at baseline was 24 ± 21 g in patients that underwent complete revascularization, 19 ± 22 g in patients with incomplete revascularization and 25 ± 21 g in patients with unsuccessful revascularization ($P=0.70$). The number of dysfunctional segments $TEI < 25\%$, and dobutamine responsive segments per patient showed no significant difference for the three groups (table 2).

Troponin levels post procedure were elevated in 10 patients that underwent complete revascularization in which new patterns of late enhancement appeared in 3 patients and in 5 patients that underwent incomplete revascularization, none of these patients developed new patterns of DE. For the 3 patients in the complete revascularization group that developed new patterns of DE maximum troponin levels were 0.65, 0.43 and 0.06 $\mu\text{g/l}$ and corresponding new infarct masses on DE were 6.7, 9.4 and 2.0 g respectively. In the 3 patients with new DE, the average myocardial infarct mass changed from 11 g to 19 g. The change in infarct mass in these 3 patients did not change the total infarct size in the complete revascularization group ($23.6\pm 21.7\text{g}$ to $23.9\pm 22.6\text{g}$). In patients

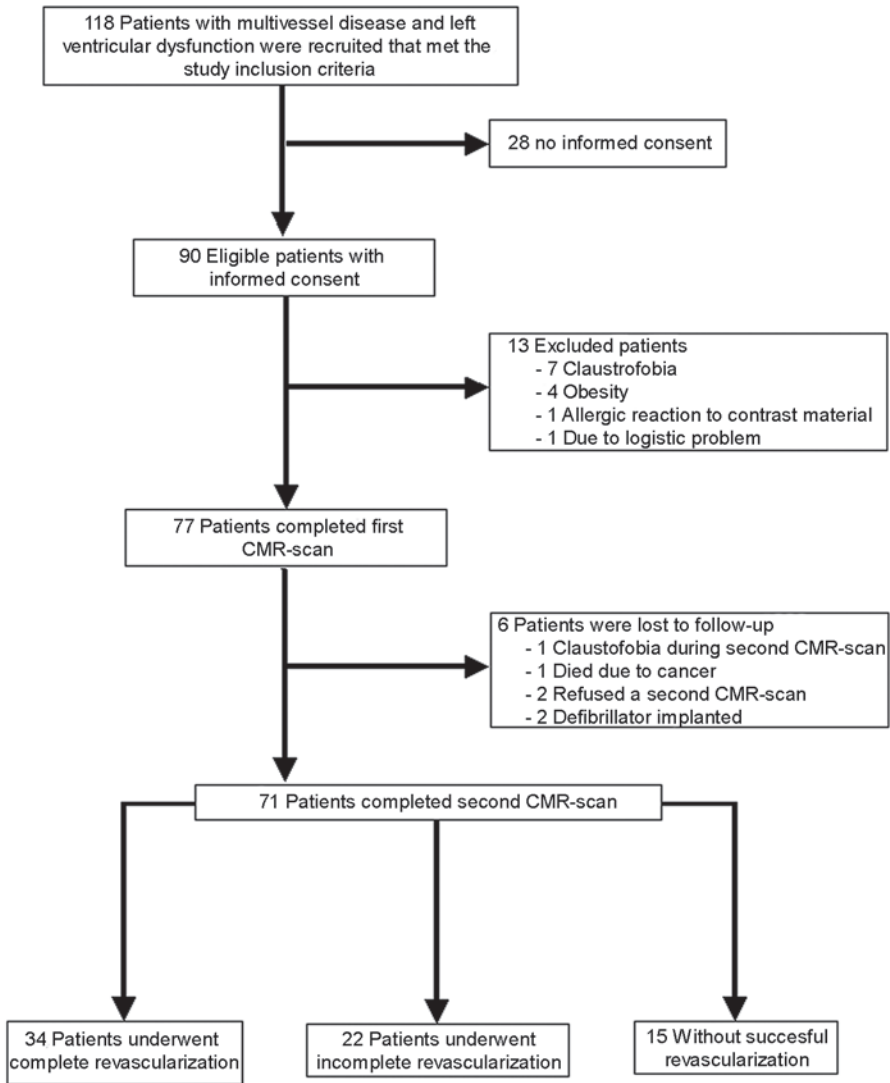


Figure 1. Flow diagram of patient recruitment - Flow diagram of patient recruitment according to the STAndards for Reporting of Diagnostic Accuracy statement CMR, cardiac magnetic resonance imaging.

without successful revascularization troponin levels were elevated in 3 patients and only 1 patient developed a new infarct pattern on DE-CMR. The new infarct mass was 2 g. Total infarct mass did not change in these patients (22.0 ± 22.2 g to 20.6 ± 22.3 g).

Table 2 Number of segments per patient perfused by a significant lesion according to the different groups.

| | Complete PCI | Incomplete PCI | Unsuccessful PCI | P-value |
|----------------------------------------|--------------|----------------|------------------|---------|
| Dysfunctional segments/patient | 5.73±2.41 | 4.52±1.12 | 5.14±2.95 | 0.38 |
| TEI<25% segments/patient | 3.03±1.83 | 2.57±1.75 | 1.86±1.35 | 0.12 |
| Dobutamine responsive segments/patient | 3.29±1.68 | 2.65±1.62 | 3.33±2.42 | 0.45 |

Left ventricular function and volumes

Pre-PCI cardiac function did not differ significantly between the 3 groups (46±12% vs. 49±11% vs. 49±13%, p=0.51). In patients with complete revascularization by PCI mean EF improved significantly from 46±12% before revascularization to 51±13% (p<0.0001) at 6 months follow-up. EF did not change significantly in patients after incomplete (49±11 to 49±10%; p=0.88) and without successful revascularization (49±13% to 47±13%; p=0.11) respectively. More detailed information is presented in table 3.

The improvement in EF and cardiac output in the group that underwent complete revascularization was significantly higher as compared to patients that underwent incomplete or unsuccessful revascularization (table 4). In patients with complete revascularization the change in global parameters was not influenced by positive troponin level after PCI or whether a CTO was treated. There was a trend toward a greater improvement in EF in patients with an baseline infarct size <24g vs. patients with an infarct size of >24g (5,4±4,4% vs. 2,8±5,1; p=0,10) (table 4).

Global contractile function and the predictive value of CMR

The change in EF was linearly related to the extent of the left ventricle that was dysfunctional but viable before PCI for TEI <25% (R=0.64; p<0.0001)(figure 2a) and for contractile reserve >7% (R=0.67; p<0.0001)(figure 2b).

According to the linear regression line for TEI, 4% improvement in EF corresponded to 25% of the left ventricle that was dysfunctional but viable, which are 4 segments before revascularization. The area under the ROC curve for DE-CMR

Table 3 Functional data at baseline and at 6 month follow-up on left ventricular function.

| | Complete PCI N=34 | Incomplete PCI N=22 | Unsuccessful PCI N=15 |
|---------------------------|----------------------|------------------------|-----------------------|
| EF% | | | |
| Baseline | 46±12 | 49±11 | 49±13 |
| 6 months | 51±13 | 49±10 | 47±13 |
| ΔEF | 4±5 | 1±5 | -2±4 |
| P-value | <0.0001 | 0.88 | 0.11 |
| ESVi (ml/m ²) | | | |
| Baseline | 56±34 | 52±23 | 47±23 |
| 6 months | 51±37 | 48±25 | 46±23 |
| ΔESVi | -5±8 | -4±10 | -1±5 |
| P-value | <0.0005 | 0.70 | 0.58 |
| EDVi (ml/m ²) | | | |
| Baseline | 99±36 | 98±22 | 87±24 |
| 6 months | 96±37 | 91±29 | 82±24 |
| ΔEDVi | -3±10 | -7±15 | -5±9 |
| P-value | 0.11 | 0.74 | 0.07 |
| Cardiac output | | | |
| Baseline | 5.5±1.0 | 6.1±1.2 | 5.7±1.2 |
| 6 months | 6.0±1.3 | 6.0±1.4 | 5.1±1.1 |
| ΔCO | 0.5±1.2 | -0.2±1.0 | -0.7±1.1 |
| P-value | 0.02 | 0.79 | 0.10 |
| SV | | | |
| Baseline | 84±16 | 96±21 | 82±18 |
| 6 months | 88±19 | 90±22 | 76±14 |
| ΔSV | 4±15 | -6±17 | -6±15 |
| P-value | 0.13 | 0.29 | 0.16 |

Numbers are presented as mean ± standard deviation. PCI, percutaneous coronary intervention; EF, ejection fraction; ESVi, end systolic volume index; EDVi, end diastolic volume index; CO, cardiac output; SV, stroke volume

Table 4 Functional data according to different subgroups

| | N | Δ EF | Δ ESVi | Δ EDVi | Δ CO | Δ SV |
|--------------------------------|----|-----------|-----------|-----------|-----------|-----------|
| Complete revascularization | 34 | 4.2±4.9 | -5.1±7.7 | -2.8±10.4 | 0.5±1.2 | 4.0±14.3 |
| Incomplete revascularization | 22 | 0.7±6.1 | -4.3±10.3 | -7.4±15.5 | -0.1±1.1 | -6.5±18.2 |
| Unsuccessful revascularization | 15 | -1.9±4.1* | -0.73±4.9 | -4.7±9.2 | -0.6±1.1* | -6.2±15.5 |
| Complete revascularization | | | | | | |
| Without CTO treatment | 14 | 3.6±5.9 | -5.5±7.3 | -1.9±8.9 | 0.6±1.2 | 6.3±16.9 |
| With CTO treatment | 20 | 4.4±4.2 | -4.7±8.0 | -3.6±11.2 | 0.4±1.2 | 2.0±12.1 |
| P value | | 0.77 | 0.50 | 0.85 | 0.36 | 0.48 |
| Complete revascularization | | | | | | |
| Infarct size <24g | 17 | 5.4±4.4 | -5.6±4.0 | -2.7±7.8 | 0.6±1.0 | 6.4±11.2 |
| Infarct size >24g | 17 | 2.8±5.1 | -4.6±9.8 | -3.1±12.4 | 0.4±1.3 | 1.5±16.4 |
| P value | | 0.10 | 0.55 | 0.62 | 0.67 | 0.30 |
| Complete revascularization | | | | | | |
| No enzymatic infarction | 24 | 4.7±4.5 | -5.8±8.9 | -4.9±10.8 | 0.1±1.0 | 4.4±13.4 |
| Enzymatic infarction | 10 | 2.9±6.2 | -5.6±4.7 | -3.3±10.3 | 0.6±1.3 | 0.6±18.3 |
| P-value | | 0.55 | 0.72 | 0.34 | 0.29 | 0.54 |

Numbers are presented as mean ± standard deviation. EF, ejection fraction; ESVi, end systolic volume index; EDVi, end diastolic volume index; CO, cardiac output; SV, stroke volume; CTO, chronic total occlusion; g, gram.* p <0.05 as compared to the group that underwent complete revascularization.

to predict improvement in EF was 0.84 (95%CI, 0.74-0.95; p<0.0001). For dobutamine-CMR, 3 dysfunctional but viable segments per ventricle were required to achieve an improvement in EF>4%. The area under the ROC curve for dobutamine-CMR to predict improvement in EF was 0.91 (95%CI, 0.82-0.99; p<0.0001). Dobutamine-CMR had a significant higher sensitivity (100% vs. 70%; p<0.0001) and specificity was not different (75% vs. 77%; p=0.80) as compared to DE-CMR. Sensitivity, specificity, PPV and NPV for both viability parameters were presented in table 5.

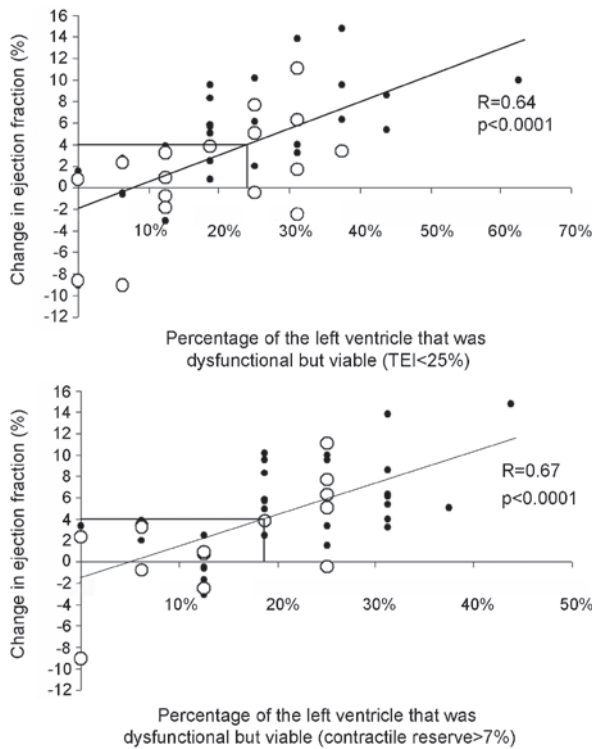


Figure 2. Prediction of change in ejection fraction - The change in left ventricular ejection fraction was related to the extent of dysfunctional but viable myocardium before revascularization using DE-CMR (a) and using dobutamine-CMR (b).

Solid circle, complete revascularization; open circle, incomplete revascularization.

Regional contractile function

Segments were stratified according to the presence or absence of viability in the perfusion territory of vessels with significant lesions. Segmental wall thickening improved significantly in patients who

underwent PCI if contractile reserve (positive change in segmental wall thickening>7%) was present or if TEI<25%. Segmental wall thickening remained unchanged in patients with unsuccessful PCI regardless if viable tissue was present (figure 3).

Table 5 Diagnostic accuracy for the prediction of improvement in global function.

| | Sensitivity (%) | Specificity (%) | PPV (%) | NPV (%) |
|---------------------------|-----------------|-----------------|-----------|-------------|
| TEI<25% | 70(50-86) | 77(58-89) | 70(47-86) | 77(58-90) |
| Contractile reserve (>7%) | 100(81-100) | 75(55-89) | 74(53-88) | 100(81-100) |

Values are presented as means and 95% confidence intervals between parenthesis; PPV, positive predictive value; NPV, negative predictive value; TEI, transmural extent of infarction.

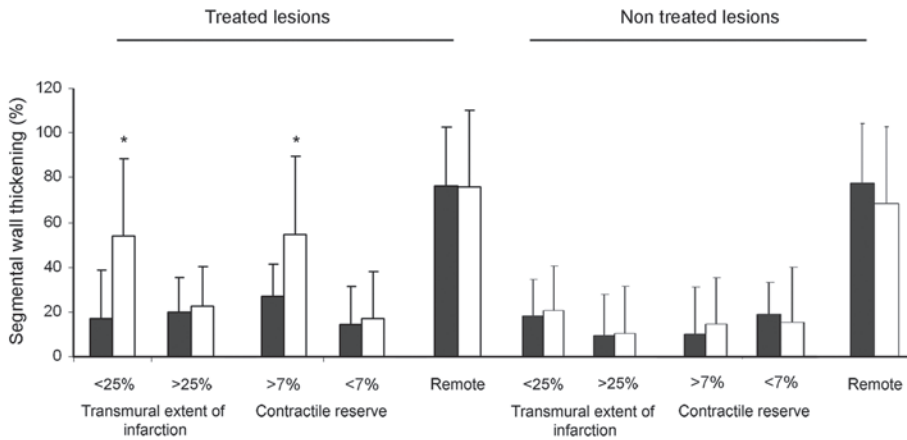


Figure 3. Segmental wall thickening for dysfunctional segments in the perfusion territory of a treated versus a non treated vessel in viable versus non viable segments - Improvement in segmental wall thickening was related to the presence of viability with MRI before percutaneous coronary intervention.

Solid bars= before PCI; open bars: 6 months after revascularization.

*p<0.05 vs. before PCI.

Discussion

To study the effect of multivessel PCI on depressed EF we used CMR as it is currently accepted as the standard of reference to determine left ventricular function (15). In addition we used both the TEI using DE-CMR and dobutamine stress CMR as potential predictors of recovery of myocardial function after PCI (12,16,17). Pre and post procedural DE-CMR can also detect new peri procedural myocardial infarction during PCI that may outweigh the potential positive effect on myocardial function.

In our study we demonstrated in patients with dysfunctional myocardium referred for PCI for multivessel coronary artery disease that complete revascularization by PCI improved EF whereas incomplete revascularization and unsuccessful revascularization did not improve EF. The extent of dysfunctional but viable myocardium per ventricle was linearly related to improvement in EF after PCI. This was reflected by the improvement in EF in patients with complete PCI by whom more dysfunctional but viable segments were revascularised than in patients with incomplete or non-succesful PCI. The change in EF could be pre-

dicted by pre-treatment CMR where dobutamine-CMR had a higher diagnostic performance than the more widely used DE-CMR.

Overall left ventricular function

The magnitude of change of EF of 4% in patients that underwent complete PCI in the present study was relatively small but in line with previous reported data about the effect of coronary artery bypass graft on left ventricular function where also an increase in EF of 4 to 5% was reported (18,19) it also should be noted that several established clinical therapies for ischemic heart failure with a demonstrated significant impact on prognosis such as angiotensin-converting enzyme inhibitor or β -blocker therapy, are associated with similar improvements in LVEF (20).

EF did not change in patients with multivessel disease followed by incomplete PCI although segments in the perfusion territory of the significant lesion in patients with incomplete PCI were dysfunctional and viable but apparently remaining non treated lesions subserving dysfunctional segments may have diluted any positive effect. Not unexpectedly an unsuccessful attempt did not improve EF. The significant increase in EF in patients that underwent complete revascularization may be a reason for the beneficial effect of complete revascularization on survival (6,7).

PCI procedure may be associated with peri-procedural myocardial infarction which may offset the potential improvement of successful revascularization of dysfunctional but viable myocardial tissue. To account for this effect we performed DE-CMR before and after the procedure to detect the occurrence of procedure related myocardial infarctions. Only 3 patients with successful complete PCI developed a peri-procedural infarction on DE-CMR, in 2 of these patients EF improved and in the other patient EF remained the same. In the patient group with an unsuccessful attempt 1 patient developed a peri procedural myocardial infarction of 2 g which is small as the mean infarct mass in these patients was 25g. In patients with incomplete PCI no peri-procedural infarcts were detected. Therefore we can conclude that the lack of change in EF in these last 2 patient groups was not influenced by peri procedural infarctions.

The improvement in EF in the present study was linearly related to the amount of dysfunctional but viable myocardium before revascularization ($R=0.64$, $p<0,001$)

for DE-CMR and $R=0,67$, $p<0,001$ for dobutamine) as was also shown by previous reported data by Kim et al. (12). They reported in a cohort of 41 patients undergoing revascularization by either PCI ($n=14$) or coronary artery bypass graft ($n=27$) that an increasing extent of dysfunctional but viable myocardium before revascularization correlated with greater improvements in EF after revascularization ($r=0.70$; $p<0.001$).

Prediction of recovery of ejection fraction

Previous studies using echocardiography or nuclear imaging have shown that improvement of EF after revascularization can be predicted with a sensitivity of 57% to 84% and a specificity of 53% to 73% (21). In our study we demonstrated that the predictive power of dobutamine-CMR was higher with a sensitivity of 100% and a specificity of 75%. However the sensitivity using DE-CMR was lower (70%) and specificity was 77%. Several reasons may explain why dobutamine CMR had a higher diagnostic performance than DE-CMR. Dobutamine stress testing is a functional parameter, the positive inotropic effects of dobutamine is a measure of functionality which mimics the potential effects of revascularization by improving contractile function in hypoperfused myocardium even in the absence of an increase in blood flow (22-24).

DE-CMR is an anatomic parameter that accurately delineates the extent of infarction which will not improve after revascularization (25) but does not provide information of the extent and the functional state of the surrounding viable myocardium. TEI is a relative value that omits the thickness of a segment and may therefore miss important information which is relevant for accurate prediction of recovery of function after revascularization therapy (13).

Limitations

The number of patient included in this study was relatively small nevertheless using CMR as the golden standard for the serial assessment of cardiac function (26,27), we were able to demonstrate a significant improvement in EF. Baseline EF tended to be lower for the group that underwent complete revascularization as compared to the other 2 groups which in theory may have influenced outcome results positively although our results for PCI are inline with results published for CABG (18,19).

The patients in the present study had a moderately reduced EF. The results may not be applicable to patients with a severe reduced EF because in these patients more non viable segments may be present, however CMR is able to detect the presence of viability which is independent on the EF. Our results may have been compromised by the occurrence of in stent restenosis because we did not perform late invasive coronary angiography. However the likelihood of in stent restenosis is low after drug eluting stent implantation and the patients that underwent complete revascularization were all symptom free at follow-up (28).

Conclusion

Left ventricular EF improves after complete revascularization and does not change after incomplete or unsuccessful revascularization in patients having multivessel coronary artery disease and dysfunctional myocardium. The change in EF after PCI could be predicted with pre treatment CMR where dobutamine-CMR had a higher diagnostic performance than DE-CMR.

References

1. Gheorghiade M, Sopko G, De Luca L, et al. Navigating the crossroads of coronary artery disease and heart failure. *Circulation* 2006;114:1202-13.
2. Afridi I, Grayburn PA, Panza JA, Oh JK, Zoghbi WA, Marwick TH. Myocardial viability during dobutamine echocardiography predicts survival in patients with coronary artery disease and severe left ventricular systolic dysfunction. *J Am Coll Cardiol* 1998;32:921-6.
3. Cortigiani L, Sicari R, Desideri A, Bigi R, Bovenzi F, Picano E. Dobutamine stress echocardiography and the effect of revascularization on outcome in diabetic and non-diabetic patients with chronic ischaemic left ventricular dysfunction. *Eur J Heart Fail* 2007;9:1038-43.
4. Meluzin J, Cerny J, Frelich M, et al. Prognostic value of the amount of dysfunctional but viable myocardium in revascularized patients with coronary artery disease and left ventricular dysfunction. Investigators of this Multicenter Study. *J Am Coll Cardiol* 1998;32:912-20.
5. Serruys PW, Morice MC, Kappetein AP, et al. Percutaneous coronary intervention versus coronary-artery bypass grafting for severe coronary artery disease. *N Engl J Med* 2009;360:961-72.
6. Hannan EL, Racz M, Holmes DR, et al. Impact of completeness of percutaneous coronary intervention revascularization on long-term outcomes in the stent era. *Circulation* 2006;113:2406-12.
7. van den Brand MJ, Rensing BJ, Morel MA, et al. The effect of completeness of revascularization on event-free survival at one year in the ARTS trial. *J Am Coll Cardiol* 2002;39:559-64.

8. Kirschbaum SW, Baks T, van den Ent M, et al. Evaluation of left ventricular function three years after percutaneous recanalization of chronic total coronary occlusions. *Am J Cardiol* 2008;101:179-85.
9. PereztoI-Valdes O, Candell-Riera J, Santana-Boado C, et al. Correspondence between left ventricular 17 myocardial segments and coronary arteries. *Eur Heart J* 2005;26:2637-43.
10. Baks T, van Geuns RJ, Duncker DJ, et al. Prediction of left ventricular function after drug-eluting stent implantation for chronic total coronary occlusions. *J Am Coll Cardiol* 2006;47:721-5.
11. Holman ER, Buller VG, de Roos A, et al. Detection and quantification of dysfunctional myocardium by magnetic resonance imaging. A new three-dimensional method for quantitative wall-thickening analysis. *Circulation* 1997;95:924-31.
12. Kim RJ, Wu E, Rafael A, et al. The use of contrast-enhanced magnetic resonance imaging to identify reversible myocardial dysfunction. *N Engl J Med* 2000;343:1445-53.
13. Wellnhofer E, Olariu A, Klein C, et al. Magnetic resonance low-dose dobutamine test is superior to SCAR quantification for the prediction of functional recovery. *Circulation* 2004;109:2172-4.
14. Thygesen K, Alpert JS, White HD. Universal definition of myocardial infarction. *Eur Heart J* 2007;28:2525-38.
15. Bellenger NG, Davies LC, Francis JM, Coats AJ, Pennell DJ. Reduction in sample size for studies of remodeling in heart failure by the use of cardiovascular magnetic resonance. *J Cardiovasc Magn Reson* 2000;2:271-8.
16. Baer FM, Theissen P, Schneider CA, et al. Dobutamine magnetic resonance imaging predicts contractile recovery of chronically dysfunctional myocardium after successful revascularization. *J Am Coll Cardiol* 1998;31:1040-8.
17. Bove CM, DiMaria JM, Voros S, Conaway MR, Kramer CM. Dobutamine response and myocardial infarct transmuralty: functional improvement after coronary artery bypass grafting--initial experience. *Radiology* 2006;240:835-41.
18. Gunning MG, Anagnostopoulos C, Knight CJ, et al. Comparison of 201Tl, 99mTc-tetrofosmin, and dobutamine magnetic resonance imaging for identifying hibernating myocardium. *Circulation* 1998;98:1869-74.
19. Selvanayagam JB, Kardos A, Francis JM, et al. Value of delayed-enhancement cardiovascular magnetic resonance imaging in predicting myocardial viability after surgical revascularization. *Circulation* 2004;110:1535-41.
20. Reffelmann T, Konemann S, Kloner RA. Promise of blood- and bone marrow-derived stem cell transplantation for functional cardiac repair: putting it in perspective with existing therapy. *J Am Coll Cardiol* 2009;53:305-8.
21. Schinkel AF, Bax JJ, Poldermans D, Elhendy A, Ferrari R, Rahimtoola SH. Hibernating myocardium: diagnosis and patient outcomes. *Curr Probl Cardiol* 2007;32:375-410.

22. Barilla F, De Vincentis G, Mangieri E, et al. Recovery of contractility of viable myocardium during inotropic stimulation is not dependent on an increase of myocardial blood flow in the absence of collateral filling. *J Am Coll Cardiol* 1999;33:697-704.
23. Lee HH, Davila-Roman VG, Ludbrook PA, et al. Dependency of contractile reserve on myocardial blood flow: implications for the assessment of myocardial viability with dobutamine stress echocardiography. *Circulation* 1997;96:2884-91.
24. Yi KD, Downey HF, Bian X, Fu M, Mallet RT. Dobutamine enhances both contractile function and energy reserves in hypoperfused canine right ventricle. *Am J Physiol Heart Circ Physiol* 2000;279:H2975-85.
25. Kim RJ, Fieno DS, Parrish TB, et al. Relationship of MRI delayed contrast enhancement to irreversible injury, infarct age, and contractile function. *Circulation* 1999;100:1992-2002.
26. Grothues F, Smith GC, Moon JC, et al. Comparison of interstudy reproducibility of cardiovascular magnetic resonance with two-dimensional echocardiography in normal subjects and in patients with heart failure or left ventricular hypertrophy. *Am J Cardiol* 2002;90:29-34.
27. Semelka RC, Tomei E, Wagner S, et al. Normal left ventricular dimensions and function: interstudy reproducibility of measurements with cine MR imaging. *Radiology* 1990;174:763-8.
28. Hoye A, Tanabe K, Lemos PA, et al. Significant reduction in restenosis after the use of sirolimus-eluting stents in the treatment of chronic total occlusions. *J Am Coll Cardiol* 2004;43:1954-8.

Interlude

Cardiac amyloidosis mimics fabry's disease in cardiac magnetic resonance imaging

Clinical Radiology 2008 Nov;63(11):1274-6.
Epub 2008 Jun 27

Sharon W Kirschbaum^{1,2}

Timo Baks^{1,2}

Marcel J M Kofflard^{1,2}

Robert-Jan M van Geuns^{1,2}

1. Department of
Cardiology, Erasmus
Medical Center,
Rotterdam, the
Netherlands

2. Department of
Radiology, Erasmus
Medical Center,
Rotterdam, the
Netherlands

Introduction

Amyloidosis is a systemic disease characterized by the extra cellular deposition of twisted β -pleated sheet fibrils (amyloid)[1]. Amyloid depositions can occur in a variety of organs, for example the heart, kidney, liver and the autonomic nervous system. Late gadolinium enhancement (LGE) in a patient with amyloidosis is in most cases observed in the subendocardium[2] although more recent studies described heterogeneous enhancement throughout the myocardium or localized most midmyocardial in a few patients[3, 4]. We present a case of a 67-year old man with biopsy proven amyloidosis and hyperenhancement of the basal inferolateral wall, which earlier has been described as typical for Fabry's disease.

Case

A 67-year old man was referred to our hospital with progressive severe dyspnoea on exertion and chest pain. His medical history showed, atrial fibrillation for which he received electrocardioversion and started amiodarone therapy. Physical examination demonstrated no evident abnormalities. The electrocardiogram at admission showed sinus rhythm with a first-degree atrioventricular block. Echocardiography demonstrated a concentric left ventricular hypertrophy, impaired systolic function, diastolic dysfunction (E/A ratio=2.0), enlarged left atrium, mild aortic valve and mitral valve insufficiency. Abdominal ultrasound demonstrated dilatation from the vena cava inferior and hepatic vein dilatation. During the evaluation of the chest pain syndrome a conventional angiogram was made which showed left ventricular pressure overload and excluded the presence of any coronary artery disease in this patient. The patient was then referred for cardiac Magnetic Resonance Imaging (CMR) for investigation of hypertrophic cardiomyopathy.

Cine images showed moderately impaired left ventricular function with ejection fraction of 43% (normal range 55-71%) and left ventricular dilatation; with an end diastolic volume of 112ml/m² (normal range 56-108ml/m²) and end systolic volume of 62 ml/m² (normal range 9-41ml/m²). Left ventricular mass was increased to 165 g/m² (normal range 45-81g/m²) with marked concentric hypertrophy. The atria were enlarged but atrial septum thickness (5 mm), the thickness of the right atrium free wall (1 mm) and atrioventricular valve thickness were normal.

Axial cine images showed bilateral pleural effusion. Late gadolinium enhancement (LGE) imaging was performed using 0.2 mmol/kg Gadoliniumdiethyltriaminepentaacetic acid (Magnevist, Schering, Germany), which demonstrated enhancement of the infero-lateral basal wall midmyocardial as shown in figure 1.

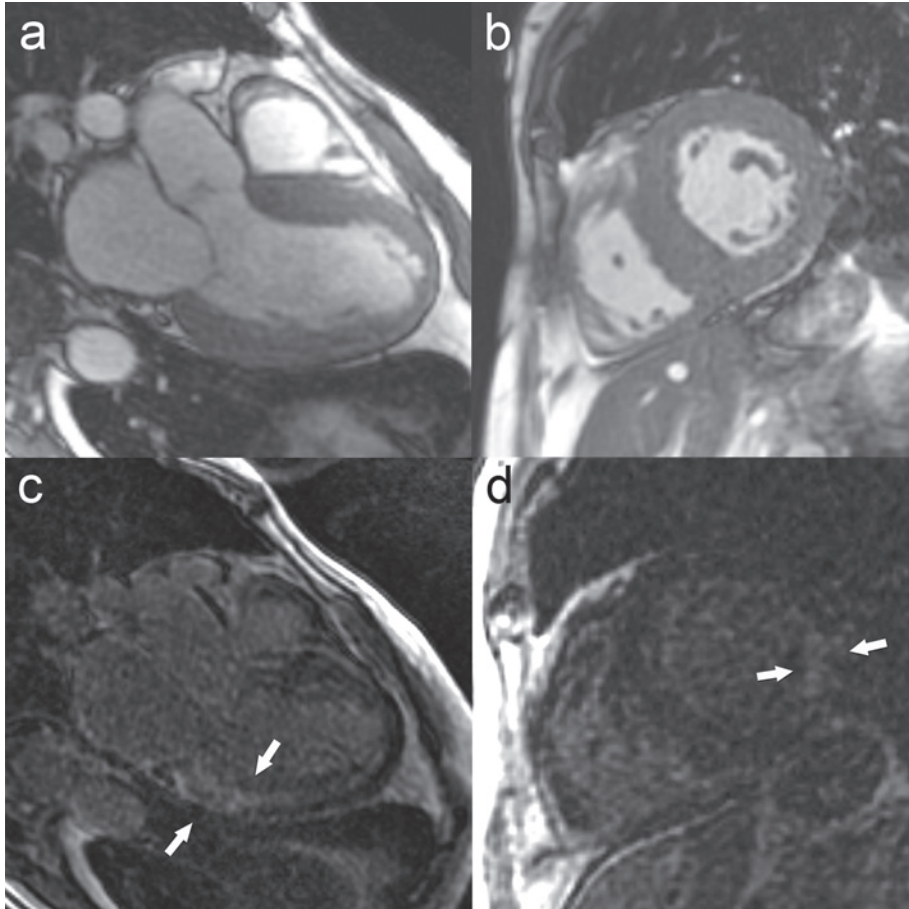


Figure 1. Cardiac Magnetic Resonance in a patient with amyloidosis. Diastolic 3-chamber long axis cine image (a) and a short axis end diastolic cine image at mid ventricular level (b) showing thickened myocardium. Corresponding late gadolinium enhancement images (c, d). Both images demonstrate enhancement in the infero-lateral basal wall at midmyocardial level (straight arrows).

The region with the positive LGE was hypokinetic. This type and the location of LGE is typically seen in patient with Fabry's disease[5]. Interestingly, accelerated Gadoliniumdiethyltriaminepentaacetic acid kinetics was present in the blood and myocardium as inversion time TI had to be increased rapidly between

scans to maintain adequately nulled myocardium. This resulted in a prolonged TI (350ms) at 10 minutes after infusion of the contrast agent. This observation strongly suggests the presence of amyloidosis. Abdominal fat aspiration biopsy confirmed the diagnosis of lambda amyloidosis. Further evaluation showed no signs of multiple myeloma or other lymphoproliferative disorders. In our case, patient was treated with a combination of melphalan, prednisolon and thalidomide, unfortunately this did not had any effect on the symptoms of this patient.

Discussion

Amyloidosis involves the heart in 50% of the patients with type AL amyloidosis and in 5% of the patients with AA amyloidosis [6]. Several findings were described in amyloidosis, for example granular appearance on echocardiography, thickened ventricular wall and systolic and diastolic dysfunction. The ECG frequently demonstrated low voltage, conduction abnormalities and arrhythmias. None of these findings is highly specific, although the combination of low voltage in the limb leads and a hypertrophic left ventricular septum or posterior wall was highly specific for cardiac involvement in systemic proven amyloidosis[7]. ECG documentation of low QRS voltages is often one of the first clues of this disease. The infiltration of the amyloid protein generally causes cardiac dysfunction, with systolic dysfunction only occurring in the late stage of the disease. The golden standard for the detection of cardiac amyloidosis is endomyocardial biopsy with the drawback of being an invasive procedure. CMR can be performed and may add diagnostic information. Maceira et al[2] showed a characteristic pattern of global subendocardial LGE and abnormal myocardial and accelerated blood pool gadolinium kinetics in patients with biopsy proven amyloidosis. They reported that the gadolinium washout from the blood was faster possibly because of gadolinium distribution into amyloid deposits throughout the body.

In our case, besides the accelerated gadolinium kinetics local LGE was observed in the basal inferolateral segments of the left ventricle. Moon et al [5]reported this as a typical predilection place for Fabry's disease. In our case, biopsy finalized the diagnosis of amyloidosis. In an overview of Marholdt et al [8]LGE in the inferolateral segments are ascribed to sarcoidosis, Fabry's disease, myocarditis or chagas disease but amyloidosis was not reported and should also be considered on our information.

References

1. Merlini G, Bellotti V. Molecular mechanisms of amyloidosis. *N Engl J Med* 2003; 349: 583-596.
2. Maceira AM, Joshi J, Prasad SK, et al. Cardiovascular magnetic resonance in cardiac amyloidosis. *Circulation* 2005; 111: 186-193.
3. vanden Driesen RI, Slaughter RE, Strugnell WE. MR findings in cardiac amyloidosis. *AJR Am J Roentgenol* 2006; 186: 1682-1685.
4. Perugini E, Rapezzi C, Piva T, et al. Non-invasive evaluation of the myocardial substrate of cardiac amyloidosis by gadolinium cardiac magnetic resonance. *Heart* 2006; 92: 343-349.
5. Moon JC, Sachdev B, Elkington AG, et al. Gadolinium enhanced cardiovascular magnetic resonance in Anderson-Fabry disease. Evidence for a disease specific abnormality of the myocardial interstitium. *Eur Heart J* 2003; 24: 2151-2155.
6. Dubrey SW, Cha K, Anderson J, et al. The clinical features of immunoglobulin light-chain (AL) amyloidosis with heart involvement. *Qjm* 1998; 91: 141-157.
7. Rahman JE, Helou EF, Gelzer-Bell R, et al. Noninvasive diagnosis of biopsy-proven cardiac amyloidosis. *J Am Coll Cardiol* 2004; 43: 410-415.
8. Mahrholdt H, Wagner A, Judd RM, Sechtem U, Kim RJ. Delayed enhancement cardiovascular magnetic resonance assessment of non-ischaemic cardiomyopathies. *Eur Heart J* 2005; 26: 1461-1474.

Part 5

Summary and Conclusions



Chapter 11

Summary and conclusions

Samenvatting en conclusies

Acknowledgements

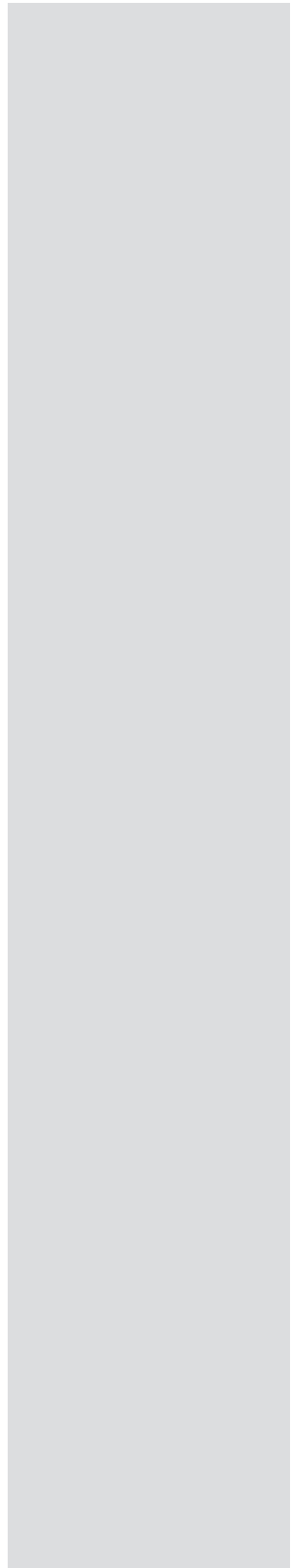
Publications

Presentations

Curriculum vitae

PhD portfolio

Summary and conclusions



Summary and conclusions

Magnetic Resonance Imaging (MRI) is an exciting non invasive imaging modality that can be used in patients with ischemic heart disease. With this technique a physician is able to accurately determine myocardial function, can identify perfusion abnormalities and allows precise assessment of the amount of scar tissue with delayed enhancement imaging. All this information can be collected in one imaging session without the use of radiation and without assumptions on left ventricular morphology as in echocardiography. In this thesis this unique imaging capability of MRI was used to study the left ventricle in an experimental setting and in patient groups for validation and also to evaluate MRI based decision making in patients with ischemic heart disease.

Validation

Cardiac MRI is nowadays considered a precise and reproducible technique for quantification of left ventricular (LV) volumes and function and these parameters are frequently used as end points in clinical trials. Still variability in measurements is present although this is relatively small compared to other techniques that can measure LV function such as LV angiography and echocardiography. Variability in measurements can be introduced during acquisition when the short axis images are positioned and planned using the long axis images and during post procedure analysis when the operator has to decide which short axis must be included in the analyses for LV functional measurement. To reduce variability in measurements we included additional 3D information from long axis images in the analysis, the combination of these images provides more detailed 3D information on the location of the mitral valve and apex as described in chapter 3. For this study a total of 40 subjects were prospectively included. The result was that the percentage interstudy variability for LV functional measurements decreased from 12 to 6% when the information of the long axis was included in the analysis.

In chapter 4 we studied the influence of papillary muscle detection on automatic image analysis. In literature the reproducibility for measurement of LV mass is good although both significant underestimation and overestimation in comparison with LV mass at autopsy have been reported. Recent improvements in MRI sequences have increased both the resolution and contrast ratios making it eas-

ier to distinguish between blood pool and muscle. Together with improvement in software this results in easier and faster identification of the papillary muscle. We used data of an animal experimental study on cell transplantation where LV mass was determined ex-vivo. All swine underwent an MRI-scan, and were sacrificed the next day. Subsequently the heart was removed and the left ventricle isolated by dissecting out the mitral and the aortic valve, the atria and the right ventricle. The computed LV mass values increased from $86.6 \pm 7.3\%$ to $92.3 \pm 6.2\%$ of the true ex-vivo mass when papillary muscle was included confirming the necessity of automatic papillary muscle detection to achieve the highest accuracy.

Detection of ischemic heart disease

Magnetic resonance perfusion (MRP) has been proposed as a non-invasive test to identify functional obstructive coronary artery disease. We compared MRP to two invasive tests available for investigation of anatomical intermediate stenoses. We studied 50 patients (male: $n=38$, mean age= 64 year) with symptoms suspicious for coronary artery disease and MRP, invasive fractional flow reserve (FFR) and coronary flow reserve (CFR) were performed. The myocardial perfusion reserve index was calculated and compared to the results of FFR and CFR. The sensitivity and specificity of myocardial perfusion reserve index for predicting a $CFR < 2.0$ was 97% and 64% and for predicting a $FFR < 0.80$, 97% and 60% respectively (Chapter 5). Therefore in patient population cardiac symptoms suspicious for coronary artery disease MRP can be used as a highly sensitive non-invasive tool to exclude hemodynamic relevant coronary artery disease similar to other non-invasive techniques such as SPECT and echocardiography. Not only MRP but also computed tomography coronary angiography (CTCA) is rapidly expanding in the diagnostic work up of patients with anginal symptoms. CTCA has a high sensitivity to detect significant coronary artery disease and is reliable to exclude the presence of coronary artery disease in patients who present with anginal symptoms. We combined function (MRP) and anatomy (CTCA) in the diagnostic work up of patients with symptoms suspicious for coronary artery disease. In this low prevalence coronary artery disease patient group the number of patients with false positive CTCA is significant, resulting in a high number of patients referred for invasive analysis. We hypothesized that MRP can identify patients that have an abnormal CTCA who require further invasive investigation. Two hundred and thirty symptomatic patients (male, 52%; age, 56 year) with anginal

symptoms underwent CTCA. In patients with a stenosis of >50%, as was visually assessed, MRP was performed and myocardial perfusion reserve index was calculated. Sensitivity and specificity for MRP in patients with a positive CTCA scan, were 96% and 78%. We concluded that the combination of CTCA followed by MRP was reliable in the selection of patients where further invasive investigation is warranted (chapter 6).

MRP provides excellent diagnostic sensitivity and NPV to detect significant coronary artery disease in patients with anginal symptoms. In addition low dose dobutamine MRI can be used to predict recovery of function after revascularization and is a useful addition to delayed enhancement MRI. We were the first to study the relation between quantitative contractile reserve and transmural extent of infarction in patients with chronic dysfunctional myocardium. We quantified contractile reserve in myocardial segments stratified according to (i) the transmural extent of infarction, (ii) end-diastolic wall thickness and (iii) thickness of the unenhanced rim in patients with chronic dysfunctional myocardium due to a chronic total occlusion (CTO) during low dose dobutamine and compared this with segmental wall thickening at follow-up (Chapter 5) . We paid particular attention to the evaluation of segments with an intermediate transmural extent of infarction between 25-75 % where we investigated the influence the epicardial viable rim on contractile reserve and improvement in function after revascularization. Significant contractile reserve was present in segments with end diastolic wall thickness >6 mm, unenhanced rim thickness >3 mm or transmural extent of infarction of <25% but only transmural extent of infarction had a significant relation with contractile reserve (OR 0.98; 95%CI 0.96-0.99; p=0.02). In segments with intermediate transmural extent of infarction (n=58) mean segmental wall thickening did not improve significantly. However segments with a hypokinetic epicardial viable rim showed contractile reserve and improved at follow-up while in segments with a normokinetic epicardial viable rim remained unchanged during dobutamine and at follow-up. Segmental wall thickening of the unenhanced rim had a significant relation with contractile reserve (OR 0.98; 95%CI 0.97-0.99; p=0.02) (chapter 7).

Magnetic resonance imaging guided management of ischemic heart disease

Left ventricular dysfunction may be the result of viable myocardium or non viable dysfunctional myocardium. The latter may not recover after revascularization therapy while viable myocardium will recover in week, months or years after revascularization. This myocardium is called hibernating myocardium where hibernation refers to regions with repetitive transient ischemia or persistent reduced myocardial blood flow that must be distinguished from infarcted myocardium. MRI allows detection of viable dysfunctional myocardium.

The improvement in cardiac function after revascularization is related to the extent of myocardial necrosis, end diastolic wall thickness, unenhanced rim thickness and the presence of contractile reserve. However the predictive accuracy of each of these parameters is moderate. In our study we have combined these parameters into a viability score. We performed cardiac MRI in patients before and 6 months after percutaneous coronary intervention (PCI) of a chronic total coronary occlusion (CTO) and demonstrated that the combination of viability parameters resulted in a higher predictive accuracy for the prediction of dysfunctional myocardial segments to improve in function after revascularization (chapter 8). The viability score may be useful for the selection of patients before PCI of a CTO. Recovery of dysfunctional but viable myocardium after revascularization is usually studied 6 months after revascularization but it is currently unknown in what time span recovery of dysfunctional myocardium can occur and recovery may still occur beyond 6 months. The time of recovery of dysfunctional myocardium is related to the extent of damage on cellular level which depends on different factors, including the duration and severity of ischemia. It has been shown that when structural changes were widespread recovery was delayed and the extent of recovery remained incomplete at 6 months.

We studied myocardial function beyond the 6 month period in segments with more extensive myocardial abnormalities (end diastolic wall thickness between 7 and 9, or transmural extent of infarction between 25-75%) at 6 months and 3 years after revascularization. We found that the restoration of flow also induce additional recovery of segments after 6 months that were not or incompletely recovered at 6 months. This indicates that treatment in this patient group is still useful in terms of improvement in cardiac function (chapter 9).

PCI is not only used in patients with single vessel disease but nowadays increasingly used in patients with multivessel disease instead of coronary artery bypass graft surgery because both therapies have the same outcome in terms of survival and rates of myocardial infarction, as long as the extent of disease is not too extensive (Syntax score <33). We were interested to study the effects of PCI on left ventricular function in patients with multivessel disease that underwent complete, incomplete and unsuccessful revascularization. Using MRI the left ventricular function was measured before and 6 months after PCI. Left ventricular function improved in patients that underwent complete revascularization and did not change in patients that underwent incomplete or unsuccessful revascularization. The outcome of pre treatment MRI predicted the improvement in ejection fraction (chapter 10).

Conclusion

In this thesis we have shown that cardiac MRI is a highly useful clinical tool to precisely quantify left ventricular function, to detect ischemia and viable dysfunctional myocardium, and to pre operatively predict the recovery of dysfunctional myocardium in patients that underwent revascularization of a chronic total occlusion or multivessel disease.

Samenvatting en conclusies

Samenvatting en conclusies

Magnetic Resonance Imaging (MRI) is een veelzijdige beeldvormende techniek die vaak gebruikt wordt voor diagnostische doeleinde bij patiënten met ischemische hartziekte. Met deze techniek kan de linkerventrikel functie van het hart, de mate van perfusie van de hartspier en de grootte van het infarct in de hartspier gemeten worden. Tijdens een MRI onderzoek wordt deze informatie verzameld zonder dat röntgenstraling of jodiumhoudend contrast nodig is. In deze thesis gebruiken we MRI zowel in dierenexperimenteel als patiënt gebonden onderzoek om enerzijds technieken om beelden te analyseren te valideren en anderzijds ischemie en vitaliteit in patiënten met ischemische hartziekten te detecteren.

Validatie

Cardiale MRI is een secure techniek met een goede reproduceerbaarheid waardoor de functie en het volume van de linkerventrikel gemeten kunnen worden zonder grote meetfouten, dit is een groot voordeel omdat deze metingen vaak worden gebruikt in klinische studies als eindpunt. Ondanks de hoge reproduceerbaarheid van deze techniek zijn variaties in metingen nog steeds aanwezig alhoewel deze variaties klein zijn ten opzichte van de variatie in metingen van de linkerventrikel bij andere imaging- modaliteiten zoals echocardiografie of linker ventrikel angiografie. Deze variatie kan ontstaan tijdens het maken van een MRI van het hart maar ook tijdens het analyseren van deze beelden. Het grootste probleem tijdens het analyseren van de beelden is de overgang van de boezem naar de ventrikel, het is daarbij lastig om aan te geven welke korte as wel nog en welke niet meer bij de linker ventrikel hoort. In hoofdstuk 3 hebben we daarom de lange as van de linker ventrikel gebruikt om niet alleen de grens aan te geven tussen de atria en de ventrikels maar ook om een meer gedetailleerde begrenzing aan te geven van het apicale gedeelte van de linker ventrikel. Veertig patiënten werden geïncludeerd in deze studie, vervolgens werden van het hart van iedere patiënt 2 MRI-scans gemaakt. De interstudievariabiliteit verminderde van 12% naar 6% wanneer de lange as van de linker ventrikel werd gebruikt bij het berekenen van de linkerventrikelfunctie.

Niet alleen de linker ventrikel functie maar ook de linker ventrikel massa kan tot in detail bestudeerd worden met MRI. Uit studies blijkt dat de massa van linker ventrikel regelmatig wordt onder- maar ook overschat wanneer deze wordt vergeleken met de massa na autopsie. Recente verbeteringen in MRI-sequenties hebben ertoe geleid dat bloed beter onderscheiden kan worden van spier. In hoofdstuk 4 is onderzocht of de papillairspier van de linker ventrikel automatisch gedetecteerd kan worden en of de papillairspier een significante invloed heeft op de totale linkerventrikel massa.

De massa van varkenshartten zijn ex vivo gewogen en vergeleken met in vivo-metingen middels een MRI-scan. De berekende linker ventrikel massa in vivo was $86.6 \pm 7.3\%$ van de linker ventrikel massa ex vivo wanneer de papillairspier massa niet meegerekend werd en $92.3 \pm 6.2\%$ van de linker ventrikel massa ex vivo wanneer de massa van de papillairspier wel meegerekend werd. Hieruit blijkt dat het van belang is deze papillairspier massa mee te nemen bij het berekenen van de massa van de linkerventrikel.

Detectie van ischemische hartziekte

Magnetic resonance perfusie (MRP) is een niet invasieve diagnostische test waarmee ischemie van de hartspier gedetecteerd kan worden. In hoofdstuk 5 hebben we deze techniek vergeleken met 2 technieken, fractionele flow reserve (FFR) en coronaire flow reserve (CFR), die beide invasief zijn en informatie geven over de bloedstroom in de kransslagaders. Om een vergelijking tussen deze technieken te maken hebben we een studie opgezet waarin we 50 patiënten hebben geïnccludeerd (38 mannen, gemiddelde leeftijd 64 jaar). Al deze patiënten hadden angineuze klachten. Ze ondergingen allemaal een MRP-scan en een angiografie van de kransslagaders. Tijdens de angiografie werd een FFR en een CFR gemeten. De myocardiale perfusie reserve index werd berekend en vergeleken met de FFR en de CFR. De sensitiviteit en specificiteit van de myocardiale perfusie reserve index om een significante CFR te voorspellen waren 97% en 64% en om een significante FFR te voorspellen, 97% en 60%. Hieruit kunnen we concluderen dat de myocardiale perfusie reserve-index een goede methode is om significante lesies die hemodynamisch relevant zijn op te sporen.

Niet alleen MRI, maar ook computed tomography coronary angiography (CTCA) is belangrijk in de diagnostiek naar ziekte van de kransslagaders. CTCA heeft een hoge negatief voorspellende waarde wat betekent dat ziekte in de kransslagaders uitgesloten kan worden. In hoofdstuk 6 hebben we 230 patiënten geïncludeerd (52% mannen, gemiddelde leeftijd 56 jaar) met stabiele angineuze klachten. MRI en CTCA werden gebruikt om hemodynamisch significant coronairlijden op te sporen. De hypothese was dat MRP het aantal patiënten met angineuze klachten, bij wie significant coronairlijden op CTCA was aangetoond en die verwezen zouden worden voor angiografie zou doen verminderen. Bij patiënten met een significante stenose op CTCA werd een MRP gemaakt en de myocardiale perfusie reserve index berekend. De sensitiviteit en specificiteit van MRP voor het detecteren van ischemie waren 96% en 78%. Hieruit kunnen we concluderen dat CTCA gevolgd door MRP betrouwbaar is voor de selectie van patiënten voor angiografie.

In hoofdstuk 7 hebben we onderzocht in 51 patiënten (gemiddelde leeftijd 60 jaar, 76% mannen) wat de mate van contractiele reserve tijdens lage dosering dobutamine (5-10 mcg/kg/min) was in de relatie tot (1) de grootte van het infarct, (2) de eind-diastolische wanddikte en (3) dikte van het niet-geïnfarceerde gedeelte. In een gedeelte van de patiënten populatie hebben we de mate van contractiele reserve voor revascularisatie vergeleken met de mate van wandverdikking 6 maanden na revascularisatie. Significante contractiele reserve was aanwezig in segmenten met een einddiastolische wand dikte van >6 mm, in segmenten met een niet-geïnfarceerde gedeelte van >3 mm en in segmenten waarbij de transmuraliteit van het infarct <25%. In een subgroep van patiënten met een hartinfarct tussen de 25-75% van de dikte van de linker ventrikel was er geen contractiele reserve aanwezig en ook geen verbetering in wandverdikking 6 maanden na percutane coronaire interventie (PCI). Echter wanneer dezelfde groep werd verdeeld in een hypokinetische en een normokinetische epicardiale vitale rand dan was contractiele reserve maar ook een verbetering in wanddikte na PCI aanwezig in de groep segmenten met een hypokinetische epicardiale vitale rand, terwijl de wandverdikking niet significant toenam in segmenten met een normokinetische epicardiale vitale rand.

Magnetic resonance imaging als leidraad voor revascularisatie therapie

De functie van de linker ventrikel kan verminderd zijn door disfunctioneel myocard dat nog vitaal is of disfunctioneel myocard dat niet meer vitaal is. Myocard dat niet vitaal is zal ook niet verbeteren na PCI terwijl chronisch hypokinetisch vitaal myocard een week, maand of jaar na PCI nog kan verbeteren. De staat waarin het hartspierweefsel dan verkeerd noemen we hibernation. Hibernation betekent "slaapstand", hierin verkeerd het myocard wanneer er te weinig zuurstofrijke bloedtoevoer is. MRI kan vitaal myocard detecteren. Er zijn verschillende parameters waarmee vitaal weefsel gedetecteerd kan worden, namelijk einddiastolische wanddikte, transmuraliteit van het infarct, de aanwezigheid van contractiele reserve en de mate van contractiliteit van de epicardiale vitale rand. Echter de voorspellende waarde van deze parameters is matig, in hoofdstuk 8 hebben we onderzocht of de voorspellende waarde beter wordt wanneer we al deze parameters voor het detecteren van vitaliteit kunnen combineren in een zogenaamde vitaliteitscore. In deze studie werden 72 patiënten geïncludeerd (87% mannen, gemiddelde leeftijd 60 jaar). Alle patiënten ondergingen voor en na de PCI-procedure een MRI-scan. De sensitiviteit en specificiteit van deze vitaliteitscore waren 91% en 84%.

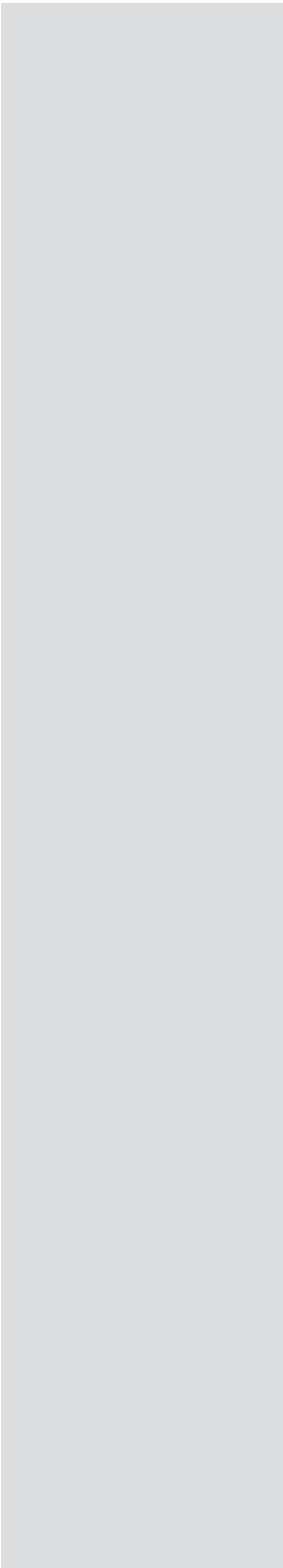
Om het effect van PCI op de functie van de hartspier te bestuderen wordt meestal een follow-up termijn van 6 maanden genomen. We weten echter niet precies hoelang het duurt voordat het myocard maximaal verbetert na PCI. Misschien verbetert het myocard ook nog wel na 6 maanden. Hoelang het duurt totdat het myocard geheel hersteld is hangt af van de mate van schade op cellulair niveau. Als de uitgebreidheid van de schade op cellulair niveau groot is dan duurt het langer voordat de functie van het myocard verbeterd is. In hoofdstuk 9 hebben we onderzocht in 21 patiënten (85% mannen, gemiddelde leeftijd 63 jaar) of de contractiliteit van de hartspier in segmenten met meer uitgebreidere schade (eind diastolische wanddikte tussen de 7-9 mm en de transmuraliteit van het infarct tussen de 25-75%), ook nog na 6 maanden verbetert. In segmenten met meer uitgebreidere schade verbeterde de functie van de hartspier ook nog na 6 maanden. Dit betekent dat PCI ook zinvol kan zijn in deze groep. PCI is niet alleen zinvol in patiënten met atherosclerose in 1 kransslagader, maar wordt ook steeds meer toegepast in patiënten bij wie sprake is van atherosclerose in meerdere kransslagaders. Wanneer de ziekte van de kransslagader niet te uitgebreid is (syn-

tax score van <33) is PCI net zo goed als bypasschirurgie. In hoofdstuk 10 hebben we het effect van PCI op de linkerventrikel functie onderzocht bij patiënten die een significante ziekte hadden in meerdere kransslagaders. In deze studie werden 71 patiënten geïncludeerd (76% mannen, gemiddelde leeftijd 62 jaar). De functie van de linker ventrikel hebben we gemeten in 3 groepen patiënten. Een groep patiënten bij wie alle vaten succesvol gedotterd werden, patiënten bij wie de PCI incompleet was en patiënten bij wie het niet gelukt was de kransslagaderen te behandelen. De mate van ziekte (syntax score) was gelijk in alle 3 de patiëntengroepen. De functie van de linker ventrikel werd berekend in alle 3 de groepen voor en 6 maanden na PCI. De linker ventrikelfunctie verbeterde alleen in de groep patiënten bij wie alle zieke kransslagaderen gedotterd werden.

Conclusie

We hebben in deze thesis laten zien dat cardiale MRI een secure methode is om de functie van de linker ventrikel tot in detail te bestuderen en ook om de aanwezigheid van ischemie en vitaliteit van de hartspier te detecteren. In specifieke patiënten populaties met een verminderde myocardfunctie en een chronisch totale occlusie en/of meervats coronairlijden zijn er aanwijzingen dat MRI als leidraad gebruikt kan worden voor PCI.

Acknowledgements



Om te beginnen zou ik graag alle patiënten en vrijwilligers die hebben meegewerkt aan dit onderzoek willen bedanken, zonder hen zou dit werk niet tot stand zijn gekomen.

Professor de Feyter, beste Pim, hoe jij een stuk tekst kan omtoveren tot een paar treffende zinnen, ongelofelijk. Veel heb ik geleerd van de momenten wanneer ik een artikel met de pen geheel herschreven “weer” terug kreeg, we er samen voor gingen zitten en het stuk door namen. Dank dat je ook nu na je pensioen nog tijd hebt voor adviezen.

Beste Robert-Jan, laagdrempelig bereid tussendoor resultaten te bespreken en naar manuscripten te kijken met opbouwend commentaar dat vaak in de avonden of in het weekend teruggestuurd werd. Ik bewonder je gedrevenheid, je enthousiasme en je originele ideeën voor nieuw onderzoek. Dank voor de altijd prettige samenwerking.

Professor Krestin, bedankt dat ik op uw afdeling heb mogen werken en gebruik heb mogen maken van alle faciliteiten die de afdeling radiologie bood, ik heb me altijd erg “thuis” gevoeld op de afdeling radiologie. En een goede samenwerking tussen cardiologie en radiologie heeft geresulteerd in dit proefschrift.

Professor Duncker, beste Dirk, graag wandelde ik weer naar de 23ste verdieping want ik wist zeker dat na een uurtje discussiëren met jou ik een enorme stortvloed aan kennis zou vergaren er weer nieuwe ideeën ontstonden voor onderzoek. Geweldig hoe jij mensen kunt enthousiasmeren voor wetenschap!

Tevens wil ik graag de overige leden van de commissie bedanken; professor Niessen, professor Zijlstra, professor Roos-Hesselink, professor van der Giessen en professor van Rossum voor de beoordeling van mijn proefschrift en hun komst bij de verdediging van dit proefschrift

Lieve Annick, beste CV, kamergenoot, altijd gezellig, toen ik wist dat er een plekje bij jou op jouw kamer vrij kwam wist ik wat me te doen stond. Gelachen met jou heb ik tijdens onze lunchuitjes naar de boeren of de Italiaan en de borrel op de vrijdagavond, bewondering heb ik voor jouw includeer-snelheid want die kan niemand overtreffen maar vooral om jouw multitask capaciteiten want moeder worden, trouwen en promoveren tegelijk dat doen er je maar weinige na!

Lieve Floor, paranimf en dierbare vriendin uit het Limburgse, per ongeluk leerde ik je kennen omdat ik naast je kwam te zitten vooraan in de klas, gelukkig maar! Vervolgens ging je naar Maastricht studeren en ik naar Rotterdam maar dat heeft ons nooit van contact weerhouden. Mooie herinneringen heb ik aan onze kampeervakanties en stapavondjes in het Weertse waarbij onze privé-taxi-chauffeurs (de moeders) onmisbaar waren!

Eric Boersma, dank voor de tijd en geduld die jij hebt om moeilijke statistiek meestal met een simpele tekening duidelijk te maken. Hierdoor werden de soms wollige vragen van reviewers voor mij toch nog duidelijk.

Speciale dank gaat ook uit naar iedereen van onze cardiale imaging groep.

Bob Meijboom, als enige haan in het onderzoek hok had je het soms zwaar te verduren met 2 kakelende kippen. Bewondering heb ik voor de manier waarop jij altijd volledig ontspannen omgaat met deadlines en met enorm lange ingewikkelde databases vol 0-en en 1-en die hebben geresulteerd in een aantal mooie publicaties in prachtige tijdschriften en een enorm dik proefschrift. Samen met Annick hebben we een leuke onderzoek tijd gehad in hok Ba-127 waar we hard gewerkt hebben maar vooral ook veel gelachen hebben!

Tirza Springeling, eindelijk weer een MRI-er tussen al het CT-geweld. Door jouw organisatietalent zaten we tijdens congressen meestal in de beste hotels op de beste locaties in de stad. Succes met het afronden van je proefschrift.

Timo Baks, veel dank voor jouw hulp in het prille begin van mijn promotietijd, met name voor het geduld dat je had mij te leren scannen aangezien mijn geduld vaak van korte duur was, helaas wisselen we elkaar zowel tijdens onze promotie als opleiding af maar gelukkig hebben we wel dezelfde hobby! Tot op het water!

Sing-Chien Yap, in no time gepromoveerd, dank voor de altijd gezellige samenwerking.

Carlos van Mieghem, vriendelijke mede zuiderling, altijd geïnteresseerd en bereid te helpen waar nodig. Bedankt voor het doen van alle combowire-met-

gen, zelfs toen je elders ging werken was je toch bereid patiënten te includeren en metingen te verrichten. Dank daarvoor.

Alexia Rossi, living abroad, thanks for all your help, sometimes last minute! I have a lot of respect the way you manage everything, good luck finishing your PhD.

Koen Nieman, bedankt voor jouw wetenschappelijke input en hulp bij dit proefschrift, altijd binnen een paar dagen een antwoord terug, dank voor onze prettige samenwerking.

Lisanne Neefjes, dank voor jouw gezelligheid, succes met het afronden van je proefschrift.

Gert-Jan ten Kate, tijdens je co-schappen begonnen met je onderzoek, knap hoor, succes met het afronden ervan.

Multiple fellows from different places all over the world have joined the research group

Niels van Pelt, all the way from Australia, thanks for checking my English grammar. "The Italians"; Francesca Pugliese, Roberto Malago, Filippo Albergina, Marco Rengo, Ermano Cupana, shearing a room full with Italians is never boring I couldn't understand any word of your conversations but when I closed my eyes it was as if I was on holiday. Thanks for teaching me how to prepare a real Italian pasta. Stamatis Kyrzopoulos, thanks for analysing MRI data.

Trialbureau cardiologie en radiologie, Saskia, Nico, Maria, Willeke, Caroline, Linda en Frans dank voor jullie ondersteuning bij de verschillende onderzoeksprojecten. Kim en Corrie dank voor jullie hulp bij de voorbereidingen voor mijn promotie.

Alle technici van het katheterisatie laboratorium wil ik graag bedanken voor hun hulp bij het verzamelen van de data. Speciale dank daarbij gaat uit naar Jurgen voor het zorgdragen voor mooie en goede CFR signalen.

Alle collega's uit het Sint Franciscus Gasthuis wil ik graag bedanken voor de prettige samenwerking en hun flexibiliteit rondom mijn promotie.

Ton en Sanne dank voor jullie hulp en jullie creatieve input tijdens het maken van dit promotieboek wat heeft geresulteerd tot een mooi geheel.

Lieve vriendinnen, dank voor de heerlijke stapavondjes en vakanties in Nederland en in het heerlijke Portugal, Italië en Spanje. Ik hoop dat er nog vele zullen volgen. Lieve Eer: huis-,club- en buurtgenoot dank voor je mental support en ik hoop dat we nooit te ver weg van mekaar zullen gaan wonen.

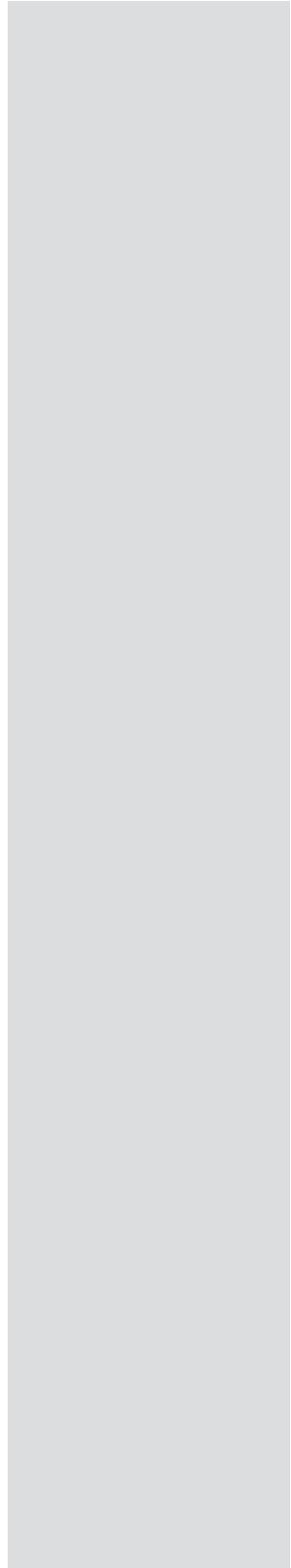
Broertje, bedankt voor je steun tijdens de laatste loodjes en ook voor het oplossen van de altijd weer zo stressvolle computer-problematiek dat was altijd erg fijn. Je woont tegenwoordig gelukkig iets dichterbij in de buurt!

Lieve Jan en José Schreurs, altijd gezellig bij jullie op de avenue, met zijn allen eten op de zondagavond en natuurlijk onze geweldige vakantie met de hele fam. in Thailand. Dank voor deze fijne momenten. Silvie, John, kleine Isabella, Guido, Janneke en Michel, dank ook voor jullie support.

Lieve pap en mam, aan jullie ben ik de meeste dank verschuldigd, dank voor de heerlijke jeugd in het fijne Limburg. Jullie laatste zetje heeft ervoor gezorgd dat ik toch naar Rotterdam ben gegaan om geneeskunde te studeren gelukkig maar! Dank voor jullie steun en liefde.

Lieve Maurice, wat ben ik gelukkig samen met jou, elke dag met jou is een feestje, ik heb je lief!

Publications



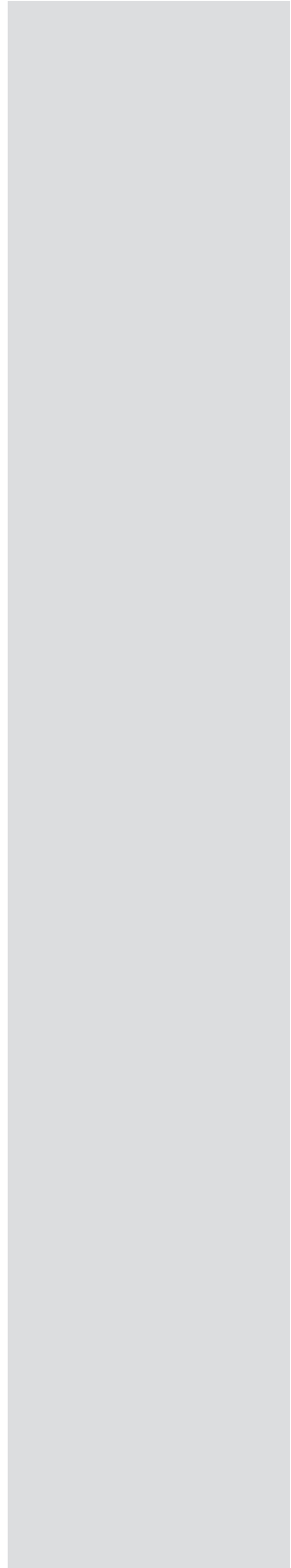
Publications

1. **Kirschbaum SW**, Baks T, Gronenschild EH, Aben JP, Weustink AC, Wielopolski PA, Krestin GP, de Feyter PJ, van Geuns RJM. Addition of the long axis information to short axis contours reduces interstudy variability of the left ventricle in cardiac magnetic resonance studies. *Invest Radiol*. 2008 Jan;43(1):1-6.
2. **Kirschbaum SW**, Baks T, van den Ent M, Sianos G, Krestin GP, Serruys PW, de Feyter PJ, van Geuns RJM. Evaluation of left ventricular function 3 years after percutaneous recanalisation of chronic total occlusion. *Am J Cardiol*. 2008 Jan 15;101(2):179-85.
3. **Kirschbaum SW**, Baks T, Kofflard MJM, van Geuns RJM. Cardiac amyloidosis mimics fabry's disease in cardiac magnetic resonance imaging. *Clinical Radiology* 2008 Nov;63(11):1274-6. Epub 2008 Jun 27.
4. **Kirschbaum SW**, Aben JP, Baks T, Wielopolski PA, Krestin GP, de Feyter PJ, van Geuns RJM. Automatic papillary muscle identification for left ventricle mass measurements in cardiac magnetic resonance imaging. *Acad Radiol*. 2008 Oct;15(10):1227-33
5. **Kirschbaum SW**, Gruszczynska K, Duncker D, Krestin GP, Serruys PW, Feyter PJ, van Geuns RJM. Quantification of regional contractile reserve in segments with non-transmural infarction in chronic dysfunctional myocardium using low dose dobutamine magnetic resonance imaging. *Journal of the american college of cardiology Cardiovasc Imaging*. 2010 Jun;3(6):614-22
6. **Kirschbaum SW**, van Geuns RJ. Magnetic resonance imaging to detect and evaluate ischemic heart disease. *Hellenic J Cardiol*. 2009 Mar-Apr;50(2):119-26. Review.
7. **Kirschbaum SW**, Springeling T, Boersma E, Moelker A, van der Giessen WJ, Serruys PW, de Feyter PJ, van Geuns RJ Complete percutaneous revascularization for multivessel disease in patients with impaired left ventricular function. Pre- and post procedural evaluation by cardiac magnetic resonance imaging. *Journal of the american college of cardiology Cardiovasc Interv*. 2010 Apr;3(4):392-400

8. **Kirschbaum SW**, Springeling T, Rossi A, Duckers E, Gutiérrez-Chico JL, Regar E, Feyter de PJ and van Geuns RJM Comparison of adenosine magnetic resonance perfusion imaging with invasive CFR and FFR in patients with suspected coronary artery disease. *International Journal of cardiology*, 2011 Febr 17;147(1):184-6
9. Soliman Oll, **Kirschbaum SW**, van Dalen B, van der Zwaan H, M. Delavary B, Vletter, van Geuns RJM, ten Cate FJ, Geleijnse M. Accuracy and Reproducibility of Quantitation of Left Ventricular Function by Real-Time Three-Dimensional Echocardiography versus Cardiac Magnetic Resonance *Am J Cardiol*. 2008 Sep 15;102(6):778-83. Epub 2008 Jul 9
10. Ramcharitar S, Meliga E, **Kirschbaum SW**, ten Cate FJ, van Geuns RJ, Serruys PW. Acute hemodynamic changes in percutaneous transluminal septal coil embolisation for obstructive hypertrophic cardiomyopathy. *Nat Clin Pract Cardiovasc Med*. 2008 Dec;5(12):806-10. Epub 2008 Oct 7
11. Krenning BJ, **Kirschbaum SW**, Soliman Oll, Nemes A, van Geuns RJM, Vletter WB, Veltman CE, ten Cate FJ, Roelandt JRTC, Geleijnse ML. Comparison of contrast agent-enhanced versus non-contrast agent-enhanced real-time three-dimensional echocardiography for analysis of left ventricular systolic function. *Am J Cardiol*. 2007 Nov 1;100(9):1485-9
12. Soliman Oll, Krenning BJ, Geleijnse ML, Nemes A, Bosch JG, van Geuns RJ, **Kirschbaum SW**, Anwar AM, Galema TW, Vletter WB, ten Cate FJ. Quantification of Left Ventricular Volumes and Function in Patients with Cardiomyopathies by Real-Time Three-Dimensional Echocardiography: A Head-to-Head Comparison Between Two Different Semi-Automated Endocardial Border Detection Algorithms. *J Am Soc Echocardiogr*. 2007 Sep;20(9):1042-9
13. Yap SC, van Geuns RJ, Meijboom FJ, **Kirschbaum SW**, McGhie JS, Simoons ML, Kilner PJ, Roos-Hesselink JW. Simplified Approach for Quantification of Aortic Valve Area by Velocity-encoded Cardiac Magnetic Resonance Imaging. *J Cardiovasc Magn Reson*. 2007;9(6):899-906
14. Cheng C, de Crom R, van haperen R, Helderma F, Mousavi Gourabi B, van Damme LCA, **Kirschbaum SW**, Slager CJ, van der Steen AFW, Krams R. The role of shear stress in Atherosclerosis. *Cell Biochem Biophys*. 2004;41(2):279-94.

15. Segers D, Cheng C, de Crom R, **Kirschbaum SW**, Oostlander AE, Helderma F, Van Wamel A., Slager CJ., Serruys PW., van der Steen AFW. Krams R. Monocyte adhesion in atherosclerosis. A biomechanical approach. *Vascular Disease Prevention*, 2005 Vol 2, nr 3.

Presentations



EuroCMR 2006

1. Sharon W. Kirschbaum; Timo Baks; Ed H Gronenschild; Jean-Paul Aben; Annick C. Weustink; Piotr A. Wielopolski; Gabriel, P. Krestin; Pim J de Feyter; Robert-Jan M van Geuns. *Poster presentation ID 44*: Reduction in interstudy variability of cardiac magnetic resonance imaging by identification of mitral valve plane and apex on long axis images.

Nederlandse Vereniging Voor Cardiologie 2006

2. Sharon W. Kirschbaum; Timo Baks; Ed H Gronenschild; Jean-Paul Aben; Annick C. Weustink; Piotr A. Wielopolski; Gabriel, P. Krestin; Pim J de Feyter; Robert-Jan M van Geuns. *Poster presentation*: Reduction in interstudy variability of cardiac magnetic resonance imaging by identification of mitral valve plane and apex on long axis images

Society of Cardiomagnetic Resonance Imaging 2007

3. Sharon W. Kirschbaum; Timo Baks; Amber Moelker; Gabriel P Krestin; Pim J de Feyter; Robert-Jan M van Geuns. *Poster presentation 440*: Influence of the papillary muscles and cardiac phase on accurate left ventricular mass measurements by CMR
4. Sharon W. Kirschbaum; Timo Baks; Ed H Gronenschild; Jean-Paul Aben; Annick C. Weustink; Piotr A. Wielopolski; Gabriel, P. Krestin; Pim J de Feyter; Robert-Jan M van Geuns. *Poster presentation 435*: Addition of the long axis information to short axis contours reduces interstudy variability of the left ventricle in cardiac magnetic resonance studies
5. Singh Yap; Robert-Jan Van Geuns; Folkert J Meijboom; Sharon W Kirschbaum; Jackie S McGhie; Maarten L Simoons; Jolien Roos-Hesselink. *Poster presentation 346 A* simplified continuity equation approach to the quantification of aortic stenosis using velocity-encoded CMR

American College of cardiology 2007

6. Sharon W. Kirschbaum; Timo Baks; Martin van den Ent; George Sianos; Gabriel, P. Krestin; Patrick W. Serruys; Pim J de Feyter; Robert-Jan M van Geuns *Poster presentation 350777* Early and Late Improvement of Left Ventricular Function After Drug-Eluting Stent Implantation for Chronic Total Occlusions.

ISMRM/ESMRMB 2007

7. Sharon W. Kirschbaum; Timo Baks; Martin van den Ent; George Sianos; Gabriel, P. Krestin; Patrick W. Serruys; Pim J de Feyter; Robert-Jan M van Geuns *Poster presentation 3864* Long-term Improvement of Left Ventricular Function after Percutaneous Recanalisation of Chronic Total Coronary Occlusions: 3 Years Follow-up

European society of cardiology 2007

8. Sharon W. Kirschbaum; Timo Baks; Martin van den Ent; George Sianos; Gabriel, P. Krestin; Patrick W. Serruys; Pim J de Feyter; Robert-Jan M van Geuns *Oral presentation 82501* Long-term improvement of left ventricular function after percutaneous recanalisation of chronic total coronary occlusions: 3 years follow-up

Nederlandse Vereniging voor cardiologie 2008

8. Sharon W Kirschbaum, Timo Baks, Martin van den Ent; Gabriel P. Krestin; Patrick W. Serruys; Pim J. de Feyter; Robert-Jan M. van Geuns. *Poster presentation* Improvement of left ventricular function after percutaneous revascularization for chronic total occlusions
9. Sharon W Kirschbaum; Alexia Rossi, Dirk J Duncker, Gabriel P. Krestin; Patrick W. Serruys; Pim J. de Feyter; Robert-Jan M. van Geuns *Poster presentation* Contractile reserve in chronic dysfunctional myocardium in patients with intermediate transmural extent of infarction

Society of Cardiomagnetic Resonance Imaging 2008

10. Sharon W Kirschbaum; Katerina Gruszczynska; Gabriel, P. Krestin; Patrick W. Serruys; Pim J de Feyter; Robert-Jan M van Geuns *Oral presentation* Contractility Reserve in Segments Non-Viable on Delayed Enhancement; Analysis with Low Dose Dobutamine MRI.
11. Sharon W Kirschbaum; Timo Baks, Martin van den Ent; George Sianos; Gabriel P. Krestin; Patrick W. Serruys; Pim J. de Feyter; Robert-Jan M. van Geuns *Poster presentation* Additional late improvement after percutaneous recanalisation of chronic total occlusions

12. Alexia. Rossi, Sharon.W. Kirschbaum, Katherina Gruszczynska, Adriaan Moelker, M.A. Cova, Gabriel.P. Krestin, Pim J de Feyter, Robert-Jan M van Geuns *Poster presentation* The number of short-axis series for MR left ventricular analysis can be reduced when a combined long-axis and short-axis analysis strategy is used

European society of cardiology 2008

13. Sharon W Kirschbaum, K. Gruszczynska, DJ. Duncker, A. Rossi, GP. Krestin, PW. Serruys, PJ. De Feyter, RJ. Van Geuns *Poster presentation 303* Contractile reserve by dobutamine cardiac magnetic resonance imaging of dysfunctional myocardial segments corresponds well with improvement in quantitative wall thickening after revascularization

RSNA 2008

14. Sharon W Kirschbaum, K Gruszczynska, A Rossi, G P Krestin, P J De Feyter, R M van Geuns *Oral presentation 6014546* Quantification of the Contractile Reserve during Low Dose Dobutamine-MRI Is a Better Predictor for Segmental Recovery than the Amount of Scar Tissue on DE-MRI in Segments with Non-transmural Extent of Infarction
15. Alexia Rossi, Sharon W Kirschbaum; Yusuf Karamermer; Peter de Jaegere; Tirza Springeling; Adriaan Moelker, Pim de Feyter, Robert-Jan van Geuns *Oral presentation 6017787* A Simplified Continuity Equation Approach to the Quantification of Stenotic Highly Calcified Aortic Valves Using Velocity-encoded CMR: Comparison with Conventional Invasive Cardiac Catheterization

Invited lecture

1. Sharon W. Kirschbaum Magnetic resonance in coronary artery disease. Thessaloniki Greece 2007
2. Sharon W. Kirschbaum Glimpse into the future: chronic total occlusion; MRI in the assessment of function and viability. EuroPCR, Barcelona, Spain, 2008

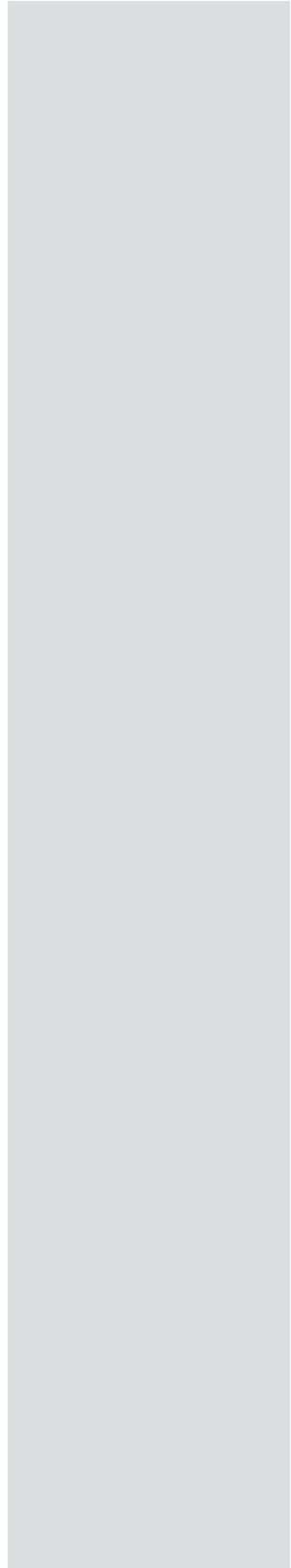
COEUR

1. Sharon W. Kirschbaum MRI and the assessment of myocardial function and viability 2007
2. Sharon W. Kirschbaum Remodelling in patients with a chronic total occlusion. 2008

METC aanvragen

1. The role of Viability testing to decide on percutaneous coronary Intervention strategies of complex Coronary Artery Disease (**VICAD**).
2. Cardiac magnetic resonance perfusion imaging for SElection of patients for additional invasive evaluation after CT coronary angiography (**CANSEL**)

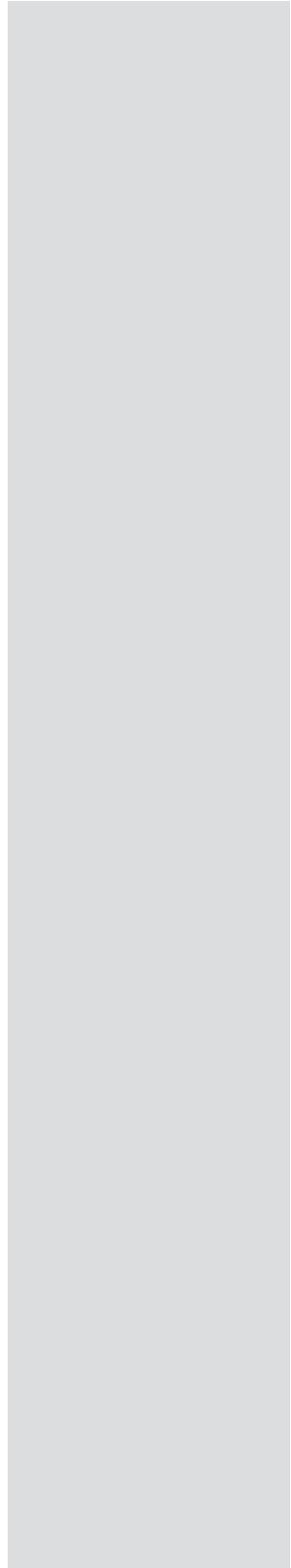
Curriculum vitae



Curriculum Vitae

Sharon Kirschbaum was born on June 15th 1980 in Weert, the Netherlands. After finishing high school in 1998 at the Philips van Horne in Weert, she studied medicine at the Erasmus University in Rotterdam. She was certified as a MD in December 2005. In December 2005 and January 2006 she worked as a fellow at the department of cardiology in the Erasmus Medical Center followed by a period as research fellow in the field of cardiac magnetic resonance imaging at the Erasmus Medical Center at the department of cardiology and radiology under supervision of Pim de Feyter and Robert-Jan van Geuns which resulted in this thesis. In April 2009 she started here cardiology training with 2 years of internal medicine in the Sint Franciscus gasthuis in Rotterdam (supervisor Dr Rietveld) which will be followed by one year at the department of cardiology in the Sint Franciscus gasthuis in Rotterdam (supervisor Dr van Mechelen). The final part of the training will be undertaken at the department of cardiology in the Erasmus Medical Center (supervisor Dr ten Cate).

PhD portfolio



| | |
|--------------------------------------------------------------------------------------------------------------------|-------------------------------------------------------------------------------------------------------------------------------------|
| Name PhD student: Sharon W Kirschbaum Erasmus MC Department: Cardiology and Radiology Research School: COEUR | PhD period: february 2006-april 2009 Promotor(s): Pim J de Feyter and Gabriel P Krestin Supervisor: Robert-Jan M van Geuns |
|--------------------------------------------------------------------------------------------------------------------|-------------------------------------------------------------------------------------------------------------------------------------|

1. PhD training

| | Year | Workload (Hours/ECTS) |
|------------------------------------------------------------------|------|--------------------------|
| General academic skills | | |
| -Biomedical English Writing and Communication | 2007 | 3 |
| Research skills | | |
| - Cardiovascular epidemiology | 2007 | 1.5 |
| - Design of cardiovascular trials | 2006 | 1.5 |
| In-depth courses (e.g. Research school, Medical Training) | | |
| - Cardiovascular imaging and diagnostics | 2006 | 1.5 |
| - Erasmus cardiac MR course | 2006 | 1.5 |
| - Pathophysiology of ischemic heart disease | 2007 | 1.5 |
| Presentations | | |
| - EuroCMR | 2006 | 0.5 |
| - Nederlandse Vereniging Voor Cardiologie | 2006 | 0.5 |
| - Society of Cardiomagnetic Resonance Imaging | 2007 | 1.5 |
| - American College of cardiology | 2007 | 3 |
| - European society of cardiology | 2007 | 3 |
| - Nederlandse Vereniging Voor Cardiologie | 2008 | 1.5 |
| - Society of Cardiomagnetic Resonance Imaging | 2008 | 3 |
| - European society of cardiology | 2008 | 1.5 |
| - EuroPCR | 2008 | 3 |
| - RSNA | 2009 | 3 |
| Other | | |
| - Cardiology and vascular medicine update and perspective | 2006 | 0.5 |
| - Cardiology and vascular medicine update and perspective | 2007 | 0.5 |
| - Cardiology and vascular medicine update and perspective | 2008 | 0.5 |

2. Teaching activities

| | Year | Workload (Hours/ECTS) |
|---------------------------------------------------------------|------|--------------------------|
| Lecturing | | |
| - MRI and the assessment of myocardial function and viability | 2006 | 0.4 |
| - Remodelling in patients with a chronic total occlusion | 2008 | 0.4 |

